Vol. 7, no. 3, 2023 eISSN 2587-8999
PEER-REVIEWED SCIENTIFIC AND THEORETICAL JOURNAL

Computational Mathematics and Information Technologies

Computational Mathematics

Mathematical Modelling

Information Technologies

www.cmit-journal.ru
DOI 10.23947/2587-8999

Computational Mathematics and Information Technologies

Peer-reviewed scientific and theoretical journal (published since 2017)

eISSN 2587-8999
DOI: 10.23947/2587-8999

Vol. 7, no. 3, 2023

The scope of "Computational Mathematics and Information Technologies" is focused on fundamental and applied research according to the following scientific sections:

1. Computational Mathematics
2. Mathematical Modelling
3. Information Technologies

Indexing:	Russian Scientific Citation Index, Crossref, Cyberleninka
Name of the body that registered the publication	Mass media registration certificate ЭЛ № ФС 77-66529 dated July 21, 2016 issued by the Federal Service for Supervision of Communications, Information Technology and Mass Media.
Founder and publisher	Federal State Budgetary Educational Institution of Higher Education Don State Technical University (DSTU).
Periodicity	Quarterly (4 issues per year)
Address of the founder and publisher	Gagarin Sq. 1, Rostov-on-Don, 344003, Russian Federation.
E-mail	CMIT-EJ@yandex.ru
Telephone	+7(863) 273–85–14
Website	https://cmit-journal.ru
Date of publication	29.09.2023

Computational Mathematics and Information Technologies

Рецензируемый научно-теоретический журнал (издаётся с 2017 года)

eISSN 2587-8999
DOI: 10.23947/2587-8999

Том 7, № 3, 2023

Журнал «Computational Mathematics and Information Technologies» ориентирован на фундаментальные и прикладные исследования по следующим научным разделам:

1. Вычислительная математика
2. Математическое моделирование
3. Информационные технологии

Индексация:	РИНЦ, CrossRef, КиберЛенинка
Наименование органа, зарегистрировавшего издание	Свидетельство о регистрации средства массовой информации ЭЛ № ФС 77 – 66529 от 21 июля 2016 г., выдано Федеральной службой по надзору в сфере связи, информационных технологий и массовых коммуникаций.
Учредитель и издатель	Федеральное государственное бюджетное образовательное учреждение высшего образования «Донской государственный технический университет» (ДГТУ).
Периодичность	4 выпуска в год
Адрес учредителя и издателя	344003, Российская Федерация, г. Ростов-на-Дону, пл. Гагарина, 1.
E-mail	CMIT-EJ@yandex.ru
Телефон	+7(863) 273–85–14
Сайт	https://cmit-journal.ru
Дата выхода в свет	29.09.2023

Contents

COMPUTATIONAL MATHEMATICS

MATHEMATICAL MODELLING

Содержание

ВЫЧИСЛИТЕЛЬНАЯ МАТЕМАТИКА

МАТЕМАТИЧЕСКОЕ МОДЕЛИРОВАНИЕ

COMPUTATIONAL MATHEMATICS
ВЫЧИСЛИТЕЛЬНАЯ МАТЕМАТИКА

UDC 519.213.2, 517.443, 517.518.45
https://doi.org/10.23947/2587-8999-2023-7-3-7-11

Short report

Semiinvariants, Senatov Moments and Density Decomposition

Alexander E Condratenko, Vitaly N Sobolev

Lomonosov Moscow State University, 1, Lenin Mountains, Moscow, Russian Federation

ae_cond@mech.math.msu.su

Abstract

It is proposed to introduce into Probability Theory courses such a new moment characteristic of random variable as Senatov moment. Naturalness of this proposal is confirmed by three views of appearance of Senatov moments. Introducing of them will answer the question about what is analogue of Taylor series of function for density.

Keywords: moments, semiinvariants, Senatov moments, Fourier transform, Fourier series, density decomposition

Acknowledgments: the authors are grateful to Professors A.V. Bulinsky, E.B. Yarova and academician A.N. Shiryaev for their attention to the work.

For citation: Condratenko AE, Sobolev VN. Semiinvariants, Senatov Moments and Density Decomposition. *Computational Mathematics and Information Technologies*. 2023;7(3):7–11. https://doi.org/10.23947/2587-8999-2023-7-3-7-11

Краткое сообщение

Семиинварианты, моменты Сенатова и разложение плотности

А.Е. Кондратенко ✉, В.Н. Соболев

Московский государственный университет им. М.В. Ломоносова, Российская Федерация, г. Москва, Ленинские горы, 1

ae_cond@mech.math.msu.su

Аннотация

Предлагается ввести в программы курсов теории вероятностей рассмотрение относительно новой моментной характеристики случайных величин — моментов Сенатова. Естественность этого предложения подтверждается тремя взглядами на возникновение моментов Сенатова, а их введение позволит ответить на вопрос, что является аналогом ряда Тейлора функции для плотности.

Ключевые слова: моменты, семиинварианты, моменты Сенатова, преобразование Фурье, ряд Фурье, разложение плотности

Благодарности: авторы выражают благодарность профессорам А.В. Булинскому, Е.Б. Яровой и академику А.Н. Ширяеву за внимание к работе.

Для цитирования: Кондратенко А.Е., Соболев В.Н. Семиинварианты, моменты Сенатова и разложение плотности. *Computational Mathematics and Information Technologies*. 2023;7(3):7–11. https://doi.org/10.23947/2587-8999-2023-7-3-7-11

Introduction. In probability theory courses, in addition to the usual moments of a random variable ξ:

$$\alpha_k = M\xi^k = \int_{-\infty}^{\infty} x^k dF(x), k \in Z_+,$$

where $F(x)$ is the distribution function of the random variable under consideration, other moment characteristics are also described, for example,
absolute moments:

$$M\,|\xi|^{k},$$

central moments:

$$M\,(\xi - M\,\xi)^{k}$$

and factorial

$$M\xi^{[k]} = M\,\xi(\xi - 1)\ldots(\xi - k + 1)$$

moments.

The central problem of probability theory — the central limit theorem — has led in its development to the appearance of two more moment characteristics, called semiinvariants, which are told to mathematics students, and Senatov moments, which are just beginning to enter the course programs.

The apparatus for determining moments proposed by V. V. Senatov can also be used in applied problems, for example, when calculating the coefficients of turbulent exchange for the equations of hydrodynamics of systems with a free surface, including marine and coastal [1].

Aim of work. Senatov's moments deserve to be included in the programs of probability theory courses. In the paper, this will be justified with the help of three questions, at first glance, unrelated to each other.

For the sake of simplicity, we will consider the random variables considered in this paper to be centered, normalized and absolutely continuous, which have moments of all natural orders, and the characteristic function:

$$f(t) = Me^{\,it\,\xi}$$

is represented by Taylor series and is absolutely integrable.

The first question. The even moments of a standard normal random variable increase and increase rapidly — the standard normal moment of the order of $2k$ is $(2k-1)!!$, $k \in N$ (in the future we will consider k a non-negative integer, unless otherwise specified). But investigating the convergence of centered and normalized convolutions to a standard normal random variable by investigating the convergence of a numerical sequence to a non-zero number is usually technically more difficult than investigating convergence to zero. Accordingly, it becomes necessary to introduce new natural moment characteristics, which for a standard normal random variable will be zero, with the exception, perhaps, of the most initial orders. Since the moments are related to the derivatives of the characteristic function by equality:

$$i^{k}\alpha_{k} = (f(t))^{(k)}_{t=0},$$

and the standard normal characteristic function is exp(-t2/2), then it is necessary to propose such a transformation of the latter so that the derivatives of the resulting composition at zero *quickly* become zero.

The use of logarithm as the first such transformation was proposed in 1889 by the Danish astronomer and mathematician Thorvald Nicolai Thiele, calling the obtained characteristics semiinvariants:

$$i^{k}\kappa_{k} = (\ln(f(t)))^{(k)}_{t=0}.$$

Indeed, $\ln(\exp(-t^2/2)) = -t^2/2$, тогда $\kappa_0 = 0$, $\kappa_1 = 0$, $\kappa_2 = 1$ и $\kappa_k = 0$ при $k > 3$.

An important exceptional property of semiinvariants: since the characteristic function of the convolution is equal to the product of the characteristic functions of the summands, the semiinvariants of the convolution are equal to the sum of the semiinvariants of the summands. But working with a complex logarithm requires special care and is often associated with significant technical difficulties.

Another transformation is no less natural — in 2001, Vladimir Vasilyevich Senatov, Professor of the Department of Probability Theory of the Faculty of Mechanics and Mathematics of the Lomonosov Moscow State University, finally determined the characteristics called Senatov moments from 2021 (after his death):

$$i^{k}\theta_{k} = (\exp(t^2/2)f(t))^{(k)}_{t=0}.$$

All the Senatov moments of a standard normal random variable are zero, except $\theta_0 = 1$.

All the mentioned moment characteristics of an arbitrary random variable exist or do not exist simultaneously, always $\kappa_0 = 0$, $\theta_0 = 1$, for centered and normalized random variables $\kappa_1 = \theta_1 = \theta_2 = 0$, $\kappa_2 = 1$.

The second question is related to the fact that the representation of a characteristic function by its Taylor series:

$$f(t) = \sum_{k=0}^{\infty} \frac{\alpha_k}{k!}(it)^{k}$$

does not allow us to find the density $p(x)$ through the inversion formula:

$$p(x) = \frac{1}{2\pi}\int_{-\infty}^{\infty} e^{-itx} f(t)dt,$$

since the Fourier transform of the power function does not exist.

It is possible to get out of the impasse with the help of semiinvariants and Senatov moments. To do this, recall that the Chebyshev-Hermite polynomials, which are eigenfunctions of the Schrodinger equation [2–3] and form an orthogonal system on the set of real numbers with the weight of the standard normal density $\varphi(x) = e^{-x^2/2}/\sqrt{2\pi}$:

$$H_k(x) = (-1)^k e^{x^2/2}\left(e^{-x^2/2}\right)^{(k)}$$

have the property (1):

$$\frac{1}{2\pi}\int_{-\infty}^{\infty} e^{-itx}(it)^k e^{-t^2/2}dt = H_k(x)\varphi(x).$$

For a characteristic function , the representation is valid:

$$f(t) = \exp(\mathrm{In}(f(t))) = \exp\left(\sum_{k=0}^{\infty}\frac{\varkappa_k}{k!}(it)^k\right) = e^{-t^2/2}\exp\left(\sum_{k=3}^{\infty}\frac{\varkappa_k}{k!}(it)^k\right),$$

and therefore property (1) allows, by presenting its second exponent with a Taylor series, to apply the inversion formula.

Similar arguments using the Senatov moments allow us to answer the third question — which analogue of the Taylor series of the function can be proposed for a random variable in the face of its density. Since:

$$f(t) = e^{-t^2/2}\left(e^{t^2/2}f(t)\right) = e^{-t^2/2}\left(\sum_{k=o}^{\infty}\frac{\theta_k}{k!}(it)^k\right) = e^{-t^2/2}\left(1+\sum_{k=3}^{\infty}\frac{\theta_k}{k!}(it)^k\right),$$

that property (1) allows you to immediately apply the inversion formula and obtain the expansion for the density in the form of the corresponding Fourier series:

$$p(x) = \varphi(x) + \sum_{k=3}^{\infty}\frac{\theta_k}{k!}H_k(x)\varphi(x).$$

For centered and normalized sums of n independent random variables, such expansions are called asymptotic [4], since all summands under the sign of the sum will tend to zero with the growth of n, which follows from the expression of the moments of convolutions through the moments of the initial distribution:

$$\frac{\theta_k(F_n)}{k!} = \sum\frac{n!}{j_0!\,j_3!\ldots j_n!}\left(\frac{\theta_3}{3!n^{\frac{3}{2}}}\right)^{j_3}\ldots\left(\frac{\theta_k}{k!n^{\frac{k}{2}}}\right)^{j_k},$$

where summation is performed over whole non-negative sets:

$$j_0+j_3+j_4+\ldots j_k=n,\ 3j_3+4j_4+\ldots kj_k=k.$$

The speed of striving for zero “triples” is interesting (Table 1):

$$\theta_k(F_n) = O\left(n - \frac{\left[\frac{k}{3}+3\left\{\frac{k}{3}\right\}\right]}{2}\right), n\to\infty.$$

Table 1

The rate of striving for zero of the “triples” of terms

k	3	4	5	6	7	8	9	10	11	…
$\frac{\left[\frac{k}{3}\right]+3\left\{\frac{k}{3}\right\}}{2}$	0.5	1	1.5	1	1.5	2	1.5	2	2.5	…

For example:

$$\theta_3(F_n)=\frac{\theta_3}{\sqrt{n}},\ \theta_4(F_n)=\frac{\theta_4}{n},\ \theta_5(F_n)=\frac{\theta_5}{n^{1,5}},\ \theta_6(F_n)=\frac{6!}{n^2}\left(\frac{n-1}{2!}\frac{\theta_3^2}{3!^2}+\frac{\theta_6}{6!}\right).$$

The *magical* connection of the Senatov moments with Chebyshev-Hermite polynomials is the following equality:

$$\theta_k=\int_{-\infty}^{\infty}H_k(x)\,dF(x).$$

V. V. Senatov defined them this way in 2001 [5], calling them Chebyshev-Hermite moments because of this connection, therefore, in literature and research until last year they are found and used under this name. Now, as a sign of memory of an outstanding scientist who worked at Moscow University and proposed, in particular, asymptotic expansions with an explicit accuracy estimate that can be brought to numerical values, we will call them Senatov moments [6].

Conclusion. The use of Senatov moments made it possible to advance the task of studying the convergence rate in the central limit theorem so qualitatively that these moment characteristics began to be perceived very naturally. This allows, according to the authors, to raise the question of their inclusion in the program of those courses in probability theory, where the central limit theorem is proved by the method of characteristic functions. And for students of mathematics, it is simply necessary to do this in order to prepare for the study of a special course “Additional chapters of probability theory”.

References

1. Sukhinov AI, Protsenko SV, Protsenko EA. Field Data Filtering for the Digital Simulation of Three-Dimensional Turbulent Flows Using The Les Approach. *Vestnik Yuzhno-Uralskogo Gosudarstvennogo Universiteta. Seriya: Matematika. Mekhanika. Fizika*. 2022;14(4): 40–51. (In Russ.). https://doi.org/10.14529/mmph220406

2. Schrodinger E. *Selected works on quantum mechanics*. Moscow: Nauka; 1976. 424 p. (In Russ.).

3. Taimanov IA, Tsarev SP. On the Moutard transformation and its applications to spectral theory and Soliton equations. *Journal of Mathematical Sciences*. 2010;170(3):371–387. https://doi.org/10.1007/s10958-010-0092-x

4. Senatov VV. *Central limit theorem: accuracy of approximation and asymptotic expansions.* Moscow: Book House “LIBROCOM”; 2009. 352 p.

5. Senatov VV. Application of the Chebyshev-Hermite moments in asymptotic decompositions. In: “Twentieth international seminar on stability problems for stochastic models”. *Theory of Probability and its Applications*. 2001;46(1):190–193.

6. Sobolev VN, Kondratenko AE. On Senatov Moments in Asymptotic Expansions in the Central Limit Theorem. *Theory of Probability and its Applications*. 2022;67(1):154–157. https://doi.org/10.4213/tvp5483

About the Authors:

Alexander E Kondratenko, Associate Professor of the Department of Probability Theory, Lomonosov Moscow State University (1, Leninskie Gory, Moscow, 119991, RF), Candidate of Physical and Mathematical Sciences, ae_cond@mech.math.msu.su

Vitaly N Sobolev, Associate Professor/PhD in specialty no. 01.01.05 Lomonosov Moscow State University (1, Leninskie Gory, Moscow, 119991, RF), Candidate of Physical and Mathematical Sciences, sobolev_vn@mail.ru

Claimed contributorship:

All authors have made an equivalent contribution to the preparation of the publication.

Received 25.07.2023
Revised 17.08.2023
Accepted 18.08.2023

Conflict of interest statement

The authors do not have any conflict of interest.

All authors have read and approved the final manuscript.

Об авторах:

Кондратенко Александр Евгеньевич, доцент кафедры теории вероятностей, Московский государственный университет им. М. В. Ломоносова (119991, РФ, г. Москва, Ленинские горы, 1), кандидат физико-математических наук, ae_cond@mech.math.msu.su

Соболев Виталий Николаевич, доцент/с.н.с. по специальности № 01.01.05 Московский государственный университет им. М. В. Ломоносова (119991, РФ, г. Москва, Ленинские горы, 1), кандидат физико-математических наук, sobolev_vn@mail.ru

Заявленный вклад соавторов:

Все авторы сделали эквивалентный вклад в подготовку публикации.

Поступила в редакцию 25.07.2023
Поступила после рецензирования 17.08.2023
Принята к публикации 18.08.2023

Конфликт интересов

Авторы заявляют об отсутствии конфликта интересов.

Все авторы одобрили окончательный вариант рукописи.

COMPUTATIONAL MATHEMATICS
ВЫЧИСЛИТЕЛЬНАЯ МАТЕМАТИКА

Original article

UDC 519.6

https://doi.org/10.23947/2587-8999-2023-7-3-12-19

Symmetrized Versions of the Seidel and Successive OverRelaxation Methods for Solving Two-Dimensional Difference Problems of Elliptic Type

Valentina V Sidoryakina ✉, Denis A Solomakha

Don State Technical University, 1, Gagarin Sq., Rostov-on-Don, Russian Federation

✉ cvv9@mail.ru

Abstract

Introduction. This article is devoted to the consideration of options for symmetrization of two-layer implicit iterative methods for solving grid equations that arise when approximating boundary value problems for two-dimensional elliptic equations. These equations are included in the formulation of many problems of hydrodynamics, hydrobiology of aquatic systems, etc. Grid equations for these problems are characterized by a large number of unknowns — from 10^6 to 10^{10}, which leads to poor conditionality of the corresponding system of algebraic equations and, as a consequence, to a significant increase in the number of iterations, necessary to achieve the specified accuracy. The article discusses a method for reducing the number of iterations for relatively simple methods for solving grid equations, based on the procedure of symmetrized traversal of the grid region.

Materials and Methods. The methods for solving grid equations discussed in the article are based on the procedure of symmetrized traversal along the rows (or columns) of the grid area.

Results. Numerical experiments have been performed for a model problem — the Dirichlet difference problem for the Poisson equation, which demonstrate a reduction in the number of iterations compared to the basic algorithms of these methods.

Discussion and Conclusions. This work has practical significance. The developed software allows it to be used to solve specific physical problems, including as an element of a software package.

Keywords: two-dimensional problem of elliptic type, iterative methods, relaxation methods, complete relaxation method, Seidel method, upper relaxation method

Funding information. The study was supported by the Russian Science Foundation grant No. 22-11-00295. https://rscf.ru/en/project/22-11-00295

Acknowledgments. The authors express their deep gratitude and sincere gratitude to Corresponding Member of the Russian Academy of Sciences, Doctor of Physical and Mathematical Sciences, Professor Alexander Ivanovich Sukhinov for discussing algorithms and research results.

For citation. Sidoryakina VV, Solomakha DA. Symmetrized Versions of the Seidel and Successive OverRelaxation Methods for Solving Two-Dimensional Difference Problems of Elliptic Type. *Computational Mathematics and Information Technologies.* 2023;7(3):12–19. https://doi.org/10.23947/2587-8999-2023-7-3-12-19

Научная статья

Симметризованные варианты методов Зейделя и верхней релаксации решения двумерных разностных задач эллиптического типа

В.В. Сидорякина ✉, **Д.А. Соломаха**

Донской государственный технический университет, Российская Федерация, г. Ростов-на-Дону, пл. Гагарина, 1

✉ cvv9@mail.ru

Аннотация

Введение. Данная статья посвящена рассмотрению вариантов симметризации двухслойных неявных итерационных методов для решения сеточных уравнений, возникающих при аппроксимации краевых задач для двумерных уравнений эллиптического типа. Данные уравнения входят в постановки многих задач гидродинамики, гидробиологии водных систем и др. Сеточные уравнения для данных задач характеризуются большим количеством неизвестных — от 10^6 до 10^{10}, что приводит к плохой обусловленности соответствующей системы алгебраических уравнений и, как следствие, к существенному росту числа итераций, необходимых для достижения заданной точности. В статье рассмотрен метод снижения числа итераций для относительно простых методов решения сеточных уравнений (метода Зейделя и верхней релаксации).

Материалы и методы. Рассматриваемые в статье методы решения сеточных уравнений базируются на процедуре симметризованного обхода по строками (или столбцами) сеточной области.

Результаты исследования. Выполнены численные эксперименты для модельной задачи — разностной задачи Дирихле для уравнения Пуассона, которые демонстрируют сокращение числа итераций по сравнению с базовыми алгоритмами данных методов.

Обсуждение и заключения. Данная работа имеет практическую значимость. Разработанное программное средство позволяет его использовать для решения конкретных физических задач, в том числе как элемента программного комплекса.

Ключевые слова: двумерная задача эллиптического типа, итерационные методы, релаксационные методы, метод полной релаксации, метод Зейделя, метод верхней релаксации

Финансирование. Исследование выполнено за счет гранта Российского научного фонда № 22-11-00295. https://rscf.ru/project/22-11-00295

Благодарности. Авторы выражают глубокую признательность и искреннюю благодарность член-корреспонденту РАН, доктору физико-математических наук, профессору Александру Ивановичу Сухинову за обсуждение алгоритмов и результатов исследования.

Для цитирования. Сидорякина В.В., Соломаха Д.А. Симметризованные варианты методов Зейделя и верхней релаксации решения двумерных разностных задач эллиптического типа. *Computational Mathematics and Information Technologies*. 2023;7(3):12–19. https://doi.org/10.23947/2587-8999-2023-7-3-12-19

Introduction. In numerical modeling of technical systems, physical phenomena and technological processes, as a rule, a significant proportion of the total amount of computational work is the solution of systems of linear algebraic equations (SLAE) that arise when the corresponding differential or integro-differential equations are discretized. A special class is represented by systems of linear algebraic equations with symmetric positive definite matrices. Depending on the proposed approach to constructing the next iterative approximation, several iterative methods for solving these SLAE are distinguished [1–3]. Among them are the methods of Seidel and Successive OverRelaxation. The popularity of these methods can be explained by their simplicity and wide popularity among researchers [4]. In this regard, there is a natural interest in studying various variants of the methods under consideration and the desire to obtain the advantages of using them.

In this article, variants of symmetrization of Seidel and Successive OverRelaxation methods for solving two-dimensional difference problems of elliptic type are considered. Based on the results of numerical calculations of the solution of the Dirichlet problem for the Poisson equation in a rectangular area, a reduction in the number of iterations compared to the basic algorithms of these methods is demonstrated. The table, which shows the dependences of the number of iterations on the number of grid nodes of the computational domain when using the methods under consideration, makes it possible to visually verify that the symmetrized version of the Successive OverRelaxation method can significantly reduce the required number of iterations to achieve a given accuracy and, as a result, reduce the calculation time.

Materials and methods

1. Seidel and Successive OverRelaxation methods. In a finite-dimensional Hilbert space , the problem of finding a solution to an operator equation is considered:

$$Ax = f, \quad A: \ H \to H, \tag{1}$$

where A is the linear operator, x is the desired function, f is the known function of the right part.

To find a solution to problem (1), we will use an implicit two-layer iterative scheme:

$$B\frac{y^{k+1} - y^k}{\tau_{k+1}} + Ay^k = f, \ B: \ H \to H, \ k = 0,1,2,..., \tag{2}$$

with an arbitrary approximation $y^0 \in H$.

Equation (2) uses the notation: B is some invertible operator; k is iteration number; y^k is the vector of the k-th iterative approximation; τ_{k+1} is the iterative parameter, $\tau_{k+1} > 0$.

To represent the Seidel iterative method in matrix form, we write the matrix as a sum of diagonal, lower triangular and upper triangular matrices:

$$A = D + L + U, \tag{3}$$

where:

$$D = \begin{pmatrix} a_{11} & 0 & ... & 0 & 0 \\ 0 & a_{22} & ... & 0 & 0 \\ ... & ... & ... & ... & ... \\ 0 & 0 & ... & a_{N-1N-1} & 0 \\ 0 & 0 & ... & 0 & a_{NN} \end{pmatrix}, \ L = \begin{pmatrix} 0 & 0 & ... & 0 & 0 \\ a_{21} & 0 & ... & 0 & 0 \\ ... & ... & ... & ... & ... \\ a_{N-11} & a_{N-12} & ... & 0 & 0 \\ a_{N1} & a_{N2} & ... & a_{NN-1} & 0 \end{pmatrix},$$

$$U = \begin{pmatrix} 0 & a_{12} & ... & a_{1N-1} & a_{1N} \\ 0 & 0 & ... & a_{2N-1} & a_{2N} \\ ... & ... & ... & ... & ... \\ 0 & 0 & ... & 0 & a_{N-1N} \\ 0 & 0 & ... & 0 & 0 \end{pmatrix}.$$

Denote by $y^k = \left(y_1^{(k)} y_2^{(k)},..., y_N^{(k)}\right)$ the vector of the k-th iterative approximation.

Using expression (3), we write the Seidel method in the form:

$$(D + L)y^{k+1} + Uy^k = f, \ k = 0,1,2,... . \tag{4}$$

Bringing the iterative scheme (4) to the canonical form of two-layer iterative schemes (2), we find:

$$(D + L)\left(y^{k+1} - y^k\right) + Ay^k = f, \ k = 0,1,2,... , \ y^0 \in H. \tag{5}$$

When comparing schemes (2) and (5), it can be seen that they will be identical at $B = D + L$, $\tau_{k+1} = 1$. Scheme (5), as well as scheme (2), will be implicit, and the operator is not self-adjoint in space H (here the operator B corresponds to the lower triangular matrix).

To accelerate the convergence of the Seidel method, it is modified by introducing a numerical parameter ω, into the iterative scheme (5), so that:

$$(D + \omega L)\frac{y^{k+1} - y^k}{\omega} + Ay^k = f, \ k = 0,1,2,... , \ y^0 \in H. \tag{6}$$

For scheme (6), the iterative method is the Successive OverRelaxation, (SOR).

The identity of schemes (6) and (2) can be observed at $B = D + \omega L$, $\tau_{k+1} = \omega$. As in the case of using the Seidel method, the matrix corresponds to the lower triangular matrix. Therefore, the introduction of the parameter ω does not take us out of the class of triangular iterative methods. The implementation of one iterative step of the scheme (6) is carried out with approximately the same cost of arithmetic operations as in the scheme (5).

Sufficient conditions for convergence of the considered schemes (5), (6) are self-conjugacy and positive definiteness of the operator A in space H [5]. In the following statement, we assume these conditions for the operator A to be fulfilled.

2. Symmetrization of Seidel and Successive OverRelaxation methods. Consider the Dirichlet difference problem for an elliptic equation. For simplicity, let's take the Dirichlet problem for the Poisson equation.

Let on a rectangular grid:

$$\omega_h = \left\{ x_{ij} = (ih_1, jh_2),\ i = 1,...,N_1,\ j = 1,...,N_2,\ h_\alpha = \frac{l_\alpha}{N_\alpha},\ \alpha = 1,2 \right\},$$

entered in a rectangle $\overline{G} = \{0 \le x_\alpha \le l_\alpha,\ \alpha = 1,2\}$, is required to find a solution to the difference problem:

$$\begin{cases} \sum_{\alpha=1}^{2} y_{\bar{x}_\alpha x_\alpha} = f(x), \quad x \in \omega_h, \\ y(x) = g(x), \quad x \in \gamma, \end{cases} \tag{7}$$

where $f(x)$ and $g(x)$ are the given functions, γ is the boundary of the grid ω_h, $\omega_h = \overline{\omega}_h \setminus \gamma$.

When solving system (7) by the Seidel method or the Successive OverRelaxation method, calculations begin at a point $x_{N_1N_2} = x_{ij}(i = N_1, j = N_2)$ and are carried out along the rows or columns of the calculated grid ω_h to a point $x_{N_1N_2} = x_{ij}(i = N_1, j = N_2)$ (the image of the grid layout is not given due to the evidence of its representation). Then the calculations start from the starting point and repeat until a solution is reached. The main idea of symmetrization of iterative methods is to add a new solution vector. Here, after the calculation is made from point x_{11} to point x_{N1N2}, it will continue further from point x_{N1N2} to point x_{11} in reverse order along the columns or rows of the grid and then repeat from the starting point.

We construct symmetrized variants of the Seidel and Successive OverRelaxation methods under the assumption that a rectangular grid with equal numbers of nodes in each of the coordinate directions is used. Let C be a matrix of permutations of size $N \times N$ ($N = N_1 = N_2$), of the form:

$$C = \begin{pmatrix} 0 & 0 & ... & 0 & a_{1N} \\ 0 & 0 & ... & a_{2N-1} & 0 \\ ... & ... & ... & ... & ... \\ 0 & a_{N-12} & ... & 0 & 0 \\ a_{N1} & 0 & ... & 0 & 0 \end{pmatrix}.$$

The iterative scheme (5) as a result of the symmetrization of the Seidel method takes the form:

$$(D + L)\left(y^{k+1} - y^k\right) + Ay^k = f,\ y^0 \in H,\ k = 0,1,2,... , k_1, \tag{8}$$

$$(D + L)C\left(y^{k+1} - y^k\right)C + ACy^kC = f,\quad y^0 = y^{k_1},\ k = k_1 + 1, k_1 + 2,... . \tag{9}$$

Sufficient convergence conditions of schemes (8)–(9) for the symmetrized Seidel method are determined from the constraints imposed on the operator (as mentioned earlier, this is a self-adjoint and positive definite operator).

Let's proceed to the construction of Symmetric Successive OverRelaxation (SSOR).

The iterative scheme (6) as a result of symmetrization takes the form:

$$(D + \omega L)\frac{y^{k+1} - y^k}{\omega} + Ay^k = f,\ y^0 \in H,\ k = 0,1,2,... , k_1, \tag{10}$$

$$(D + \omega L)C\frac{y^{k+1} - y^k}{\omega}C + ACy^kC = f,\quad y^0 = y^{k_1},\ k = k_1 + 1, k_1 + 2,... . \tag{11}$$

Sufficient convergence conditions of schemes (10)–(11) for the symmetrized Successive OverRelaxation method at any initial approximation are inherited by sufficient convergence conditions of schemes (8)–(9). However, in addition to these restrictions, an additional condition imposed on the iterative parameter is required: ω: $0 < \omega < 2$ [5].

3. Complete symmetrization of the Seidel method and the Successive OverRelaxation method. The idea of complete symmetrization methods is close to the methods of ordinary symmetrization. However, when solving problem (7) by the method of complete symmetrization, iterations can start from any corner of a rectangular grid ω_h and calculations are performed in rows or columns (i.e., either from point x_{11} to point $x_{N_1-1N_2-1}$, or from point $x_{N_1-1N_2-1}$ to point x_{11}, or from point x_{1N_2-1} to point x_{N_1-11}, or from point x_{N_1-11}, to point x_{1N_2-1}).

The difference scheme corresponding to the complete symmetrized Seidel method can be represented as:

$$(D + L)\left(y^{k+1} - y^k\right) + Ay^k = f_1,\ y^0 \in H,\ k = 0,1,2,... , k_1, \tag{12}$$

$$(D+L)\left(y^{k+1}-y^{k}\right)+Ay^{k}=f_1,\ y^0\in H,\ k=0,1,2,\dots,\ k_1, \tag{13}$$

$$(D+L)C\left(y^{k+1}-y^{k}\right)+ACy^{k}=f,\quad y^0=y^{k_1},\ k=k_1+1,k_1+2,\dots\ k_2. \tag{14}$$

$$(D+L)C\left(y^{k+1}-y^{k}\right)C+ACy^{k}C=f,\quad y^0=y^{k_3},\ k=k_3+1,k_3+2,\dots\ . \tag{15}$$

Sufficient conditions for convergence of schemes (12)–(15) for a complete symmetrized Seidel method are determined from the constraints imposed on the operator A.

The difference scheme corresponding to the Complete Symmetric Successive OverRelaxation method can be represented as:

$$(D+\omega L)\frac{y^{k+1}-y^{k}}{\omega}+Ay^{k}=f,\ y^0\in H,\ k=0,1,2,\dots,\ k_1, \tag{16}$$

$$(D+\omega L)C\frac{y^{k+1}-y^{k}}{\omega}+ACy^{k}=f,\quad y^0=y^{k_1},\ k=k_1+1,k_1+2,\dots\ k_2. \tag{17}$$

$$(D+\omega L)\frac{y^{k+1}-y^{k}}{\omega}C+Ay^{k}C=f,\quad y^0=y^{k_2},\ k=k_2+1,k_2+2,\dots\ k_3. \tag{18}$$

$$(D+\omega L)C\frac{y^{k+1}-y^{k}}{\omega}C+ACy^{k}C=f,\quad y^0=y^{k_3},\ k=k_3+1,k_3+2,\dots\ . \tag{19}$$

Sufficient convergence conditions of the Complete Symmetric Successive OverRelaxation method coincide with sufficient convergence conditions of the complete symmetrized Seidel method, and a restriction on the iterative parameter is added: ω: $0 < \omega < 2$.

Results. We illustrate the calculation results using the described methods on a grid ω_h at $N = N_1 = N_2$.

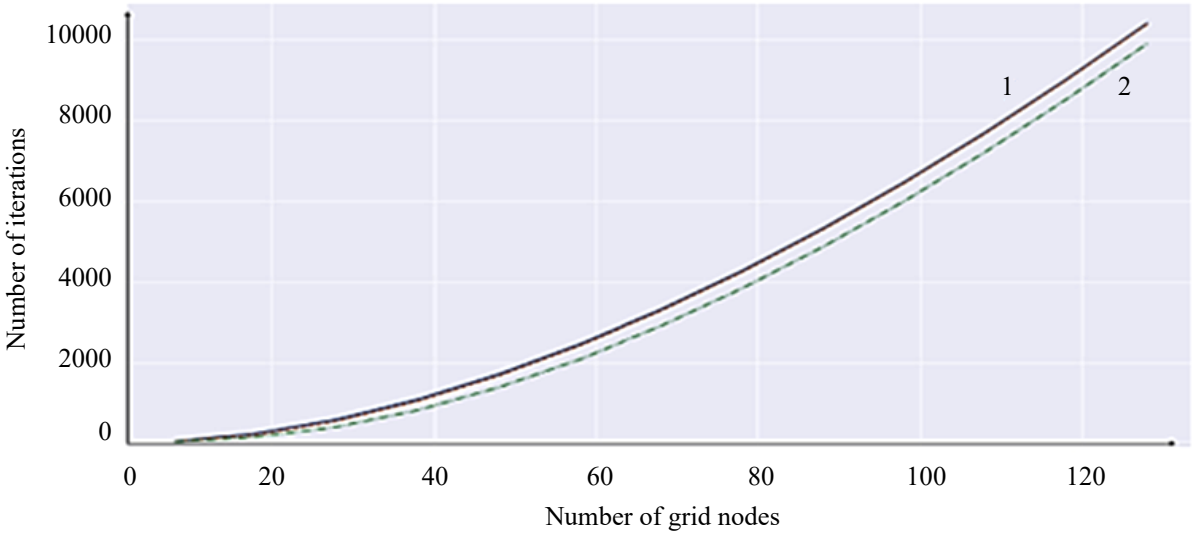

Fig. 1. Graph of the dependence of the number of iterations on the number of grid nodes when solving the problem using: 1 — the Seidel method and the symmetrized Seidel method (the lines coincide);
2 — the complete symmetrized Seidel method

The problem is solved:

$$\begin{cases}\sum\limits_{\alpha=1}^{2} y_{\bar{x}_\alpha x_\alpha}=f(x), & x\in\omega_h,\\ y(x)=0, & x\in\gamma.\end{cases} \tag{20}$$

The function of the right part $f(x)$ was chosen in such a way that $y(x) = x_1(x–x_1)x_2(x–x_2)$ is an exact solution to the problem (20).

For the Symmetric Successive OverRelaxation method and the Symmetric Successive OverRelaxation method, the iterative parameter ω was chosen according to the formula [5]:

$$\omega=\frac{2}{1+\sin(\pi/n)}.$$

The calculations are performed until the accuracy $\varepsilon = 10^{-4}$ is reached, where $\varepsilon = \frac{\left\|r^{N(\varepsilon)}\right\|_C}{\left\|r^0\right\|_C}$, $\left\|r^{N(\varepsilon)}\right\|_C$ is the grid norm C of the discrepancy at the final iteration, at which the specified accuracy is achieved, $\left\|r^0\right\|_C$ is the norm from the initial discrepancy.

Figures 1 and 2 show the results of calculations related to the solution of problem (20) using the considered iterative methods. The dependence of the number of grid nodes on the number of iterations required to achieve the required accuracy is demonstrated ε.

In accordance with the graphs (Fig. 1), a slight decrease in the required number of iterations for the symmetrized Seidel method should be noted. The complete Symmetric Successive OverRelaxation method requires significantly fewer iterations compared to its unsymmetrized counterpart. In terms of the costs of arithmetic operations per iteration, the basic methods and their symmetrized analogues differ slightly.

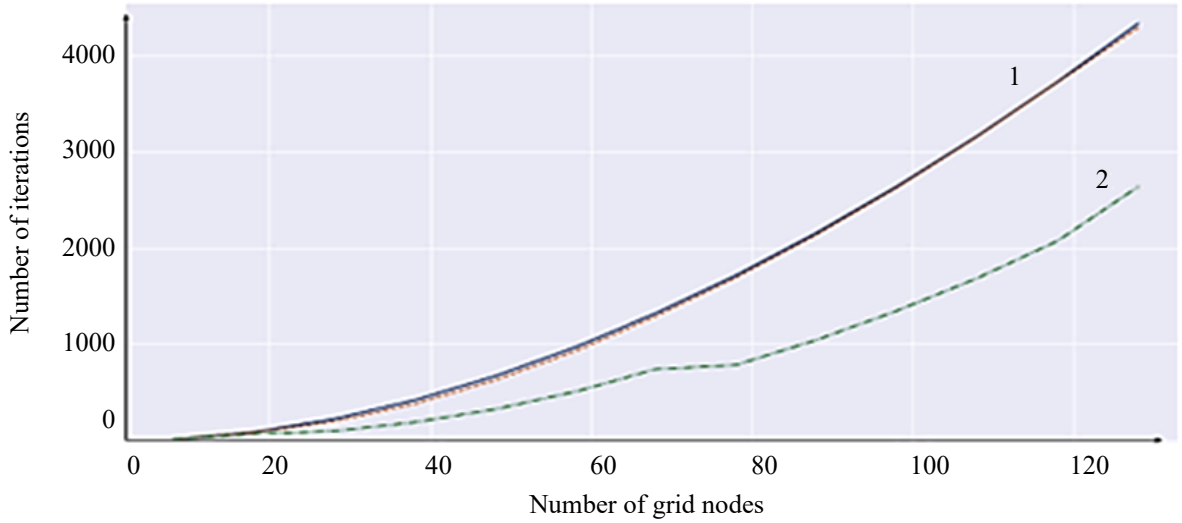

Fig. 2. Graph of the dependence of the number of iterations on the number of grid nodes when solving the problem using: 1 — the Successive OverRelaxation and the Symmetric Successive OverRelaxation method (the lines coincide); 2 — the complete Symmetric Successive OverRelaxation method

This is confirmed by a comparative analysis of the data obtained, shown in Table 1.

Table 1

Calculation results using various iterative methods

Iterative method	$N = 32$	$N = 64$	$N = 128$
Seidel method	757	2947	10420
Symmetrized Seidel method	714	2914	10400
Complete symmetrization of the Seidel method	538	2550	9914
Successive OverRelaxation method	281	1131	4335
Symmetric Successive OverRelaxation method	253	1111	4293
Complete Symmetric Successive OverRelaxation method	101	521	2637

Discussion and Conclusions. The article proposes methods of symmetrization for the Seidel and the Successive OverRelaxation methods. The use of a complete Symmetric Successive OverRelaxation method can significantly reduce the number of iterations required to achieve a given accuracy. It helps to halve the required number of iterations without additional computational costs. This work has practical significance. The developed software tool makes it possible to use it to solve specific physical problems, including as an element of a software package [6–9].

References

1. Meligy ShA, Youssef IK. Relaxation parameters and composite refinement techniques. *Results in Applied Mathematics.* 2022;15(1):100282. https:doi.org/10.1016/j.rinam.2022.100282

2. Weiss R, Podgajezki I, Hafner H, et al. Iterative methods for solving systems of linear equations, from the past to the future. *Mathematical modelling*. 2001;13(2):39–50.

3. Saw BC, Man S, Bairagi A, et al. Gauss-Seidel and Sor Methods for Solving Intuitionistic Fuzzy System of Linear Equations. *Computer Sciences & Mathematics*. 2023;7(1):47.

4. Allahviraloo T. Successive over relaxation iterative method for fuzzy system of linear equations. *Applied Mathematics and Computation.* 200;162(1):189–196. https:/doi.org//10.1016/j.amc.2003.12.085

5. Samarskiy AA, Nikolaev ES. *Methods for solving grid equations*. Moscow: Nauka; 1978. 592 p.

6. Sidoryakina VV. Efficient algorithms for the numerical solution of the coupled sediment and suspended matter transport problems in coastal systems. In: *Proceedings of the 21st International Workshop on Computer Science and Information Technologies (CSIT 2019) Series: Atlantis Highlights in Computer Sciences*. 2019;(3):243–248. https://doi.org/10.2991/csit-19.2019.42

7. Sukhinov AI, Sukhinov AA, Sidoryakina VV. Uniqueness of solving the problem of transport and sedimentation of multicomponent suspensions in coastal systems structures. *Journal of Physics: Conference Series*. 2020;1479(1):012081. https://doi.org/10.1088/1742-6596/1479/1/012081

8. Sukhinov AI, Sidoryakina VV. About correctness of the suspension transport and sedimentation model, taking into account bottom relief changes. *Computational Mathematics and Information Technologies Electronic Journal.* 2018;2(2):76–90. https://doi.org/10.23947/2587-8999-2018-2-76-90

9. Sidoryakina VV, Sukhinov AI. Correctness study and numerical implementation of a linearized two-dimensional sediment transport problem. *Computational Mathematics and Mathematical Physics*. 2017;57(6):978–994. https://doi.org/10.7868/S0044466917060138

About the Authors:

Valentina V Sidoryakina, Associate Professor of the Department of Mathematics and Computer Science, Don State Technical University (1, Gagarin Sq., Rostov-on-Don, 344003, RF), Candidate of Physical and Mathematical Sciences, MathSciNet, eLibrary.ru, ORCID, ResearcherID, ScopusID, cvv9@mail.ru

Denis A Solomakha, 4th year Student of the Department of Mathematics and Computer Science, Don State Technical University (1, Gagarin Sq., Rostov-on-Don, 344003, RF), eLibrary.ru, solomakha.05@yandex.ru

Claimed contributorship:
all authors have made an equivalent contribution to the preparation of the publication.

Received 04.08.2023
Revised 29.08.2023
Accepted 30.08.2023

Conflict of interest statement
the authors do not have any conflict of interest.

All authors have read and approved the final manuscript.

Об авторах:

Сидорякина Валентина Владимировна, доцент кафедры математики и информатики, Донской государственный технический университет (344003, РФ, г. Ростов-на-Дону, пл. Гагарина, 1), кандидат физико-математических наук, MathSciNet, eLibrary.ru, ORCID, ResearcherID, ScopusID, cvv9@mail.ru

Соломаха Денис Анатольевич, студент 4 курса кафедры «Математика и информатика», Донской государственный технический университет (344003, РФ, г. Ростов-на-Дону, пл. Гагарина, 1), eLibrary.ru, solomakha.05@yandex.ru

Заявленный вклад соавторов:
все авторы сделали эквивалентный вклад в подготовку публикации.

Поступила в редакцию 04.08.2023
Поступила после рецензирования 29.08.2023
Принята к публикации 30.08.2023

Конфликт интересов
Авторы заявляют об отсутствии конфликта интересов.

Все авторы прочитали и одобрили окончательный вариант рукописи.

COMPUTATIONAL MATHEMATICS
ВЫЧИСЛИТЕЛЬНАЯ МАТЕМАТИКА

Original article

UDC 519.6

https://doi.org/10.23947/2587-8999-2023-7-3-20-27

Application of a Modification of the Grid-Characteristic Method using Overset Grids for Explicit Interface Description to Modelling the Relief of the Ocean Shelf

Vladislav O Stetsyuk

Moscow Institute of Physics and Technology (National Research University), 1A, build 1, Kerchenskaya St., Moscow, Russian Federation

stetsyuk@phystech.edu

Abstract

Introduction. The problem of modelling the propagation of elastic waves is of great practical importance when conducting seismic exploration. Based on it, a model of the environment under study is being built. At the same time, the quality of the constructed model is determined by the accuracy of solving the modelling problem, which ensures constantly increasing requirements for modelling accuracy. For accurate modelling, it is important to correctly describe and take into account the boundaries of the media. At the same time, the quality of the constructed model is determined by the accuracy of solving the modelling problem, which ensures constantly increasing requirements for modelling accuracy.

Materials and Methods. We have studied a modification of the grid-characteristic method on rectangular grids using overset grids to describe the interface of media of complex shape. This approach has previously been used to describe the earth's surface when conducting simulations on land. This paper describes its application in modelling the relief of the ocean shelf.

Results. The use of the overset grid reduces the modelling error, the number of parasitic waves and artifacts and makes it possible to get a more visual picture.

Discussion and Conclusions. Overset grids can be used to describe the interface of media in modelling seismic exploration of the ocean shelf. Their use makes it possible to increase the accuracy of modelling and reduce the number of artifacts compared to using only one grid.

Funding information: This work was funded by Russian Scientific Foundation (project no. 21-11-00139).

Keywords: grid-characteristic method, overset grid, chimera grid, shelf seismic exploration

For citation. Stetsyuk VO. Application of a modification of the grid-characteristic method using overset grids for explicit interface description to modeling the relief of the ocean shelf. *Computational Mathematics and Information Technologies.* 2023;7(3):20–27. https://doi.org/10.23947/2587-8999-2023-7-3-20-27

Научная статья

Применение модификации сеточно-характеристического метода с использованием наложенных сеток для явного выделения границы раздела сред при моделировании рельефа океанического шельфа

В.О. Стецюк

Московский физико-технический институт (национальный исследовательский университет), Российская Федерация, г. Москва, ул. Керченская, 1А, корп. 1

✉stetsyuk@phystech.edu

Аннотация

Введение. Задача моделирования распространения упругих волн имеет большое практическое значение при проведении сейсморазведки, поскольку на ее основе выполняется построение модели исследуемой среды. При этом качество построенной модели определяется точностью решения задачи моделирования, что обеспечивает постоянно возрастающие требования к точности моделирования. Для точного моделирования важно корректно описывать и учитывать границы раздела сред. При этом важным фактором остается ресурсоемкость используемого метода моделирования, поскольку использование менее ресурсоемких методов позволяет выполнить больше итераций расчета для инверсии или использовать сетки с меньшим шагом для повышения точности.

Материалы и методы. В данной работе рассматривается модификация сеточно-характеристического метода на прямоугольных сетках, использующая наложенные сетки для описания границы раздела сред сложной формы. Данный подход ранее использовался для описания поверхности земли при проведении моделирования на суше. В данной работе описывается его применение при моделировании рельефа океанического шельфа.

Результаты исследования. Использование наложенной сетки позволяет уменьшить погрешность моделирования, количество паразитных волн и артефактов и получить более наглядную картину.

Обсуждение и заключения. Наложенные сетки могут быть применены для описания границы раздела сред при моделировании сейсморазведки океанического шельфа. Их использование позволяет повысить точность моделирования и снизить количество артефактов по сравнению с использованием только одной сетки.

Финансирование: работа выполнена при финансовой поддержке Российского научного фонда (проект № 21-11-00139).

Ключевые слова: сеточно-характеристический метод, метод наложенных сеток, метод сеток-химер, шельфовая сейсморазведка

Для цитирования. Стецюк В.О. Применение модификации сеточно-характеристического метода с использованием наложенных сеток для явного выделения границы раздела сред при моделировании рельефа океанического шельфа. *Computational Mathematics and Information Technologies*. 2023;7(3):20–27. https://doi.org/10.23947/2587-8999-2023-7-3-20-27

Introduction. The elastic and acoustic wavespropagation in the medium is studied by many scientific and engineering disciplines. Among the most important practical tasks considered by these disciplines are seismic stability analysis, non-destructive defect detection and seismic exploration. Numerical modeling is widely used in solving all these problems. Two main types of modeling tasks can be distinguished — in fact, the task of moderating the propagation of wave disturbances in a medium with known properties (a direct task) and the task of constructing a model of the medium based on known characteristics of the source signal and receiver readings (an inverse problem). These tasks are not independent, the solution of the inverse problem usually relies on several iterations of solving the direct problem and making refinements to the model.

It is necessary to take into account its features and limitations, as well as the amount of computing resources it requires, when choosing a numerical method used for modeling. The finite element method, the finite difference method and the grid-characteristic method are widely used to simulate the propagation of mechanical waves.

The finite element method [1] uses non-structural meshes, most often tetrahedral, which makes it possible to describe with good accuracy the boundaries of the modeling area, as well as the inhomogeneities and joints between layers lying inside it. This method is based on the approximation of the desired function inside each of the cells using a given basis. It also makes it possible to describe absorbing boundary conditions well using the PML method [2]. Its main disadvantage is its high resource intensity.

The main idea of the finite difference method is to replace differentiation operations in the simulated equation with non-differential expressions determined by the difference scheme used. Finite-difference schemes usually use structural rectangular grids. Their advantage is low resource consumption with good accuracy [3].

The grid-characteristic method [4; 5] is in many ways similar to the finite difference method. Instead of directly replacing differentiation with a difference expression, he uses variable substitution, which allows him to move from the original equation to the transfer equation. This transfer equation is solved by searching for the characteristics along which the values are transferred. In this paper, a modification of the grid-characteristic method is used, in which, instead of using characteristics, the transfer equation is solved using difference schemes.

In cases when methods based on structural grids are used for modeling, and in the field of modeling there are boundaries of complex shape, there is a need to somehow adapt the method to describe them. In this paper, overset curved grids are used to describe curved boundaries. The choice of this method is due to its good accuracy and low resource consumption. Earlier in [6] it was shown how this method can be used to describe a free surface of a complex shape, and in this paper it is used to describe the interface of media.

Materials and methods

1. Physical model. The processes of wave propagation in elastic and acoustic media are studied. Let's first consider the elastic medium model. At a point with a radius vector $\bar{x}$ we denote the displacement vector at time t as $u(\vec{x},t)$. Newton's second law on the i axis will have the form [7]:

$$\rho\frac{\partial^2 u_i}{\partial t^2}-\sum_j \frac{\partial \sigma_{ij}}{\partial x_i}-f_i=0.$$

We assume that all offsets are small. Then we can write down Hooke's law:

$$\sigma_{ij}=\sum_{k=1,l=1}^{3,3} C_{ijkl}\,\in_{kl},$$

where C_{ijkl} is called the stiffness tensor, and ε_{ij} is the Cauchy–Green strain tensor:

$$\in_{i,j}=\frac{1}{2}\left(\frac{\partial u_i}{\partial x_j}+\frac{\partial u_j}{\partial x_i}+\sum \frac{\partial u_i}{\partial x_l}\frac{\partial u_j}{\partial x_l}\right)\approx\frac{1}{2}\left(\frac{\partial u_i}{\partial x_j}+\frac{\partial u_j}{\partial x_i}\right).$$

The tensors σ and ε are symmetric and, therefore, contain no more than 6 independent components each. The C_{ijkl} tensor is also symmetric, so the number of its independent components does not exceed 21, and it can be written in Voigt notation [8] as a 6×6 symmetric matrix. In this paper, only isotropic media are considered. In such environments, this matrix is further simplified and has the form [9]:

$$C_{\alpha\beta}=\begin{bmatrix}\lambda+2\mu & \lambda & \lambda & 0 & 0 & 0\\ \lambda & \lambda+2\mu & \lambda & 0 & 0 & 0\\ \lambda & \lambda & \lambda+2\mu & 0 & 0 & 0\\ 0 & 0 & 0 & \mu & 0 & 0\\ 0 & 0 & 0 & 0 & \mu & 0\\ 0 & 0 & 0 & 0 & 0 & \mu\end{bmatrix}.$$

You can enter the displacement velocity vector at point v as a derivative of the displacement vector in time. The system of equations will take the form:

$$\rho\frac{\partial\vec{v}}{\partial t}=(\nabla\cdot\sigma)^T+\vec{f},$$

$$\frac{\partial\sigma}{\partial t}=\lambda(\nabla\cdot\vec{v})\mathbf{I}+\mu\left(\nabla\otimes\vec{v}+\nabla\otimes\vec{v}\right)^T).$$

The parameters λ and μ are called Lame parameters.Together with the density, they set the properties of the medium at the point. The velocities of longitudinal and transverse waves can be expressed through them as follows:

$$c_p=\sqrt{\frac{\lambda+2\mu}{\rho}},$$

$$c_s=\sqrt{\frac{\mu}{\rho}}.$$

The continuity equation and the Euler equation are used to describe acoustic media. Denote the pressure, density and velocity at a point with a radius vector $\bar{x}$ в at time t as p_A (x,t), ρ_A (x,t) and vA (x,t) respectively. The equations have the following form [10]:

$$\frac{\partial \rho_A}{\partial t} + \nabla \cdot \left(\rho_A \vec{v}_A\right) = 0,$$

$$\frac{\partial \vec{v}_A}{\partial t} + \left(\vec{v}_A \nabla\right)\vec{v}_A = -\frac{1}{\rho_A}\nabla p.$$

In this paper, we consider problems in which the media are at rest before the propagation of wave disturbances. In addition, changes in pressure and density caused by wave propagation are assumed to be small compared to their values at rest. Denote the pressure and density at rest at the selected point as p_0 (x,t) and ρ_0 (x,t), and their changes caused by propagating waves, as $p(x,t)$ and $\rho(x,t)$. In the assumptions above, the equations of the acoustic medium can be reduced to this form:

$$\frac{\partial v}{\partial t} + \frac{1}{\rho_0}\nabla p = 0,$$

$$\frac{\partial p}{\partial t} + \rho_0 c^2 \nabla \cdot \vec{v} = 0.$$

In the approximation used, the propagation of acoustic waves can be considered as a special case of the propagation of elastic waves in a medium where only *P*-waves propagate. The parameters of such an elastic medium will be set by the following relations:

$$c_p = c\sqrt{\frac{\lambda}{\rho}},$$

$$c_s = 0,$$

$$\mu = 0.$$

2. Grid-characteristic method. Consider the application of the grid-characteristic method for solving equations describing an elastic medium. Let's collect all the unknowns in these equations into one vector [11]:

$$q = [v_1, v_2, v_3, \sigma_{11}, \sigma_{22}, \sigma_{33}, \sigma_{23}, \sigma_{13}, \sigma_{12}].$$

Let's put the derivatives for each of the coordinates together. We obtain a matrix equation of the following form:

$$\frac{\partial}{\partial t}\mathbf{q} - \mathbf{A_1}\frac{\partial}{\partial x_1}\mathbf{q} - \mathbf{A_2}\frac{\partial}{\partial x_2}\mathbf{q} - \mathbf{A_3}\frac{\partial}{\partial x_3}\mathbf{q} = 0.$$

We will perform splitting by spatial coordinates [12], that is, we will divide one system into three different ones, one for each axis. Since initially the system of equations is hyperbolic, it is possible to perform diagonalization of matrices A_i:

$$\mathbf{A}_i = \mathbf{\Omega}_i^{-1}\mathbf{\Lambda}_i\mathbf{\Omega}_i,$$

where $\mathbf{\Lambda}_i$ is a diagonal matrix consisting of eigenvalues $\mathbf{A}_i$, and $\mathbf{\Omega}_i$ consists of columns equal to eigenvectors $\mathbf{A}_i$.

Next, you can replace the variable $\omega_i = \Omega_i q$, after which the systems along the axes will take the form:

$$\frac{\partial}{\partial t}\omega_i + \mathbf{\Lambda}_i\omega_i = 0.$$

Since the matrices $\mathbf{\Lambda}_i$ are diagonal, we are actually dealing with a set of separate transfer equations for each of the components ω_i. These individual transfer equations can be solved using the method of characteristics [4], but in this paper finite-difference schemes are used to solve them.

Thus, the time step of modeling occurs as follows: first, a transition to new variables and transfer equations is performed, then a time step is performed in these variables, after which a reverse replacement is performed and new values of the original variables in the grid nodes are calculated.

3. The method of overset grids. The method of overset grids, first described in [13], allows us to combine the advantages of using curved grids, which make it possible to describe well the boundaries of complex shapes with low resource consumption of structural grids. When using this method, the main grid is first constructed — a large structural grid covering the entire modeling area. After that, the areas near the borders that need to be described are covered with separate curved grids of smaller size. If the areas covered by overset grids make up an insignificant part of the entire modeling area, then the share of computing resources spent on calculation in overset grids is insignificant, that is, the addition of overset grids in this case does not lead to a noticeable increase in the resource intensity of the calculation.

When using overset grids, the time step of modelling is performed in two stages. First, a time step is performed independently on each of the grids. After that, the values are transferred between the grids. In areas that are covered by overset grids, the values in the nodes of the main grid are overwritten by the values from the corresponding overset grids. For each of the overset grids, several nodes closest to the boundary of the layers along all axes are called ghost nodes (phantom nodes). The values in these nodes are not used to calculate new values in the nodes of the main grid, but on the contrary, the values in them are overwritten by the values from the main grid [6]. The number of phantom node layers used is determined based on the difference scheme used, in our case it is equal to two, since a five-point difference scheme is used.

Since the nodes of the main and overset grids do not match, and for each grid at each time, the function values are known only in the nodes, interpolation is used to calculate new values during rewriting. Since there are no changes in the geometry of the computational domain in the problems considered in this paper, the grid nodes remain stationary during the calculation. This allows you to transfer part of the calculations required for interpolation to the preprocessing stage to save computing resources during the calculation. During this preprocessing, for all nodes of the main grid, the values in which will be overwritten, there are nodes of the overset grid, the values in which will participate in the calculation of new values in the node of the main grid and the summation weight, and, conversely, for the phantom nodes of the overset grids, the source nodes of the values from the main grid and their weights are searched. Thus, only weighted summation with known coefficients is performed during the calculation.

Commonly used methods of multidimensional interpolation include the nearest neighbor method, the inverse distance method [14], the natural neighborhood method (also known as the Sibson method [15]) and local basis decomposition methods. In the calculation in this paper, the method of local decomposition by radial type functions (Radial Basis Function, RBF) was used.

Computational experiment. The propagation of wave disturbances from a point source was simulated. The size of the simulated area was 1080×1320 meters, the upper boundary of the area coincided with the water surface, and the lower one was at a depth of 720 meters. The source of the disturbances was located near the water surface. Receivers were also located near the surface. The depth map was taken from the dataset [16]. The density of the shelf medium was assumed to be equal to 2400 kg /m^3, the velocities of longitudinal and transverse waves in it were 2850 m/s and 1650 m/s, respectively. The speed of waves in the water was assumed to be equal to 1500 m/ s, and the density of water was 1050 kg /m^3. The Riker pulse was used as the source signal. The time step of the simulation was 1 ms.

Two main approaches to modelling this area were considered. In the first approach, only one rectangular grid of 180×220×120 nodes with a step of 6 meters along all axes was used. Depending on whether the nodes are above or below the bottom surface, they were assigned the physical properties of the water or the bottom material. When using this approach, the interface of the media actually had a ladder structure. In the second approach, an additional curved grid of 192×234×11 nodes with a step of about 6 meters was used to describe the interface of the media, the shape of which repeated the interface. Figure 1 shows an illustration of the description of the interface in these ways is shown in Figure 1.

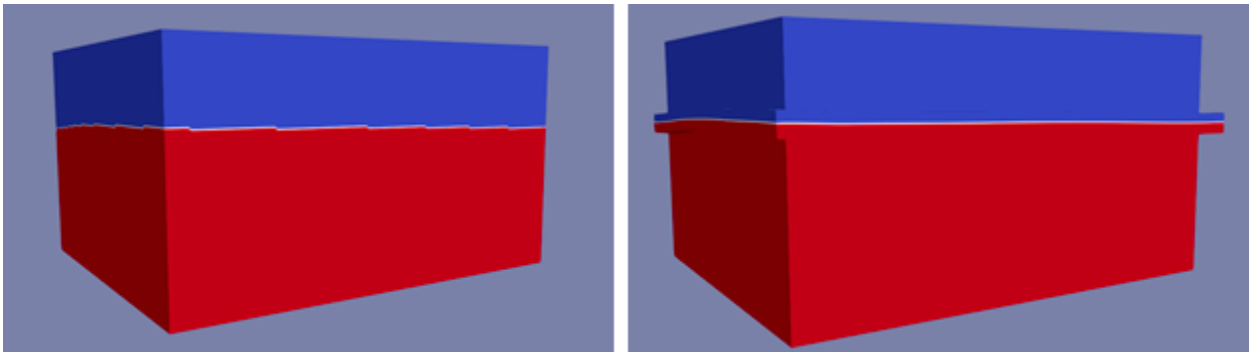

a) *b)*

Fig. 1. Modelling of the interface:
a) without using overset grid; b) using overset grid

In this case, there are two ways to use overset grids. You can use two overset grids, each of which will be on one side of the border and set a contact condition between them, or you can limit yourself to one grid in which there will be nodes with different properties. In this experiment, the second approach was used, since nodes with different properties are still present in the main grid, but if the areas on different sides of the border were described by two different main grids, then using the first approach would be preferable.

Results. Using the receiver readings obtained during the simulation, synthetic seismograms of the vertical component of the displacement velocity were constructed (Fig. 2).

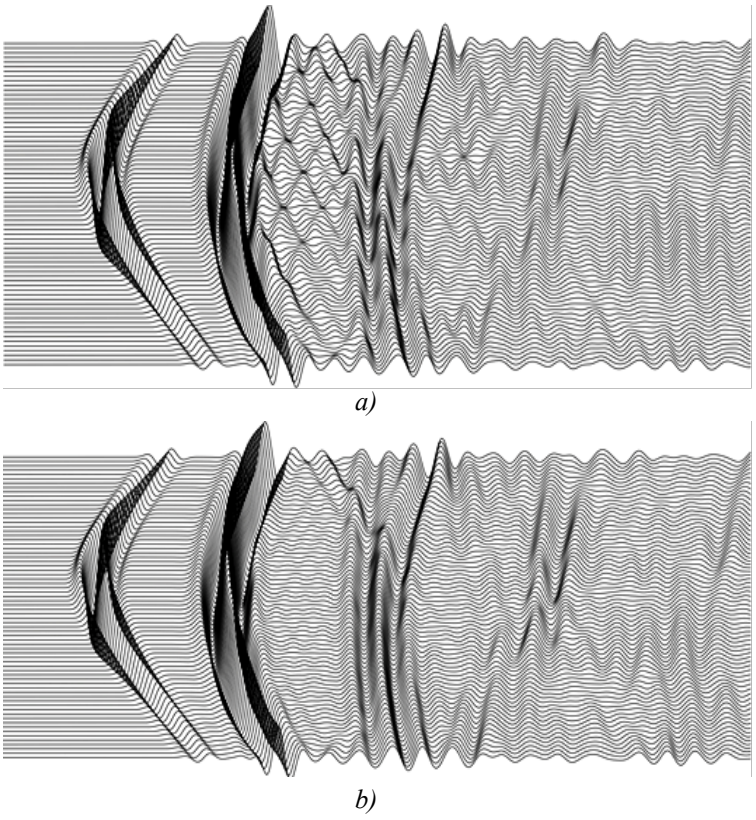

a)

b)

Fig. 2. Synthetic seismograms of the vertical component of the displacement velocity:
a) without using overset grid; b) using overset grid

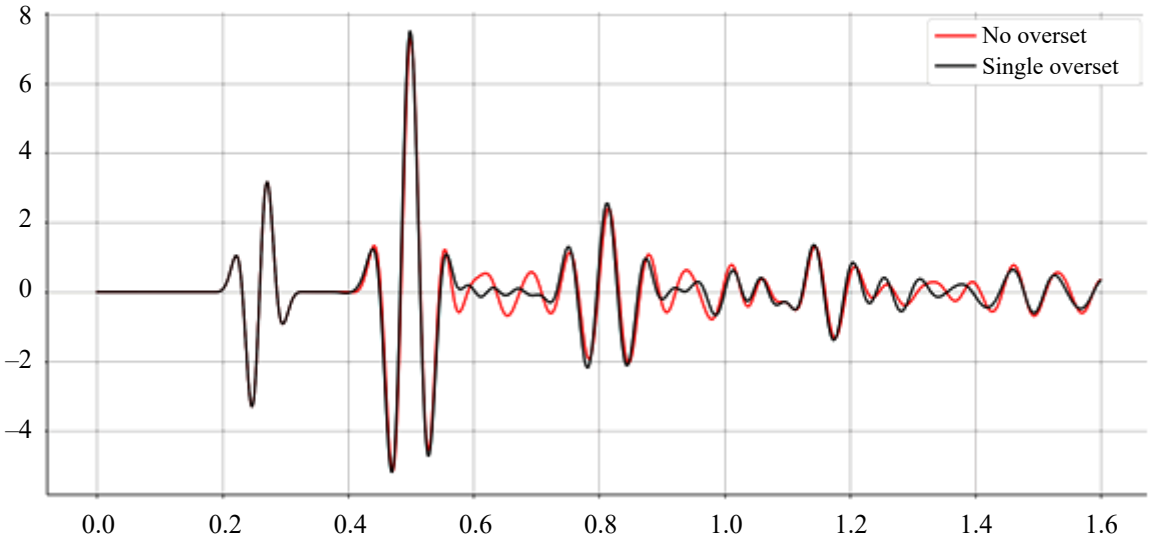

Fig. 3. Comparison of seismogram readings on one receiver

It can be seen that these seismograms are qualitatively the same, but on the seismogram, which was built using a overset grid to describe the interface of the media, the waves are visible better, and the number of artifacts and noise is less. Figure 3 shows a comparison of the readings of one of the receivers.

This comparison also confirms the conclusion made: the use of the overset grid makes it possible to reduce the modelling error, the number of parasitic waves and artifacts and get a more visual picture.

At the same time, the increase in the calculation time when adding the overset grid was insignificant and did not exceed 10 % of the calculation time using a single grid.

Discussion and Conclusions. In this study, it is shown that overset grids, previously used to isolate a free boundary when modelling near the earth's surface on land, can also be used to describe the interface of media when modelling seismic exploration of the ocean shelf. Their use makes it possible to increase the accuracy of modelling and reduce the number of artifacts compared to using only one grid. At the same time, the use of overset grids does not lead to a significant increase in the resource intensity of the computing complex. In addition, the overset grids do not require modification of the main computational grid or significant changes to the modelling process. From this we can conclude that the use of overset grids in such tasks is often justified, since it allows you to increase accuracy with little cost.

The proposed method can also be used to describe the boundaries of geological layers in a solid medium, since there is no fundamental difference between these tasks. However, additional modifications of the method may be required there to take into account cases when several interface boundaries meet at one point. The study of this issue has not yet been conducted, but it can serve as a topic for subsequent works.

References

1. Zienkiewicz OC, Taylor RL, Robert L, et al. *The finite element method : its basis and fundamentals*. 7th ed. Elsevier, 2013. 756 p.

2. Komatitsch D, et al. A perfectly matched layer absorbing boundary condition for the second-order seismic wave equation. *Geophysical Journal International*. 2003;154(1):146–153. https://doi.org/10.1046/J.1365-246X.2003.01950.X

3. Zang N, Zhang W, Chen X. An overset-grid finite-difference algorithm for simulating elastic wave propagation in media with complex free-surface topography. *Geophysics*. 2021:86(4):1–97. https://doi.org/10.1190/geo2020-0915.1

4. Magomedov KM, Kholodov AS. On the construction of difference schemes for hyperbolic equations based on characteristic relations. *Journal of Computational Mathematics and Mathematical Physics*. 1969;9(2):158–176. (In Russ.). https://doi.org/10.1016/0041-5553(69)90099-8

5. Magomedov KM, Kholodov AS. *Grid-characteristic numerical methods*, 2nd ed. Moscow: Yurayt, 2023. 313 p. (In Russ.).

6. Khokhlov NI, Stetsyuk VO, Mitskovets IA. Overset grids approach for topography modelling in elastic-wave modelling using the grid-characteristic method. *Computer Research and Modelling*. Institute of Computer Science. 2019;11(6):1049–1059. https://doi.org/10.20537/2076-7633-2019-11-6-1049-1059

7. Novatsky V. *Theory of elasticity*. Moscow: Mir, 1975. 872 p. (In Russ.).

8. Voigt W. *Lehrbuch der kristallphysik (mit ausschluss der kristalloptik)*. Leipzig; Berlin: B.G. Teubner, 1910. 998 p.

9. Landau LD, Lifshits EM. Theoretical physics, in 10 vols. *Theory of Elasticity*, 5th ed., by DA Mirtov (ed.). Moscow: Fizmatlit, 2003. Vol. 7. 264 p. (In Russ.).

10. Landau LD, Lifshits EM. Theoretical physics. Textbook, in 10 t. *Hydrodynamics*, 6th ed., by LP Pitaevsky (ed.). Moscow: Fizmatlit, 2015. Vol. 6. 728 P.

11. Favorskaya AV, et al. Modelling the wave phenomena in acoustic and elastic media with sharp variations of physical properties using the grid-characteristic method. *Geophys Prospecting*. Blackwell Publishing Ltd, 2018;66(2):1485–1502. https://doi.org/10.1111/1365-2478.12639

12. LeVeque RJ. *Finite Volume Methods for Hyperbolic Problems*. Cambridge University Press, 2002. https://doi.org/10.1017/CBO9780511791253

13. Benek JA, Steger JL, Dougherty FC, et al. *Chimera: A Grid-Embedding Technique*. 1986. 300 p.

14. Shepard D. A two-dimensional interpolation function for irregularly-spaced data. In: *Proceedings of the 1968 23rd ACM National Conference, 27–29 August 1968*. New York, 1968. Pp. 517–524. https://doi.org/10.1145/800186.810616

15. Sibson R. A *Brief Description of Natural Neighbor Interpolation*, by V Barnett (ed.). Interpreting Multivariate Data, John Wiley & Sons, New York, 1981. Pp. 21–36.

16. Butman B, Danforth WW, Clark JH, et al. *Bathymetry and backscatter intensity of the sea floor of the Hudson Shelf Valley*. U.S. Geological Survey, 2017. https://doi.org/10.5066/F7C53J1Z

About the Author:

Vladislav O Stetsyuk, Assistant, Moscow Institute of Physics and Technology (National Research University), (bldg. 1, 1A, Kerchenskaya Street, Moscow, 117303, RF), Math-Net.Ru, stetsyuk@phystech.edu

Received 24.07.2023
Revised 16.08.2023
Accepted 17.08.2023

Conflict of interest statement
The author does not have any conflict of interest.

The author has read and approved the final manuscript.

Об авторе:
Стецюк Владислав Олегович, ассистент, Московский физико-технический институт (национальный исследовательский университет), (РФ, 117303, г. Москва, ул. Керченская, 1А, корп. 1), Math-Net.Ru, stetsyuk@phystech.edu

Поступила в редакцию 24.07.2023
Поступила после рецензирования 16.08.2023
Принята к публикации 17.08.2023

Конфликт интересов
Автор заявляет об отсутствии конфликта интересов.

Автор прочитал и одобрил окончательный вариант рукописи.

COMPUTATIONAL MATHEMATICS
ВЫЧИСЛИТЕЛЬНАЯ МАТЕМАТИКА

UDC 519.6
https://doi.org/10.23947/2587-8999-2023-7-3-28-38

Original article

Grid-characteristic Method using Superimposed Grids in the Problem of Seismic Exploration of Fractured Geological Media

Ivan A Mitkovets, Nikolay I Khokhlov

Moscow Institute of Physics and Technology (National Research University), 1A, build 1, Kerchenskaya St., Moscow, Russian Federation

k_h@inbox.ru

Abstract

Introduction. Seismic exploration in conditions of heterogeneity of the environment is an urgent topic for the oil and gas industry. Consequently, the development of numerical methods for solving the direct problem of seismic exploration remains relevant as a necessary link in the development and improvement of methods for solving the inverse problem. The Schonberg thin crack model has performed well in the numerical solution of problems requiring explicit consideration of geological inhomogeneities.

Materials and Methods. In this paper, we consider a modification of the grid-characteristic method using superimposed grids. The presented approach makes it possible to conduct computational experiments, explicitly taking into account fractured inhomogeneities with arbitrary spatial orientation. For this, in addition to the basic regular computational grid, there is the concept of superimposed grids. Inhomogeneities, such as cracks, are described within the framework of the superimposed grid and, in turn, have no restrictions associated with the main grid. Thus, by performing an interpolation operation between the superimposed main grids, we can bypass the requirement of alignment of cracks and edges of the main grid.

Results. The proposed approach made it possible to study the dependence of the anisotropy of the seismic response of a fractured cluster on the dispersion of the angles of inclination of the cracks.

Discussion and Conclusions. A modification of the grid-characteristic method using superimposed grids is proposed to explicitly account for fractured inhomogeneities in a heterogeneous geological environment.

Funding information. The research was carried out at the expense of the grant of the Russian Science Foundation No. 21-11-00139. https://rscf.ru/project/21-11-00139/

Keywords: grid-characteristic method, superimposed grids, chimeric grids, seismics, seismic exploration, heterogeneous geological environment

For citation. Mitkovets IA, Khokhlov NI. Grid-characteristic method using superimposed grids in the problem of seismic exploration of fractured geological media. *Computational Mathematics and Information Technologies*. 2023;7(3):28–38. https://doi.org/10.23947/2587-8999-2023-7-3-28-38

Научная статья

Сеточно-характеристический метод с использованием наложенных сеток в задаче сейсморазведки трещиноватых геологических сред

И.А. Митьковец, Н.И. Хохлов

Московский физико-технический институт (национальный исследовательский университет), Российская Федерация, г. Москва, ул. Керченская, 1А, корп. 1

k_h@inbox.ru

Аннотация

Введение. Сейсморазведка в условия гетерогенности среды является актуальной темой для нефтегазовой промышленности. Следовательно, остается актуальным развитие численных методов решения прямой задачи сейсморазведки как необходимого звена при разработке и усовершенствовании методов решения обратной

задачи. Модель тонкой трещины Шонберга хорошо себя показала при численном решении задач, требующих явного учета геологических неоднородностей.

Материалы и методы. В данной работе авторы рассматривают модификацию сеточно-характеристического метода применением наложенных сеток. Представленный подход позволяет проводить вычислительные эксперименты, явно учитывая трещиноватые неоднородности с произвольной пространственной ориентацией. Для этого помимо основной регулярной вычислительной сетки водится понятие наложенных сеток. Неоднородности, такие как трещины, описываются в рамках наложенной сетки и, в свою очередь не имеют ограничений, связанных с основной сеткой. Таким образом, производя операцию интерполирования между наложенными основными сетками, мы можем обойти требование соосности трещин и ребер основной сетки.

Результаты исследования. Предлагаемый подход позволил произвести исследование зависимости анизотропии сейсмического отклика трещиноватого кластера от дисперсии углов наклона трещин.

Обсуждение и заключения. Предложена модификация сеточно-характеристического метода с применением наложенных сеток для явного учета трещиноватых неоднородностей в гетерогенной геологической среде.

Финансирование. Исследование выполнено за счет гранта Российского научного фонда № 21-11-00139. https://rscf.ru/project/21-11-00139/

Ключевые слова: сеточно-характеристический метод, наложенные сетки, химерные сетки, сейсмика, сейсморазведка, гетерогенная геологическая среда

Для цитирования. Митьковец И.А., Хохлов Н.И. Сеточно-характеристический метод с использованием наложенных сеток в задаче сейсморазведки трещиноватых геологических сред. *Computational Mathematics and Information Technologies.* 2023;7(3):28–38. https://doi.org/10.23947/2587-8999-2023-7-3-28-38

Introduction. Methods of search and exploration of oil and gas fields include an effective solution to the inverse problem of seismic exploration in a heterogeneous geological environment. This becomes inherently important, given that the known oil and gas deposits are gradually being exhausted, and in order to maintain the production level, it is necessary to search for new deposits or extract minerals from already developed deposits using modern methods. Often, potential sites are located in regions rich in fractured heterogeneities. Additionally, modern technologies for increasing production at the fields provide for the use of such a tool as hydraulic fracturing. Modern approaches to hydraulic fracturing based on multi-stage procedures open up opportunities for the resumption of production even in those fields that have been recognized as exhausted for many years. The geophysical information collected as a result of seismic exploration makes it possible to simulate the process of hydraulic fracturing, which is a critical element for adapting the technology to a specific field. Taking into account the location of existing cracks, as well as taking into account the fracture parameters (which can be determined using seismic exploration), it is possible to control the shape of the resulting rupture. Such control over the shape of the created crack is relevant because of the risk of traffic jams in the formed channels, which can lead to their blocking and, as a result, to a decrease in the efficiency of field operation. For the success of this kind of manipulation, the presence of an accurate picture of the structure of cracks and faults hidden under the earth›s surface is of paramount importance.

The data in the process of seismic exploration, obtained on a variety of seismic sensors located at an insignificant depth in the earth›s surface, are interpreted by modern methods of computational mathematics to recreate a model of the geological environment in the studied area. However, it is difficult to verify the results obtained in this way due to the lack of an opportunity to obtain a detailed and qualitative model of the geological environment by alternative methods. Thus, in order to develop the capabilities and accuracy of modern methods for solving the inverse problem of seismic exploration, it is critically important to develop the capabilities and accuracy of methods for solving the direct problem of seismic exploration.

Several techniques are known that take into account the presence of fractured structures when modeling the propagation of elastic perturbation waves in genuine geological formations. One of the most common is a mathematical approach based on the linear sliding model proposed by Schonberg (LSM), which was described in an article published in 1980 [1], and received further experimental confirmation in other sources [2–3]. Nevertheless, when modeling areas with faults, the use of anisotropic models [4] turns out to be most effective at large wavelengths, although it does not take into account most of the characteristics. An alternative method for modeling a zone with faults is the explicit approach [5], which has its advantages. Other techniques were also studied, including the addition of additional nodes, as shown in [6–7], as well as the use of additional computational grids to describe the wave propagation process inside the fault [8].

The authors present a new version of the grid-characteristic method [9], which uses the technique of overset grids. The first concepts of this approach were outlined in the source [10]. One of the initial works devoted to the application of overset (or adaptive) computational grids was the work of authors named Berger and Joseph [11], as well as Steger

and Benek [12–13]. The idea of using overset grids has been successfully developed and is currently being used to solve various problems, as shown in studies [14–18]. The innovativeness of the methodology proposed by the authors lies in the use of overset grids in solving the problems of seismic exploration of fractured areas and in organizing these grids around cracks in such a way that the Jacobian of the transformation tends to unity. In this study, the authors focus on 2D geological models.

Materials and Methods

1. The equation of elasticity. One of the key equations in the linear theory of elasticity is considered to be the Hooke equation, which provides a connection between the stress tensor and the strain tensor [19–20]. The equations of conservation of mass and momentum are also used to describe the process of wave propagation in a medium. A more complex representation of elastic media is possible using extended equations that take into account nonlinear and inhomogeneous characteristics of the medium. These equations may contain nonlinear relationships between stress and strain, and a variety of physical processes, such as anisotropy or energy dissipation, can also be taken into account. Within the framework of the study, a model of a linear elastic and isotropic medium was chosen to solve the generalized problem of modelling the propagation of a seismic wave in the ground. This model has been studied in a number of previous papers [21–24].

Newton's second law is fulfilled at each point of a linear elastic medium:

$$\rho \vec{\boldsymbol{v}}_t = \left(\nabla \cdot \mathbf{T}\right)^{\mathrm{T}}, \tag{1}$$

where $\mathbf{T}$ is Cauchy stress tensor, ρ is the density of the medium, $\boldsymbol{v}$ is the velocity of movement of the medium.

Hooke's law in tensor form has the form:

$$\mathbf{T} = \lambda tr\left(\varepsilon\right)\mathbf{I} + 2\mu\varepsilon, \tag{2}$$

$$\varepsilon = \frac{1}{2}\left(\nabla \otimes \boldsymbol{u} + \left(\boldsymbol{u} \otimes \nabla\right)^{\mathrm{T}}\right), \tag{3}$$

where $\boldsymbol{u}$ is the displacement tensor, $\mathbf{I}$ is the unit tensor, λ and μ are Lame parameters, the elastic deformation characteristics, ε is the strain tensor, $\otimes$ is the tensor product operator $\left(\nabla \otimes \boldsymbol{v}\right)_{i,j} = \nabla_i \boldsymbol{v}_j$.

Taking into account the effect of an external force $\vec{f}$, from equations (1)–(3) it is possible to obtain a system of equations for a linear elastic isotropic medium in the following form:

$$\mathbf{T} = \lambda\left(\nabla \cdot \vec{\boldsymbol{v}}\right)\mathbf{I} + \mu\left(\nabla \otimes \vec{\boldsymbol{v}} + \left(\nabla \otimes \vec{\boldsymbol{v}}\right)^{\mathrm{T}}\right), \tag{4}$$

$$\rho \vec{\boldsymbol{v}}_t = \left(\nabla \cdot \mathbf{T}\right)^{\mathrm{T}} + \vec{f}. \tag{5}$$

The system of equations (4) and (5) can be represented as a system of differential equations, here and further in the work we assume the absence of an external force:

$$\frac{\partial}{\partial t}\mathbf{T}_{ij} = \lambda\left(\sum_k \frac{\partial \upsilon_k}{\partial x_k}\right) I_{ij} + \mu\left(\nabla_i \upsilon_j + \nabla_j \upsilon_i\right), \tag{6}$$

$$\rho \frac{\partial}{\partial t}\boldsymbol{v}_j = \frac{\partial \mathbf{T}_{ji}}{\partial x_i}. \tag{7}$$

The system of differential equations of the theory of linear elasticity (6) and (7) can be represented in matrix form, which is convenient to use when studying the characteristic methods of computational mathematics. We introduce the notation $\vec{u} = (u_1, \ldots u_5)^T = (v_1, v_2, \boldsymbol{T}_{11}, \boldsymbol{T}_{22}, \boldsymbol{T}_{12})^T$, then the system of equations in the Cartesian coordinate system takes the form:

$$\frac{\partial u}{\partial t} + \mathbf{A_1}\frac{\partial \mathbf{u}}{\partial x_1} + \mathbf{A_2}\frac{\partial \mathbf{u}}{\partial x_2} = 0, \tag{8}$$

$$\mathbf{A_1} = -\begin{bmatrix} 0 & 0 & \rho^{-1} & 0 & 0 & 0 \\ 0 & 0 & 0 & 0 & 0 & \rho^{-1} \\ \lambda + 2\mu & 0 & 0 & 0 & 0 & 0 \\ \lambda & 0 & 0 & 0 & 0 & 0 \\ 0 & \mu & 0 & 0 & 0 & 0 \end{bmatrix}, \tag{9}$$

$$\mathbf{A}_2 = -\begin{bmatrix} 0 & 0 & 0 & 0 & 0 & \rho^{-1} \\ 0 & 0 & 0 & 0 & \rho^{-1} & 0 \\ 0 & \lambda & 0 & 0 & 0 & 0 \\ 0 & \lambda+2\mu & 0 & 0 & 0 & 0 \\ \mu & 0 & 0 & 0 & 0 & 0 \end{bmatrix}. \tag{10}$$

To describe the elastic properties of the medium, it is convenient to use sound wave velocities: longitudinal C_p and transverse C_s. The longitudinal velocity reflects the velocity of the wave in the direction of force, the transverse velocity in the perpendicular direction. They are calculated through the Lame parameters and the density of the medium as follows:

$$C_p = \sqrt{\frac{\lambda+2\mu}{\rho}}, \tag{11}$$

$$C_s = \sqrt{\frac{\mu}{\rho}}. \tag{12}$$

In this paper, the model of a two-shore thin Schonberg crack is used to simulate the propagation of elastic waves in the presence of cracks. In the case when the crack is oriented along the OY axis, the boundary conditions have the form:

$$\boldsymbol{T}^0_{xx} = \boldsymbol{T}^1_{xx},$$

$$\boldsymbol{T}^0_{xy} = \boldsymbol{T}^1_{xy},$$

$$\frac{\partial \boldsymbol{T}^0_{xx}}{\partial t} = K_T\left(v^1_x + v^0_x\right),$$

$$\frac{\partial \boldsymbol{T}^0_{xy}}{\partial t} = K_N\left(v^1_y + v^0_y\right).$$

where the indices 0 and 1 are used to mark the ratio of the magnitude to the left and right sides of the crack, respectively, K_T and K_N are the crack parameters, which in our case of a thin liquid-filled crack are equal:

$$K_T = \infty,$$
$$K_N = 0.$$

2. Grid-characteristic method. To obtain a numerical solution of a system of equations describing a linear elastic medium, a grid-characteristic method is used. This method was first presented in [25–27]. In the context of this study, which is limited to the numerical solution of a system of hyperbolic equations, it can be argued that for the matrix $\mathbf{A}_j$ there are always N eigenvalues and N linearly independent eigenvectors. This in turn confirms the possibility of the existence of an inverse matrix for $\mathbf{\Omega}_j$. Then, taking into account the splitting by components, equation (8) takes the form:

$$\frac{\partial \boldsymbol{u}}{\partial t} = \mathbf{\Omega}_j^{-1}\mathbf{\Lambda}_j\mathbf{\Omega}_j\frac{\partial \boldsymbol{u}}{\partial x_j}, j = 1,2, \tag{13}$$

where $\mathbf{\Omega}_j$ consists of columns that are the eigenvectors of the matrix $\mathbf{A}_j$, and $\mathbf{\Lambda}_j$ is a diagonal matrix consisting of the eigenvalues of the matrix $\mathbf{A}_j$. At the same time, $\mathbf{\Lambda}_j$ for any j has the same form:

$$\Lambda = \text{dia g}\sqrt{(\lambda+2\mu)/\rho}, -\sqrt{(\lambda+2\mu)/\rho}, \sqrt{\mu/\rho}, -\sqrt{\mu/\rho}, -\sqrt{\mu/\rho}, \ 0,0,0. \tag{14}$$

Taking into account expressions (11) and (12), equation (14) can be reduced to the form:

$$\Lambda = \text{diag}\{C_p, -C_p, C_s, -C_s, C_s, -C_s, 0,0,0\}.$$

Let's make a characteristic replacement of the variables $\boldsymbol{v} = \mathbf{\Omega}\boldsymbol{u}$ ($\boldsymbol{u} = \mathbf{\Omega}^{-1}\boldsymbol{v}$) in equation (13), b multiply on the left by the matrix $\mathbf{\Omega}^{-1}$:

$$\frac{\partial \boldsymbol{v}}{\partial t} + \Lambda\frac{\partial \boldsymbol{v}}{\partial x} = 0.$$

Thus, the calculation of the value for each element of the vector u at the subsequent time step, denoted as n+1, is carried out provided that the value of $\boldsymbol{v}^{(n+1)}$ is known: $\boldsymbol{u}^{n+1} = \mathbf{\Omega}^{-1}\boldsymbol{v}^{n+1}$.

3. Overset grids. Direct interpolation is carried out from the main grid to the external nodes of the overset grid at the start of each stage of the computational process, which is limited to a certain time step, after performing calculations in the nodes of the main computational grid. This action is necessary to take into account the changes in the intensity and vector displacement of the medium caused by the wave propagation process within the main grid. After that, new values are calculated in the nodes of the overset grid. At the end of each time step, reverse interpolation occurs from the nodes of the overset grid to the main one. This process ensures synchronization of changes that took place during this stage of calculations. This approach is due to the need to take into account the influence of various inhomogeneities represented in the overset grids when performing calculations at the next time stage [28].

The authors used the bilinear interpolation function to find the values of the desired functions at a point by the values of the function at four known points:

$$F_{x,y} = b_1 + b_2 x + b_3 y + b_4 xy.$$

Application of overset grids

1. Implementation. A continuous medium can be represented using a single basic rectangular grid when applying a overset grid to determine the position of an inclined crack . At the same time, cracks can be defined using overset grids, which are arranged according to the orientation of each individual crack. The method of calculating a straight crack on a regular rectangular grid and its application within the framework of the grid-characteristic method were described in detail in the scientific work [9]. It is important to note that the application of the overset grid is not mandatory to account for cracks that are coaxial with the edges of the main computational grid.

Figure 1 shows the location of the grids and cracks used, and the nodes of the overset grid involved in the interpolation between the grids are also indicated. In the figure, the borders of the main rectangular regular grid representing the environment are represented in black. The edges of the overset grid are highlighted in blue. Additional «ghost» nodes of the overset grid are marked in green, where interpolation from the main grid is performed. The orange color highlights the part of the nodes of the overset grid from where the interpolation occurs. The red line indicates the location of the crack.

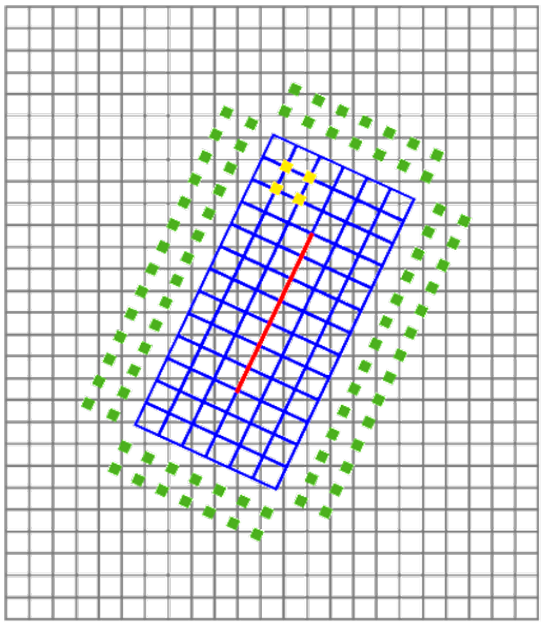

Fig. 1. Using the overset grid to account for the crack

2. Verification. To assess the accuracy of the proposed modification, we will compare the readings obtained on virtual receivers during the simulation of the interaction of an elastic wave with a crack. In one case, the crack coincides with the horizontal axis of the main grid, and in the other, it is rotated relative to this axis using the overset grid. To make such a turn, it is necessary to correctly process the data received from virtual receivers, as well as correctly rotate the crack and the receivers and the elastic wave source.

Figure 2 (a, b) shows the wave patterns at one of the time points for the compared productions, as well as the location of the receivers and the overset grid.

The initial conditions assumed the presence of elastic perturbations of the plane front, given by a Gaussian function with a width of 10 meters. The front of the initiated plane wave was rotated relative to the simulated crack by an angle of 30 degrees. The length of the thin crack was 52 meters. In the calculation using the overset grid, the wave-crack-receivers

system was rotated by an angle of 30 degrees. The receivers were placed on a line perpendicular to the simulated crack and passing through its center, at a distance of 30 meters from it. The longitudinal velocity of the elastic wave in the medium was C_p = 3000 м/с, the transverse velocity was C_s = 1500 м/с, the time step was dt = 0.0002 seconds, the spatial step of the grids was h= 2.0.

Figures 3 and 4, for receivers above the crack and behind it, respectively, show a comparison of the values of the components of the displacement velocity of the medium obtained as a result of the experiments described above.

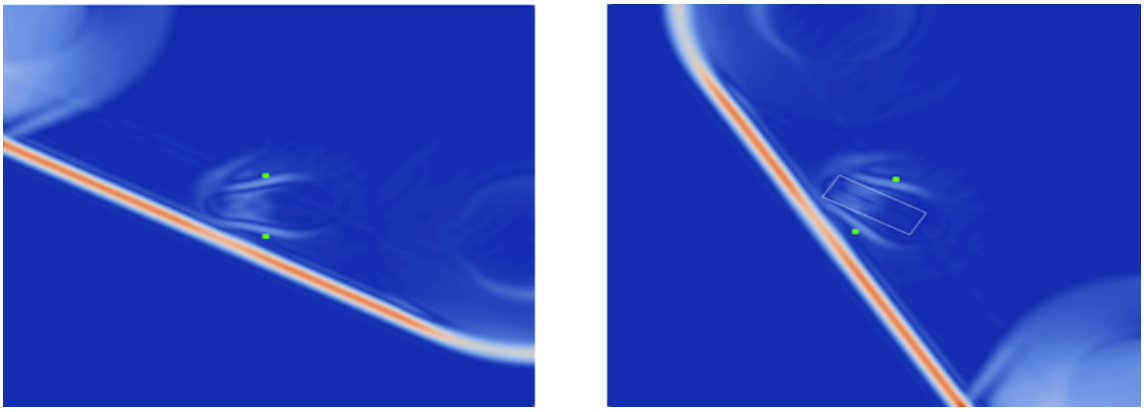

a) *b)*

Fig. 2. Wave patterns at one of the time points: a) without using the superimposed grid (the position of the receivers is marked in green); b) using the superimposed grid marked in white, green is receivers

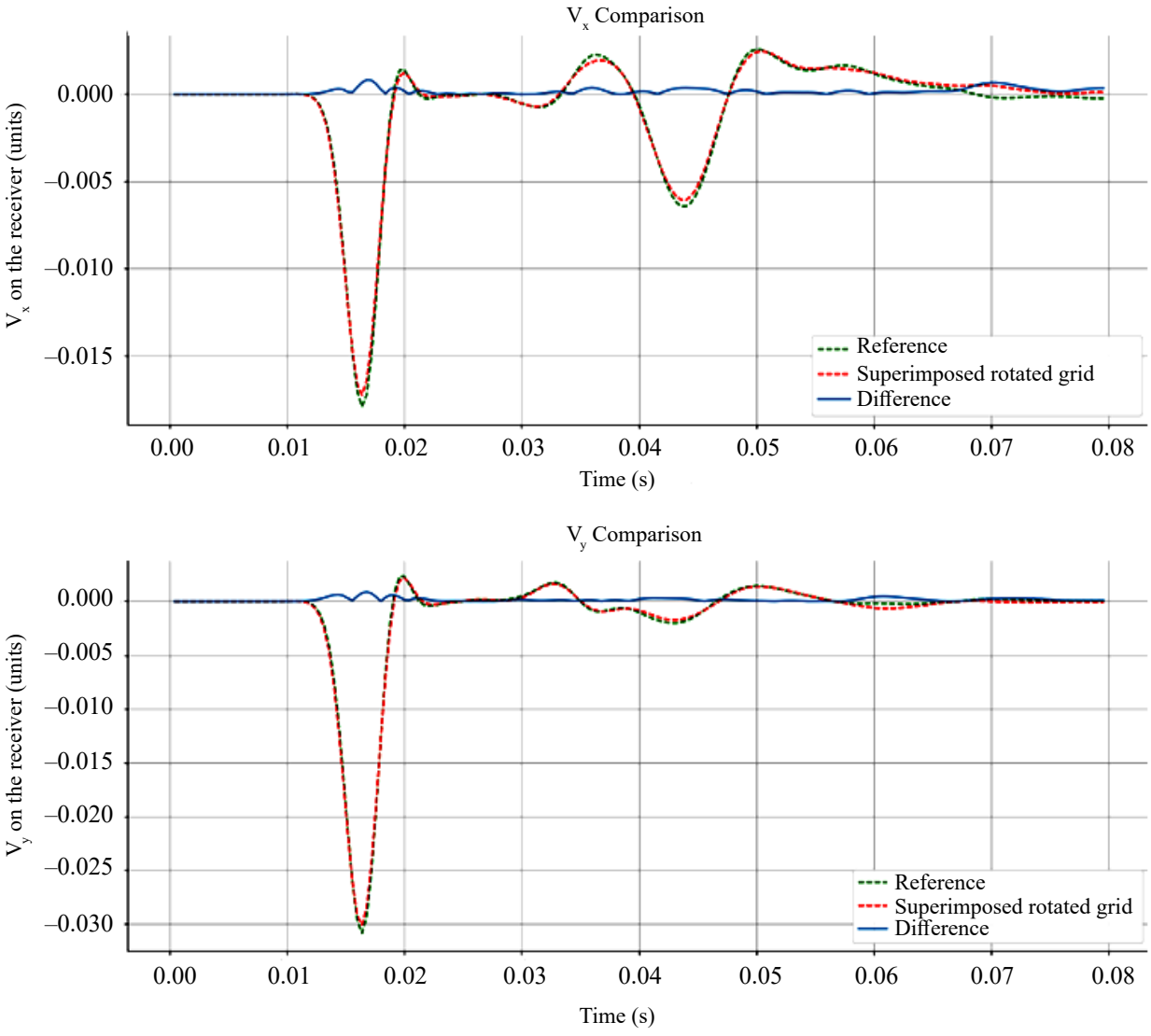

Fig. 3. Comparison of signals on receivers above the crack

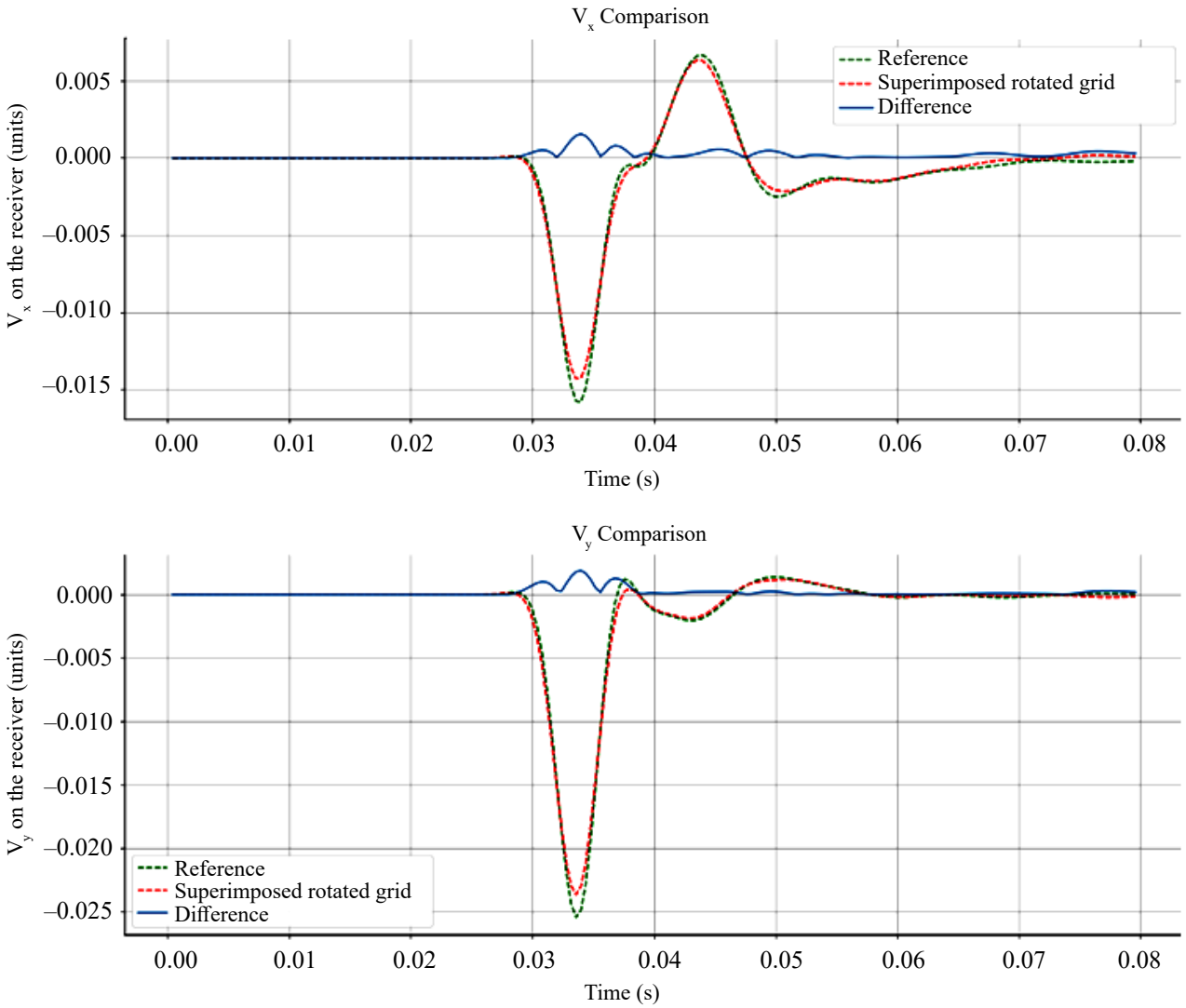

Fig. 4. Comparison of signals on receivers under the crack

Research results. The analysis of the anisotropy of the seismic response of a fractured cluster in an elastic geological medium, interconnected with the dispersion of the slope of cracks, was carried out. A similar analysis related to the anisotropy of the seismic response of a fractured cluster, depending on the variable distance between the cracks and the frequency of the source, was carried out in [29]. The problem of numerical simulation of the seismic response from fractured clusters of subvertical cracks using the grid-characteristic method has been considered in a number of scientific articles [30–33].

Within the framework of this study, a fixed distance of 30 meters was used between vertically and horizontally adjacent cracks. A total of 128 cracks were placed, which were organized into 8 layers and 16 columns. Each crack was inclined at an arbitrary angle relative to the vertical and had a length of 10 meters. In each individual experiment, the angles of rotation of the cracks corresponded to a normal distribution with an average value of 45 degrees and a variance varying from 0 to 20 degrees. The scheme of the problem and the location of the crack cluster in the simulated half-space are shown in Figure 5.

In a number of computational experiments, a 50-meter-long plane wave source was used, which fell vertically and was set by the Riker function. The time integration step was $3 \cdot 10^{-4}$ seconds, the total number of steps was 3000. To register the seismic response in the experiments, 300 receivers were used, evenly distributed at a depth of 6 meters from the surface of the simulated area. In order to isolate the seismic response from the wave passing through the receivers, during the processing of the results, the readings of the receivers during the experiment, less than 0.0801 seconds, were ignored. The longitudinal velocity of the elastic wave in the medium was $C_p = 3000$ m/s, the transverse velocity was $C_s = 1500$ m/s, the spatial step of the grids was $h = 2.0$.

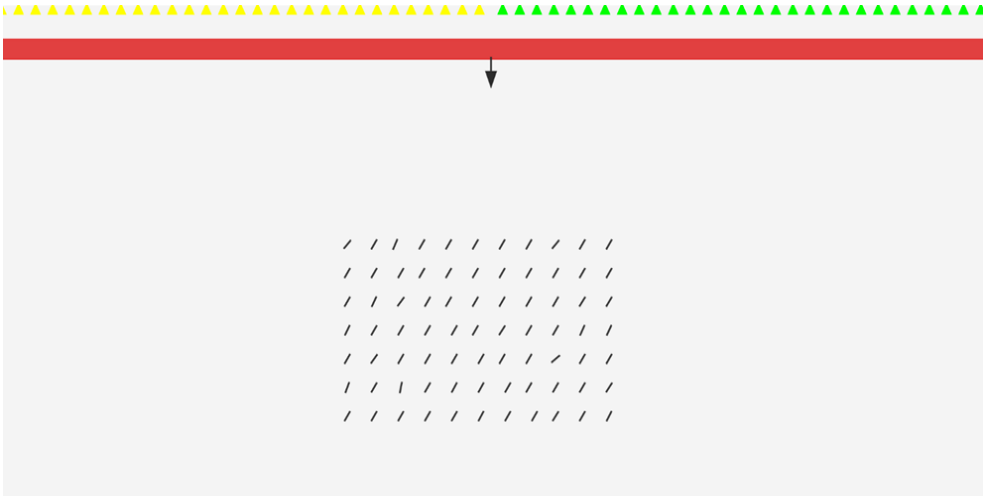

Fig. 5. The scheme of the computational experiment. Yellow and green triangles indicate the “left“ and “right” groups of receivers

To assess the anisotropy of the seismic response, the receivers used were divided into two equal groups: a group of receivers with index L was located to the left of the middle (along the axis O_x) of the main overset grid, and a group of receivers with index R was located to the right. Let the displacement velocity of the medium in the projection on the O_x axis, registered at the end of the i-th computational step, on the j-th virtual receiver in the group L be denoted $V^{i,j}_{x,L}$ (for the projection on the O_y axis respectively $V^{i,j}_{y,L}$). Then the anisotropy of the seismic response A in a given experiment can be calculated using the following formulas:

$$E_R = \sum_{i=1}^{150} \sum_{j=267}^{3000} \left(\left(V^{i,j}_{x,L} \right)^2 + \left(V^{i,j}_{y,L} \right)^2 \right),$$

$$E_L = \sum_{i=1}^{150} \sum_{j=267}^{3000} \left(\left(V^{i,j}_{x,R} \right)^2 + \left(V^{i,j}_{y,R} \right)^2 \right),$$

$$A = \frac{E_L - E_R}{E_L + E_R}.$$

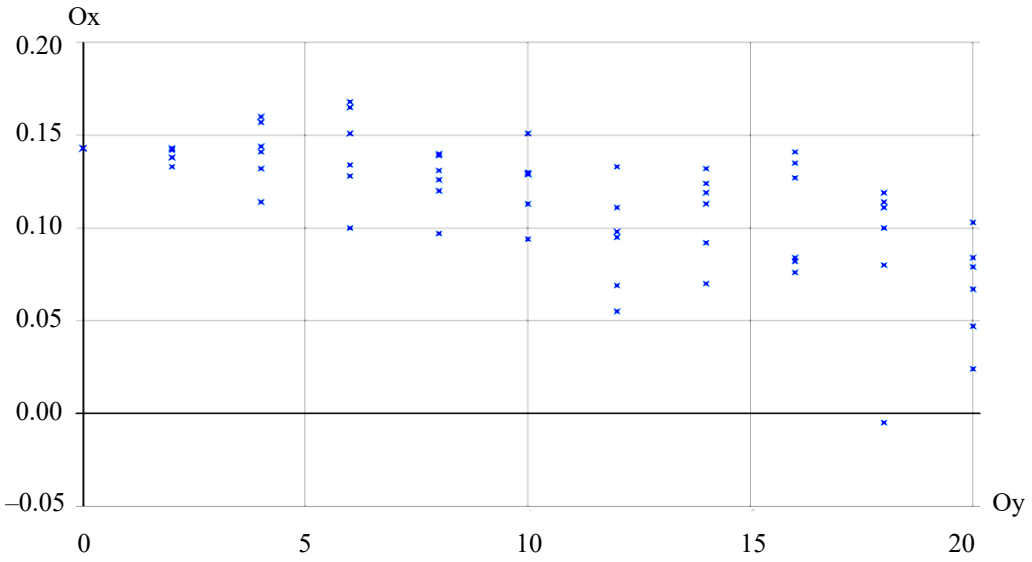

Fig. 6. Dependence of anisotropy on the dispersion of the slope of cracks in the cluster

Discussion and conclusions. A modification of the grid-characteristic method using overset grids is proposed to explicitly account for fractured inhomogeneities in a heterogeneous geological environment.

A verification study was carried out, which showed the high accuracy of the proposed approach and does not introduce a significant error compared to using the classical implementation of the thin Schonberg crack in the grid-characteristic method and at the same time expands a number of applied problems available for numerical modeling by this method.

The dependence of the anisotropy of the seismic response on the fractured cluster depending on the dispersion of the angle of inclination of the cracks in the latter is investigated. The obtained dependence shows a significant spread of results, which demonstrates the complexity of the inverse problem of seismic exploration of heterogeneous geological structures.

In conclusion, it can be concluded that the use of overset grids makes it possible to explicitly take into account geological inhomogeneities, such as cracks, when numerically solving the problem of modeling the propagation of elastic waves in a geological medium. The presented approach to the description of inhomogeneities has a high potential in computational mathematics and arouses interest in its further study.

References

1. Schoenberg M. Elastic Wave Behavior Across Linear Slip Interfaces. *The Journal of the Acoustical Society of America.* 1980;68:1516–21. https://doi.org/10.1121/1.385077

2. Pyrak-Nolte LJ, Myer LR, Cook NGW. Anisotropy in Seismic Velocities and Amplitudes from Multiple Parallel Fractures. *Journal of Geophysical Research: Solid Earth*. 1990;95:11345–58. https://doi.org/10.1029/JB095IB07P11345

3. Chaur-Jian H, Schoenberg M. Elastic Waves Through a Simulated Fractured Medium. *Geophysics*.1993;58:924–1060. https://doi.org/10.1190/1.1443487

4. Backus GE. Long-Wave Elastic Anisotropy Produced by Horizontal Layering. *Journal of Geophysical Research*. 1962;67:4427–40. https://doi.org/10.1029/JZ067I011P04427

5. Zhang J. Elastic Wave Modeling in Fractured Media with an Explicit Approach. *Geophysics*. 2005;70. https://doi.org/10.1190/1.2073886

6. Slawinski RA, Krebes ES. Finite-Difference Modeling of SH-Wave Propagation in Nonwelded Contact Media. *Geophysics*. 2002;67:1656–63. https://doi.org/10.1190/1.1512753

7. Slawinski RA, Krebes ES. The Homogeneous Finite-Difference Formulation of the p-SV-Wave Equation of Motion. *Studia Geophysica Et Geodaetica.* 2002;46:731–51. https://doi.org/10.1023/A:1021133606779

8. Zhang J, Gao H. Elastic Wave Modelling in 3-d Fractured Media: An Explicit Approach. *Geophysical Journal International.* 2009;177:1233–41. https://doi.org/10.1111/J.1365-246X.2009.04151.X

9. Favorskaya AV, Zhdanov MS, Khokhlov NI, et al. Modelling the wave phenomena in acoustic and elastic media with sharp variations of physical properties using the grid-characteristic method. *Geophysical Prospecting.* 2018;66(8):1485–1502.

10. Ruzhanskaya A, Khokhlov N. Modelling of Fractures Using the Chimera Grid Approach. In 2nd Conference on Geophysics for Mineral Exploration and Mining. *European Association of Geoscientists & Engineers*. 2018;1:1–5.

11. Berger MJ, Oliger J. Adaptive mesh refinement for hyperbolic partial differential equations. *Journal of Computational Physics.* 1984;53(3):484–512.

12. Steger JL, Dougherty FC, Benek JA. *A chimera grid scheme.* 1983;5:55–70.

13. Steger JL, Benek JA. On the use of composite grid schemes in computational aerodynamics. *Computer Methods in Applied Mechanics and Engineering*. 1987;64(1):301–320.

14. Chan W. Overset grid technology development at NASA Ames Research Center. *Computers & Fluids*. 2009; 38:496–503.

15. Mayer UM, Popp A, Gerstenberger A, et al. 3D fluid–structure-contact interaction based on a combined XFEM FSI and dual mortar contact approach. *Computational Mechanics*. 2010;46(1):53–67.

16. Zhang Y, Yim SC, Del Pin F. A nonoverlapping heterogeneous domain decomposition method for three-dimensional gravity wave impact problems. *Computers & Fluids*. 2015;106:154.

17. Nguyen VT, Vu DT, Park WG, et al. Navier–Stokes solver for water entry bodies with moving Chimera grid method in 6DOF motions. *Computers & Fluids*. 2016;140:19–38.

18. Formaggia L, Vergara C, Zonca S. Unfitted extended finite elements for composite grids. *Computers & Mathematics with Applications.* 2018;76(4):893–904.

19. Lurie AI. *Theory of Elasticity*. Moscow: Nauka. 1970. 940 p. (In Russ.).

20. Nowacki V. *Theory of Elasticity*. Moscow: MIR. 1975. 872 p. (In Russ.).

21. Keiiti A, Richards PG. *Quantitative Seismology*, 2nd ed. Quse. 2002;68:1546.

22. Randall J LeVeque. *Finite Volume Methods for Hyperbolic Problems*. 2002. https://doi.org/10.1017/CBO9780511791253

23. Zhdanov MS. *Geophysical Inverse Theory and Regularization Problems*. Elsevier Science Ltd. 2002;609.

24. Zhdanov MS. *Inverse Theory and Applications in Geophysics.* Elsevier Inc. 2015. https://doi.org/10.1016/C2012-0-03334-0

25. Ivanov DV, Kondaurov VI, Petrov IB, et al. Calculation of Dynamic Deformation and Distructure of Elastic-Plastic Body by Grid-Characteristic Methods. *Mathematical Modeling.* 1990;2:11–29. http://mathscinet.ams.org/mathscinet-getitem?mr=1124094

26. Golubev VI, Petrov IB, Khokhlov NI. Numerical Simulation of Seismic Activity by the Grid-Characteristic Method. Computational *Mathematics and Mathematical Physics*. 2013;53:1523–1533. https://doi.org/10.1134/S0965542513100060

27. Magomedov KM, Kholodov AS. The Construction of Difference Schemes for Hyperbolic Equations Based on Characteristic Relations. *USSR Computational Mathematics and Mathematical Physics*. 1969;9(2):158–76. https://doi.org/10.1016/0041-5553(69)90099-8

28. Petrov IB, Khokhlov NI. Modeling 3D Seismic Problems Using High-Performance Computing Systems. *Mathematical Models and Computer Simulations*. 2014;6:342–50. https://doi.org/10.1134/S2070048214040061

29. Kvasov IE, Pankratov SA, Petrov IB. Numerical Study of Dynamic Processes in a Continuous Medium with a Crack Initiated by a Near-Surface Disturbance by Means of the Grid-Characteristic Method. *Mathematical Models and Computer Simulations.* 2011;3:399–409. https://doi.org/10.1134/S2070048211030070

30. Kvasov IE, Petrov IB. Numerical Study of the Anisotropy of Wave Responses from a Fractured Reservoir Using the Grid-Characteristic Method. *Mathematical Models and Computer Simulations*. 2012;4:336–43. https://doi.org/10.1134/S2070048212030064

31. Muratov MV, Petrov IB. Estimation of Wave Responses from Subvertical Macrofracture Systems Using a Grid Characteristic Method. *Mathematical Models and Computer Simulations*. 2013;5:479–91.

32. Golubev VI, Petrov IB, Khokhlov NI. Numerical Simulation of Seismic Activity by the Grid-Characteristic Method. *Computational Mathematics and Mathematical Physics*. 2013;53:1523–33. https://doi.org/10.1134/S0965542513100060

33. Favorskaya AV, Petrov IB. The Use of Full-Wave Numerical Simulation for the Investigation of Fractured Zones. *Mathematical Models and Computer Simulations*. 2019;11:518–30. https://doi.org/10.1134/S2070048219040069

About the Authors:

Ivan A Mitkovets, PhD student, Moscow Institute of Physics and Technology (National Research University) (bldg. 1, 1A, Kerchenskaya St., Moscow, 117303, RF), ORCID, mitkovets@phystech.edu

Nikolay I Khokhlov, Associate Professor, Head of the Department of Computer Science and Computational Mathematics, Moscow Institute of Physics and Technology (National Research University) (bldg. 1, 1A, Kerchenskaya St., Moscow, 117303, RF), Candidate of physical and mathematical Sciences, ORCID, Math-Net.Ru, elibrary.ru, ResearcherID, k_h@inbox.ru

Claimed contributorship:

all authors have made an equivalent contribution to the preparation of the publication.

Received 24.07.2023
Revised 16.08.2023
Accepted 17.08.2023

Conflict of interest statement

the authors do not have any conflict of interest.

All authors have read and approved the final manuscript.

Об авторах:

Иван Анатольевич Митьковец, аспирант, Московский физико-технический институт (национальный исследовательский университет) (РФ, 117303, г. Москва, ул. Керченская, 1А, корп. 1), ORCID, mitkovets@phystech.edu

Николай Игоревич Хохлов, доцент, заведующий кафедрой информатики и вычислительной математики, Московский физико-технический институт (национальный исследовательский университет) (РФ, 117303, г. Москва, ул. Керченская, 1А, корп. 1), кандидат физико-математических наук, ORCID, Math-Net.Ru, elibrary.ru, ResearcherID, k_h@inbox.ru

Заявленный вклад соавторов:
все авторы сделали эквивалентный вклад в подготовку публикации.

Поступила в редакцию 24.07.2023
Поступила после рецензирования 16.08.2023
Принята к публикации 17.08.2023

Конфликт интересов
Авторы заявляют об отсутствии конфликта интересов.

Все авторы прочитали и одобрили окончательный вариант рукописи.

MATHEMATICAL MODELING
МАТЕМАТИЧЕСКОЕ МОДЕЛИРОВАНИЕ

Original article

UDC 519.6
https://doi.org/10.23947/2587-8999-2023-7-3-39-48

Mathematical Model of Three-Component Suspension Transport

Alexander I Sukhinov[1], **Inna Yu Kuznetsova**[1,2]

[1]Don State Technical University, 1, Gagarin Square, Rostov-on-Don, Russian Federation
[2]Supercomputers and Neurocomputers Research Center, 106, Italian Lane, Taganrog, Russian Federation

inna.yu.kuznetsova@gmail.com

Abstract

Introduction. Prediction of suspension deposition zones is required to assess and minimize the negative impact on the ecosystem of the reservoir during dredging within the framework of large-scale engineering projects, prediction of suspension deposition zones is required to assess and minimize the negative impact on the ecosystem of the reservoir. It is necessary to build a mathematical model that takes into account many factors that have a significant impact on the accuracy of forecasts. The aim of the work is to construct a mathematical model of transport of multicomponent suspension, taking into account the composition of the soil (different diameter of the suspension particles), the flow velocity of the water flow, the complex geometry of the coastline and bottom, wind stresses and friction on the bottom, turbulent exchange, etc.

Materials and Methods. A mathematical model for the transport of a multicomponent suspension and an approximation of the proposed continuous model with the second order of accuracy with respect to the steps of the spatial grid are described, considering the boundary conditions of the Neumann and Robin type. The approximation of the hydrodynamics model is obtained based on splitting schemes by physical processes, which guarantee fulfillment mass conservation for discrete model.

Results. The proposed mathematical model formed the basis of the developed software package that allows to simulate the process of sedimentation of a multicomponent suspension. The results of the work of the software package on the model problem of sedimentation of a three-component suspension in the process of soil dumping during dredging are presented.

Discussions and Conclusions. The mathematical model of transport of three-component suspension is described and software implemented. The developed software allows to simulate the process of deposition of suspended particles of various diameters on the bottom, and to evaluate its effect on the bottom topography and changes in the bottom composition. The developed software package also allows to analyze the process of sediment movement in the case of resuspension of multicomponent bottom sediments of the reservoir, which causes secondary pollution of the reservoir.

Keywords: suspension transport, multicomponent suspension, three-dimensional hydrodynamics model, splitting schemes, numerical methods

Funding information. The research was carried out at the expense of the grant of the Russian Science Foundation no. 22-11-00295. https://rscf.ru/project/22-11-00295/

For citation. Sukhinov AI, Kuznetsova IYu. Mathematical model of three-component suspension transport. *Computational Mathematics and Information Technologies*. 2023;7(3):39–48. https://doi.org/10.23947/2587-8999-2023-7-3-39-48

Научная статья

Математическая модель транспорта трехкомпонентной взвеси

А.И. Сухинов[1], И.Ю. Кузнецова[1,2]

[1]Донской государственный технический университет, Российская Федерация, г. Ростов-на-Дону, пл. Гагарина, 1
[2]НИЦ супер-ЭВМ и нейрокомпьютеров, Российская Федерация, Ростовская область, г. Таганрог, пер. Итальянский, 106

inna.yu.kuznetsova@gmail.com

Аннотация

Введение. При проведении дноуглубительных работ в рамках реализации масштабных инженерных проектов требуется прогнозирование зон осаждения взвеси для оценки и минимизации негативного влияния на экосистему водоема. Для решения подобных задач необходимо построение математической модели, учитывающей множество факторов, оказывающих существенное влияние на точность прогнозов. Целью работы является построение математической модели транспорта многокомпонентной взвеси, учитывающей состав грунта (различный диаметр частиц взвеси), скорость течения водного потока, сложную геометрию береговой линии и дна, ветровые напряжения и трение о дно, турбулентный обмен и др.

Материалы и методы. Описана математическая модель транспорта многокомпонентной взвеси и аппроксимация предложенной непрерывной модели со вторым порядком точности относительно шагов пространственной сетки с учетом граничных условий второго и третьего рода. Аппроксимация модели гидродинамики представлена на основе схем расщепления по физическим процессам, которая обеспечивает выполнение закона сохранения массы в разностной схеме.

Результаты исследования. Предлагаемая математическая модель легла в основу разработанного программного комплекса, позволяющего моделировать процесс осаждения многокомпонентной взвеси. Приведены результаты работы программного комплекса на модельной задаче осаждения трехкомпонентной взвеси в процессе дампинга грунта при проведении дноуглубительных работ.

Обсуждения и заключения. Описана программная математическая модель транспорта трехкомпонентной взвеси. Разработанный программный комплекс позволяет моделировать процесс осаждения взвешенных частиц различного диаметра на дно и оценивать его влияние на рельеф и изменение состава дна. Разработанный программный комплекс также позволяет анализировать процесс движения наносов в случае взмучивания многокомпонентных донных отложений водоема, вызывающий вторичное загрязнение водоема.

Ключевые слова: транспорт взвеси, многокомпонентная взвесь, трехмерная модель гидродинамики, схемы расщепления, численные методы

Финансирование. Исследование выполнено за счет гранта Российского научного фонда № 22-11-00295. https://rscf.ru/project/22-11-00295/

Для цитирования. Сухинов А.И., Кузнецова И.Ю. Математическая модель транспорта трехкомпонентной взвеси. *Computational Mathematics and Information Technologies*. 2023;7(3):39–48. https://doi.org/10.23947/2587-8999-2023-7-3-39-48

Introduction. The implementation of large-scale engineering projects, such as the construction of bridges, the expansion of the water area accessible to navigation, requires work that has a significant impact on both the bottom relief and the ecosystem of the reservoir as a whole. For example, during dredging, a significant amount of suspension enters the water, which in the process of settling to the bottom or secondary agitation can negatively affect the productive and destructive processes of the aquatic ecosystem [1–2]. To assess the possible damage caused to the ecosystem during the dumping of soil during dredging, it is necessary to pre-assess the areas of the water area in which the suspension will settle and in which its agitation is possible, which leads to secondary pollution of the water body. To predict the deposition zones of suspended particles, a mathematical model of suspension transport is proposed based on a system of initial boundary value problems, including the calculation of hydrodynamic characteristics of the water area and suspension transport.

We describe an approach to the approximation of a continuous model with a second order of accuracy with respect to the steps of the spatial grid , taking into account the boundary conditions of the second and third kind for the proposed three — dimensional model of multicomponent suspension transport . The proposed mathematical model of the transport of suspended particles is supplemented by a three-dimensional model of hydrodynamics, which allows calculating the fields of the velocity vector of the water flow [3–4]. The proposed mathematical model formed the basis of the developed

software package that allows modeling the deposition process of multicomponent suspension. The results of the work of the software package on the model problem of deposition of a three-component suspension in the process of dumping soil during dredging are presented.

Materials and methods

1. Problem statement. To construct a mathematical model of multicomponent suspension transport, we use the diffusion-convection equation, which can be written in the following form [3]:

$$(c_r)_t' + (uc_r)_x' + (vc_r)_y' + ((w+w_{s,r})\,c_r)_z' = \left(\mu (c_r)_x'\right)_x' + \left(\mu (c_r)_y'\right)_y' + \left(\nu (c_r)_z'\right)_z' + F_r\,, \tag{1}$$

where c_r is the concentration of the r-th fraction of the suspension, mg/l; $\mathbf{V}=\{u,v,w\}$ are the components of the velocity vector of the water flow, m/s; $w_{s,r}$ is the deposition rate of the r-th fraction of the suspension, m/s; μ, ν are the horizontal and vertical components of the turbulent exchange coefficient, respectively, m^2/s; F_r is the function describing the intensity of the distribution of sources of the rth fraction of the suspension, mg/ (l·s).

Equation (1) is considered under the following initial $c_r(x, y, z, 0) = c_{0r}(x, y, z)$ and boundary conditions:

– on the free surface: $(c^n)_z' = 0$;

– near the bottom surface: $\nu (c_r)_z' = -w_{s,r} c_r$;

– on the side surface: $(c_r)_{\mathbf{n}}' = 0$, if $(\mathbf{V}, \mathbf{n}) \geq 0$, and $\mu (c_r)_{\mathbf{n}}' = (\mathbf{V}, \mathbf{n}) c_r$, if $(\mathbf{V}, \mathbf{n}) < 0$, where $(\mathbf{V}, \mathbf{n})$ is the normal component of the velocity vector, $\mathbf{n}$ is the normal vector directed inside the computational domain.

The diffusion-convection equation (1) is supplemented with a three-dimensional model of the hydrodynamics of shallow water bodies [5] to calculate the velocity vector of the water flow:

– equations of motion (Navier-Stokes):

$$\begin{aligned} u_t' + uu_x' + vu_y' + wu_z' &= -P_x'/\rho + (\mu u_x')_x' + (\mu u_y')_y' + (\nu u_z')_z', \\ v_t' + uv_x' + vv_y' + wv_z' &= -P_y'/\rho + (\mu v_x')_x' + (\mu v_y')_y' + (\nu v_z')_z', \\ w_t' + uw_x' + vw_y' + ww_z' &= -P_z'/\rho + (\mu w_x')_x' + (\mu w_y')_y' + (\nu w_z')_z' + g, \end{aligned} \tag{2}$$

– the continuity equation in the case of variable density:

$$\rho_t' + (\rho u)_x' + (\rho v)_y' + (\rho w)_z' = 0. \tag{3}$$

where P is the pressure, Pa; ρ is the density, kg/m^3; g is the acceleration of gravity, m/s^2.

The system of equations (2)–(3) is considered under the following boundary conditions:

– the entrance $u = u_0, v = v_0, P_{\mathbf{n}}' = 0, V_{\mathbf{n}}' = 0$;

– lateral border (shore and bottom) $\rho\mu u_{\mathbf{n}}' = -\tau_x, \rho\mu v_{\mathbf{n}}' = -\tau_y, V_{\mathbf{n}} = 0, P_{\mathbf{n}}' = 0$;

– upper bound $\rho\mu u_{\mathbf{n}}' = -\tau_x$, $\rho\mu v_{\mathbf{n}}' = -\tau_y$, $w = -\omega - P_t'/(\rho g)$, $P_{\mathbf{n}}' = 0$,

where ω is the intensity of liquid evaporation, τ_x, τ_y are the components of the tangential stress.

2. Approximation of the suspended particles transport problem. Let us consider an approximation of the three-dimensional problem of transport of a one-component suspension based on the expression (1) (for each individual fraction, the equation is written similarly):

$$c_t' + (uc)_x' + (vc)_y' + (wc)_z' = \left(\mu c_x'\right)_x' + \left(\mu c_y'\right)_y' + \left(\nu c_z'\right)_z', \tag{4}$$

where the velocity component w implicitly takes into account the deposition rate of the suspension fraction in question w_s.

We introduce a uniform grid in time $\overline{\omega}_\tau = \left\{t^n = n\tau;\ n = \overline{0, N_t};\ N_t\tau = T\right\}$, where τ is the time step, N_t is the number of time layers, T is the duration of the modeling interval.

Suppose that the calculated area is inscribed in a parallelepiped $G = \left\{0 < x < L_x, 0 < y < L_y, 0 < z < L_z\right\}$ we obtain the closure of the area G by joining the faces of the parallelepiped, that is, we define as $\overline{G} = \left\{0 \leq x \leq L_x, 0 \leq y \leq L_y, 0 \leq z \leq L_z\right\}$.

Thus, we come to the chain of initial boundary value problems:

$$(c^n)_t' + \operatorname{div}\left(\mathbf{V} \cdot c^n\right) = \operatorname{div}\left(\mathbf{k} \cdot \operatorname{grad}\ c^n\right), \tag{5}$$

where $\mathbf{k} = \{\mu, \mu, \nu\}$ is the coefficient of turbulent exchange, $(x, y, z, t) \in G \times [0 < t \leq T]$, $t_{n-1} < t \leq t_n$, $cn\,(x, y, z, t_{n-1}) = c^{n-1}$ (x, y, z, t_{n-1}), (x, y, z, t_{n-1}), $(x, y, z) \in G$.

In this case, the initial and boundary conditions will be written as:

– initial condition $c\,(x, y, z, 0) = c_0\,(x, y, z)$, $(x, y, z) \in \overline{G}$;

– boundary condition on a free surface: $(c_r)_z' = 0;$, $(x, y, z) \in \Sigma_0$;

– boundary condition at the bottom: $\nu(c^n)_z' = -w_s c^n$, $(x, y, z) \in \Sigma_H$;

– boundary condition on the lateral surface: $(c^n)_{\mathbf{n}}' = 0$, if $(\mathbf{V}, \mathbf{n}) \geq 0$ and $\mu(c_r)_{\mathbf{n}}' = (\mathbf{V}, \mathbf{n})c_r$, , if $(\mathbf{V}, \mathbf{n}) < 0$,

where $\Sigma_0 = \{0 \leq x \leq L_x, 0 \leq y \leq L_y, z = 0\}$ is the upper face of the parallelepiped $\overline{G}$, $\Sigma_H = \{0 \leq x \leq L_x, 0 \leq y \leq L_y, z = L_z\}$ is the lower face of the parallelepiped $\overline{G}$..

Let's write down a term describing the convective transfer of suspended substances in a symmetrical form. Such an approach to the discretization of the problem will allow us to construct a difference operator with the property of skew symmetry [6]:

$$\operatorname{div}(\mathbf{V} \cdot c^n) = \frac{1}{2}\left[u\frac{\partial c^n}{\partial x} + v\frac{\partial c^n}{\partial y} + w\frac{\partial c^n}{\partial z} + \frac{\partial}{\partial x}\left(uc^n\right) + \frac{\partial}{\partial y}\left(vc^n\right) + \frac{\partial}{\partial z}\left(wc^n\right)\right]. \tag{6}$$

To approximate problem (5) , we introduce a uniform computational grid $\overline{\omega} = \overline{\omega}_x \times \overline{\omega}_y \times \overline{\omega}_z$, where:

$$\overline{\omega}_x = \left\{x_i : x_i = ih_x;\ i = \overline{0, N_x};\ h_x N_x = L_x\right\},$$
$$\overline{\omega}_y = \left\{y_j : y_j = jh_y;\ j = \overline{0, N_y};\ h_y N_y = L_y\right\},$$
$$\overline{\omega}_z = \left\{z_k : z_k = kh_z;\ k = \overline{0, N_z};\ h_z N_z = L_z\right\},$$

where h_x, h_y, h_z are the steps in the spatial coordinate directions O_x, O_y and O_z , respectively, N_x, N_y, N_z , are the numbers of nodes of the computational grid in each of the spatial directions, L_x, L_y, L_z are the lengths of the computational intervals in each of the spatial directions..

The set of internal nodes of the computational grid is denoted as ω_x, ω_y, ω_z.

The approximation of problem (5) on a space-time grid $\overline{\omega}_\tau \times \overline{\omega}$ is performed by specifying the velocities (convective transfer coefficients) at the nodes of the grids shifted by half a step along the coordinate directions O_x and O_y.

For the convective transport operator given in symmetric form (6) in equation (5), we have:

$$Cc^n \equiv \frac{1}{2h_x}\left(u^n\left(x + 0.5h_x, y, z\right)\cdot\overline{c}^n\left(x + h_x, y, z\right) - u^n\left(x - 0.5h_x, y, z\right)\cdot\overline{c}^n\left(x - h_x, y, z\right)\right) +$$
$$+\frac{1}{2h_y}\left(v^n\left(x, y + 0.5h_y, z\right)\cdot\overline{c}^n\left(x, y + h_y, z\right) - v^n\left(x, y - 0.5h_y, z\right)\cdot\overline{c}^n\left(x, y - h_y, z\right)\right) + \tag{7}$$
$$+\frac{1}{2h_z}\left(w^n\left(x, y, z + 0.5h_z\right)\cdot\overline{c}^n\left(x, y, z + h_z\right) - w^n\left(x, y, z - 0.5h_z\right)\cdot\overline{c}^n\left(x, y, z - h_z\right)\right),$$

where $\overline{c}^n$ denotes a grid function $\overline{c}^n \equiv c(x, y, z, t_n)$, $(x, y, z) \in \omega$, and through c^n denotes a sufficiently smooth function of continuous variables (x, y, z, t).

For the diffusion transfer operator in equation (5) we have:

$$Dc^n \equiv \frac{1}{h_x}\left(\mu\left(x + 0.5h_x, y, z\right)\frac{\overline{c}^n\left(x + h_x, y, z\right) - \overline{c}^n\left(x, y, z\right)}{h_x} -\right.$$
$$\left. -\mu\left(x - 0.5h_x, y, z\right)\frac{\overline{c}^n\left(x, y, z\right) - \overline{c}^n\left(x - h_x, y, z\right)}{h_x}\right) + \frac{1}{h_y}\left(\mu\left(x, y + 0.5h_y, z\right)\frac{\overline{c}^n\left(x, y + h_y, z\right) - \overline{c}^n\left(x, y, z\right)}{h_y} - \right. \tag{8}$$
$$\left. -\mu\left(x, y - 0.5h_y, z\right)\frac{\overline{c}^n\left(x, y, z\right) - \overline{c}^n\left(x, y - h_y, z\right)}{h_y}\right) + \frac{1}{h_z}\left(\nu\left(x, y, z + 0.5h_z\right)\frac{\overline{c}^n\left(x, y, z + h_z\right) - \overline{c}^n\left(x, y, z\right)}{h_z} - \right.$$
$$\left. -\nu\left(x, y, z - 0.5h_z\right)\cdot\frac{\overline{c}^n\left(x, y, z\right) - \overline{c}^n\left(x, y, z - h_z\right)}{h_z}\right).$$

Taking into account the recorded approximations (7)–(8), we obtain the following type of approximation of equation (5) in the inner nodes of the grid:

$$\frac{\bar{c}^{n}-\bar{c}^{n-1}}{\tau}+\frac{1}{2h_x}\left(u^n(x+0.5h_x,y,z)\bar{c}^n(x+h_x,y,z)-u^n(x-0.5h_x,y,z)\bar{c}^n(x-h_x,y,z)\right)+$$
$$+\frac{1}{2h_y}\left(v^n(x,y+0.5h_y,z)\bar{c}^n(x,y+h_y,z)-v^n(x,y-0.5h_y,z)\bar{c}^n(x,y-h_y,z)\right)+$$
$$+\frac{1}{2h_z}\left(w^n(x,y,z+0.5h_z)\bar{c}^n(x,y,z+h_z)-w^n(x,y,z-0.5h_z)\bar{c}^n(x,y,z-h_z)\right)=$$
$$=\frac{1}{h_x}\left(\mu(x+0.5h_x,y,z)\frac{\bar{c}^n(x+h_x,x,z)-\bar{c}^n(x,y,z)}{h_x}-\mu(x-0.5h_x,y,z)\frac{\bar{c}^n(x,y,z)-\bar{c}^n(x-h_x,y,z)}{h_x}\right)+$$
$$+\frac{1}{h_y}\left(\mu(x,y+0.5h_y,z)\frac{\bar{c}^n(x,y,z)-\bar{c}^n(x,y,z)}{h_y}-\mu(x,y-0.5h_y,z)\frac{\bar{c}^n(x,y,z)-\bar{c}^n(x,y-h_y,z)}{h_y}\right)+$$
$$+\frac{1}{h_z}\left(v(x,y,z+0.5h_z)\cdot\frac{\bar{c}^n(x,y,z+h_z)-\bar{c}^n(x,y,z)}{h_z}-v(x,y,z-0.5h_z)\frac{\bar{c}^n(x,y,z)-\bar{c}^n(x,y,z-h_z)}{h_z}\right). \quad (9)$$

We supplement the obtained approximation (9) with initial and boundary conditions. To set boundary conditions on the bottom, free and lateral surfaces of the considered area it is convenient to introduce an expanded grid [7] $\bar{\omega}^* = \bar{\omega}_x^* \times \bar{\omega}_y^* \times \bar{\omega}_z^*$, where

$$\bar{\omega}_x^* = \{x_i : x_i = ih_x;\ i = \overline{-1, N_x+1};\ h_x N_x = L_x\},$$
$$\bar{\omega}_y^* = \{y_j : y_j = jh_y;\ j = \overline{-1, N_y+1};\ h_y N_y = L_y\},$$
$$\bar{\omega}_z^* = \{z_k : z_k = kh_z;\ k = \overline{-1, N_z+1};\ h_z N_z = L_z\}.$$

In the future, we will assume that:

$$\bar{c}^n(x,y,z) = 0, \quad (10)$$

where $\bar{\omega}^* \setminus \bar{\omega}$ are the boundary nodes of the grid $\bar{\omega}^*$.

We also consider the values of the components of the velocity vector of the aqueous medium in the grid nodes $\bar{\omega}^* \setminus \bar{\omega}$ with fractional index values to be known. For grid nodes $\bar{\omega}^* \setminus \bar{\omega}$, that are located outside the reservoir, the values of the velocity vector components are set to zero.

In the case of flows on the lateral faces of the region G, coinciding in the direction with the external normals to the faces (case $(\mathbf{V}, \mathbf{n}) \geq 0$), the Neumann boundary conditions take place. This case can be written as:

$$u^n(0.5h_x,y,z)+u^n(-0.5h_x,y,z)<0,$$
$$u^n(L_x-0.5h_x,y,z)+u^n(L_x+0.5h_x,y,z)>0,$$
$$v^n(x,0.5h_y,z)+v^n(x,-0.5h_y,z)<0, \quad (11)$$
$$v^n(x,0.5h_y,z)+v^n(x,-0.5h_y,z)<0,$$

We write down an approximation of the boundary conditions of the second kind for the convective transport operator. Consider the case $x = 0$, $0 < y < L_y$, $0 < z < L_z$. In this case, the expression can be considered as a difference approximation of the convective term:

$$\frac{1}{2h_x}\left(u^n(0.5h_x,y,z)\bar{c}^n(h_x,y,z)-u^n(-0.5h_x,y,z)\bar{c}^n(-h_x,y,z)\right)$$

Expression (12) approximates the convective term with an error $O(h^2_x)$. In addition to the form (12), the approximation of the convective term with an error $O(h^2_x)$ can be written as:

$$\frac{\bar{c}^n(h_x,y,z)-\bar{c}^n(-h_x,y,z)}{2h_x}=0,$$

from where we get:

$$\bar{c}^n(-h_x, y, z) = \bar{c}^n(h_x, y, z). \tag{13}$$

From approximations (12) and (13) we obtain:

$$C_x\left(c^n\right)\Big|_{x=0} \equiv \frac{1}{2h_x}\bar{c}^n\left(h_x, y, z\right)\left(u^n\left(0.5h_x, y, z\right) - u^n\left(-0.5h_x, y, z\right)\right). \tag{14}$$

Similarly, the cases $x = L_x$, $y = 0$, $y = Ly$, $z = 0$ (boundary condition on a free surface) are written. We get:

$$C_x\left(c^n\right)\Big|_{x=L_x} \equiv \frac{1}{2h_x}\cdot\bar{c}^n\left(L_x - h_x, y, z\right)\cdot\left(u^n\left(L_x + 0.5h_x, y, z\right) - u^n\left(L_x - 0.5h_x, y, z\right)\right), \tag{15}$$

$$C_y\left(c^n\right)\Big|_{y=0} \equiv \frac{1}{2h_y}\cdot\bar{c}^n\left(x, h_y, z\right)\cdot\left(v^n\left(x, 0.5h_y, z\right) - v^n\left(x, -0.5h_y, z\right)\right), \tag{16}$$

$$C_y\left(c^n\right)\Big|_{y=L_y} \equiv \frac{1}{2h_y}\cdot\bar{c}^n\left(x, L_y - h_y, z\right)\cdot\left(v^n\left(x, L_y + 0.5h_y, z\right) - v^n\left(x, L_y - 0.5h_y, z\right)\right), \tag{17}$$

$$C_z\left(c^n\right)\Big|_{z=0} \equiv \frac{1}{2h_z}\cdot\bar{c}^n\left(x, y, h_z\right)\cdot\left(w^n\left(x, y, 0.5h_z\right) - w^n\left(x, y, -0.5h_z\right)\right). \tag{18}$$

We write down an approximation of the boundary conditions of the second kind for the diffusion transfer operator. Consider the case $x = 0$, $0 < y < L_y$, $0 < z < L_z$. In this case, the expression can be considered as a difference approximation of the diffusion term on an extended grid:

$$D_x\left(c^n\right)\Big|_{x=0} \equiv \frac{1}{h_x}\left(\mu(0.5h_x, y, z)\frac{\bar{c}^n(h_x, y, z) - \bar{c}^n(0, y, z)}{h_x} - \right.$$
$$\left. - \mu(-0.5h_x, y, z)\cdot\frac{\bar{c}^n(0, y, z) - \bar{c}^n(-h_x, y, z)}{h_x}\right). \tag{19}$$

When the first condition of (11) is fulfilled, we obtain that $\bar{c}^n(-h_x, y, z) = \bar{c}^n(h_x, y, z)$. Then, taking into account the last equality and expression (19), we obtain the following approximation of the diffusion transfer operator in the case: $x = 0$, $0 < y < L_y$, $0 < z < L_z$:

$$D_x\left(c^n\right)\Big|_{x=0} \equiv \frac{1}{h_x^2}\left(\left(\mu\left(0.5h_x, y, z\right) + \mu\left(-0.5h_x, y, z\right)\right)\left(\bar{c}^n\left(h_x, y, z\right) - \bar{c}^n\left(0, y, z\right)\right)\right). \tag{20}$$

Similarly, the cases $x = L_x$, $y = 0$, $y = L_y$ are written. For example, in the case $x = L_x$, $0 < y < L_y$, $0 < z < L_z$, when the second condition from (11) is met and taking into account equality $\bar{c}^n(L_x + h_x, y, z) = \bar{c}^n(L_x - h_x, y, z)$, we get:

$$D_x\left(c^n\right)\Big|_{x=L_x} \equiv \frac{1}{h_x^2}\left(\left(\mu\left(L_x + 0.5h_x, y, z\right) + \mu\left(L_x - 0.5h_x, y, z\right)\right)\left(\bar{c}^n\left(L_x - h_x, y, z\right) - \bar{c}^n\left(L_x, y, z\right)\right)\right). \tag{21}$$

Similarly for $y = 0$ and $y = L_y$:

$$D_y\left(c^n\right)\Big|_{y=0} \equiv \frac{1}{h_y^2}\left(\left(\mu\left(x, 0.5h_y, z\right) + \mu\left(x, -0.5h_y, z\right)\right)\left(\bar{c}^n\left(x, h_y, z\right) - \bar{c}^n\left(x, 0, z\right)\right)\right), \tag{22}$$

$$D_y\left(c^n\right)\Big|_{y=L_y} \equiv \frac{1}{h_y^2}\left(\left(\mu\left(x, L_y + 0.5h_y, z\right) + \mu\left(x, L_y - 0.5h_y, z\right)\right)\left(\bar{c}^n\left(x, L_y - h_y, z\right) - \bar{c}^n\left(x, L_y, z\right)\right)\right). \tag{23}$$

For a free surface (case $y = 0$) taking into account $v(x, y, -0{,}5h_z) = 0$ the approximation of the diffusion operator is written as:

$$D_z\left(c^n\right)\Big|_{z=0} \equiv \frac{1}{h_z^2}\nu\left(x, y, 0.5h_z\right)\left(\bar{c}^n\left(x, y, h_z\right) - \bar{c}^n\left(x, y, 0\right)\right). \tag{24}$$

Consider the approximation of the diffusion transfer operator on the bottom surface ($z = L_z$) on an extended grid. Formally , the approximation of the diffusion term can be written as:

$$D_z\left(c^n\right)\Big|_{z=L_z} \equiv \frac{1}{h_z}\left(\nu\left(x, y, L_z + 0.5h_z\right)\frac{\left(\bar{c}^n\left(x, y, L_z + h_z\right) - \bar{c}^n\left(x, y, L_z\right)\right)}{h_z} - \right. \tag{25}$$

$$-\nu(x,y,L_z-0.5h_z)\frac{\left(\overline{c}^n(x,y,L_z)-\overline{c}^n(x,y,L_z-h_z)\right)}{h_z}\Bigg).$$

Let's use a second-order approximation of the accuracy $O(h^2_z)$ of the boundary condition of the third kind $\nu(c^n)'_z=-w_s c^n$, the relation:

$$\nu(x,y,L_z)\frac{\left(\overline{c}^n(x,y,L_z+h_z)-\overline{c}^n(x,y,L_z-h_z)\right)}{2h_z}=-w_s\overline{c}^n(x,y,L_z). \tag{26}$$

Let 's use the ratio:

$$\nu(x,y,L_z)=\frac{1}{2}\left(\nu(x,y,L_z+0.5h_z)+\nu(x,y,L_z-0.5h_z)\right)+O\left(h_z^2\right). \tag{27}$$

Substituting (27) into (26), we get:

$$\left(\nu(x,y,L_z+0.5h_z)+\nu(x,y,L_z-0.5h_z)\right)\frac{\left(\overline{c}^n(x,y,L_z+h_z)-\overline{c}^n(x,y,L_z-h_z)\right)}{4h_z}=-w_s\overline{c}^n(x,y,L_z). \tag{28}$$

From equation (28) we have:

$$\overline{c}^n(x,y,L_z+h_z)=-\frac{4w_s h_z}{\left(\nu(x,y,L_z+0.5h_z)+\nu(x,y,L_z-0.5h_z)\right)}\overline{c}^n(x,y,L_z)+\overline{c}^n(x,y,L_z-h_z). \tag{29}$$

Then the approximation of the diffusion term in the diffusion-convection equation of the suspension has the form:

$$D_z\left(c^n\right)\Big|_{z=L_z}\equiv\frac{1}{h_z}\Bigg(\frac{4w_s\nu(x,y,L_z+0.5h_z)}{\nu(x,y,L_z+0.5h_z)+\nu(x,y,L_z-0.5h_z)}\overline{c}^n(x,y,L_z)+$$

$$+\frac{1}{h_z}\nu(x,y,L_z+0.5h_z)\left(\overline{c}^n(x,y,L_z-h_z)-\overline{c}^n(x,y,L_z)\right)- \tag{30}$$

$$-\nu(x,y,L_z-0.5h_z)\frac{\left(\overline{c}^n(x,y,L_z)-\overline{c}^n(x,y,L_z-h_z)\right)}{h_z}\Bigg).$$

In a similar way , it is possible to obtain an approximation of the convective operator for $z = L_z$:

$$C_z\left(c^n\right)\Big|_{z=L_z}\equiv\frac{1}{2h_z}\Bigg(\frac{4w_s h_z w^n(x,y,z+0.5h_z)}{\nu(x,y,L_z+0.5h_z)+\nu(x,y,L_z-0.5h_z)}\overline{c}^n(x,y,L_z)+ \tag{31}$$

$$+\left(w^n(x,y,L_z+0.5h_z)-w^n(x,y,L_z-0.5h_z)\right)\overline{c}^n(x,y,L_z-h_z)\Bigg).$$

The obtained approximations of the diffusion (30) and convective (31) transfer operators at the boundary nodes (at $z = L_z$) are suitable for bottoms with different morphological characteristics ("liquid" bottom, impermeable bottom, etc.) when the turbulent exchange coefficient v is set accordingly.

After constructing the scheme, it is necessary to investigate the monotonicity, stability and convergence of the difference scheme. The study of these properties uses physically motivated constraints of the Peclet grid number and the Courant number and is based on the maximum grid principle and, due to the limited scope of the article, is not given here.

3. Approximation of three-dimensional hydrodynamics model. To approximate the model (2)–(3), we will carry out on the calculated grid $\overline{\omega}=\overline{\omega}_\tau\times\overline{\omega}_h$.. To approximate the model (2)–(3), we use splitting schemes for physical processes [8]. According to this method, the initial model of hydrodynamics (2)–(3) will be divided into three subtasks [6, 9].

The first subtask is represented by the diffusion-convection equation, on the basis of which the components of the field of the velocity vector of the water flow on the intermediate time layer are calculated:

$$\frac{\widetilde{u}-u}{\tau}+u\overline{u_x}'+v\overline{u_y}'+w\overline{u_z}'=\left(\mu\overline{u_x}'\right)_x'+\left(\mu\overline{u_y}'\right)_y'+\left(\nu\overline{u_z}'\right)_z',$$

$$\frac{\widetilde{v}-v}{\tau}+u\overline{v_x}'+v\overline{v_y}'+w\overline{v_z}'=\left(\mu\overline{v_x}'\right)_x'+\left(\mu\overline{v_y}'\right)_y'+\left(\nu\overline{v_z}'\right)_z',$$

$$\frac{\widetilde{w}-w}{\tau}+u\overline{w_x}'+v\overline{w_y}'+w\overline{w_z}'=\left(\mu\overline{w_x}'\right)_x'+\left(\mu\overline{w_y}'\right)_y'+\left(\nu\overline{w_z}'\right)_z'+g\left(\frac{\rho_0}{\rho}-1\right),$$

where u, v, w are the components of the velocity vector on the previous time layer; $\tilde{u},\tilde{v},\tilde{w}$ are the components of the velocity vector on the intermediate time layer; $\bar{u} = \sigma\tilde{u} + (1-\sigma)u$, $\sigma \in [0,1]$ is the weighting factor or the weight of the scheme.

Based on the second subtask, the pressure field is calculated:

$$P''_{xx} + P''_{yy} + P''_{zz} = \frac{\hat{\rho} - \rho}{\tau^2} + \frac{(\hat{\rho}\tilde{u})'_x}{\tau} + \frac{(\hat{\rho}\tilde{v})'_y}{\tau} + \frac{(\hat{\rho}\tilde{w})'_z}{\tau}.$$

Based on the third subtask, the components of the field of the velocity vector of the water flow on the next time layer are calculated using explicit formulas:

$$\frac{\hat{u} - \tilde{u}}{\tau} = -\frac{1}{\hat{\rho}} P'_x, \quad \frac{\hat{v} - \tilde{v}}{\tau} = -\frac{1}{\hat{\rho}} P'_y, \quad \frac{\hat{w} - \tilde{w}}{\tau} = -\frac{1}{\rho} P'_z,$$

where $\hat{u},\hat{v},\hat{w}$ are the components of the velocity vector on the current time layer.

The approximation of the problem of calculating the velocity field of the water medium by spatial variables is performed on the basis of the balance method.

Results. Based on the presented mathematical model of multicomponent suspension transport, a software package in *C++* has been developed that takes into account various factors that affect the accuracy of the forecasts obtained, among which one can distinguish the complex geometry of the bottom and coastline, wind currents and friction on the bottom, the presence of a significant gradient in the density of the aquatic environment.

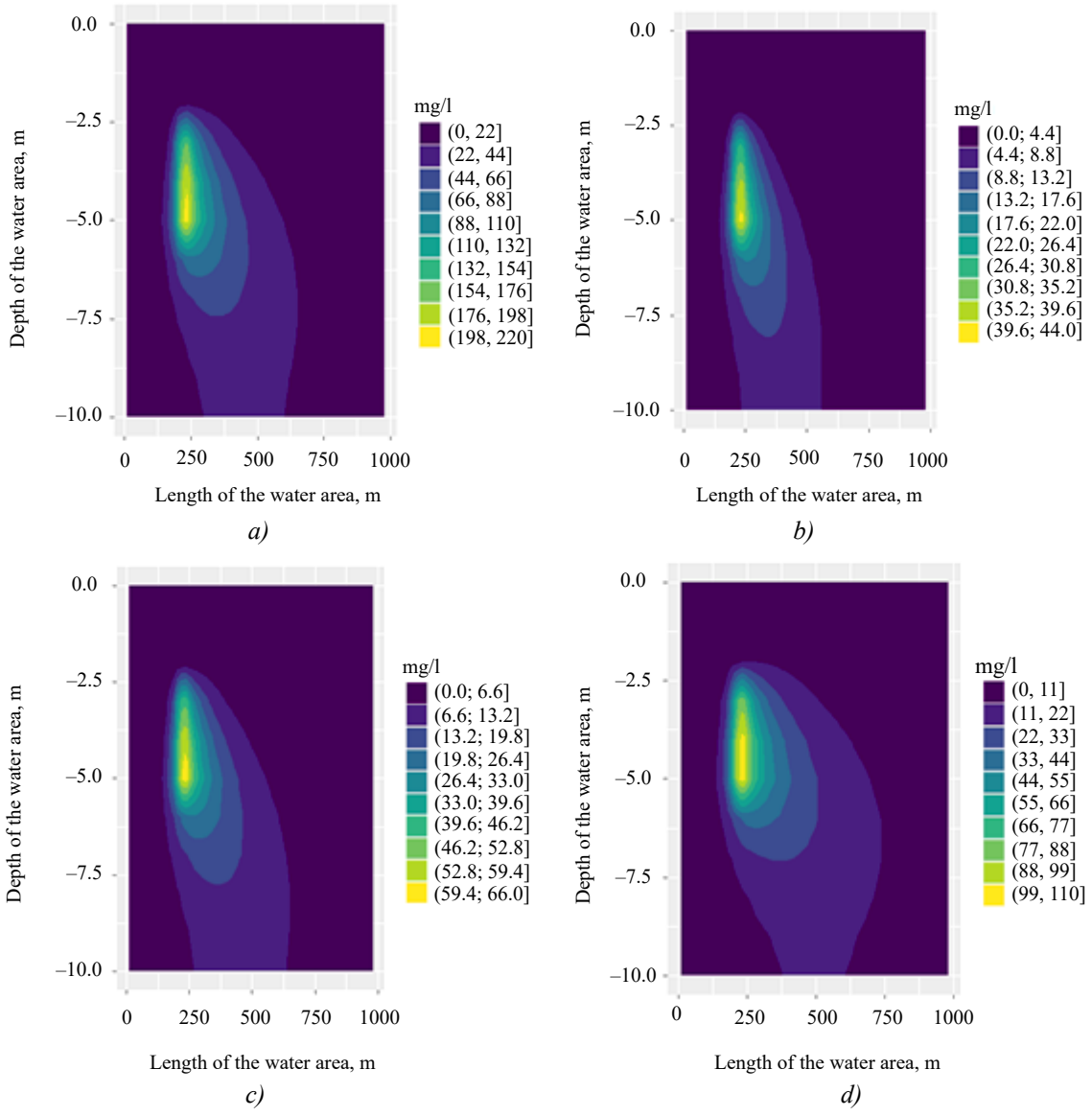

Fig. 1. Concentration of the suspension in the water column 2 hours after unloading

The developed software package allows you to calculate:

– the velocity of the water flow based on the system of equations (2)–(3);

– the process of transport of suspended particles in the water column, taking into account the obtained flow velocity of the water flow;

– the process of settling the suspension on the bottom based on the model (1)–(3).

As an example of the work of the software package, we present the results of numerical modeling of the problem of transport of three-component suspension when modeling the process of dumping soil during dredging.

Parameters of the calculated area: length — 1 km; width — 720 m; depth — 10 m.

The parameters of the calculated grid: the steps along the horizontal and vertical spatial coordinates were 10 and 1 m, respectively; the calculated interval was 2 hours, the time step was 5 seconds. The O_x axis is directed along the calculated area, the O_y axis is along the width of the calculated area, the O_z axis is along the depth of the calculated area (from 0 to –10 m, where the mark 0 corresponds to the water surface, –10 to the bottom of the reservoir).

Input parameters of the model: the average distance from the point of unloading the soil to the bottom of the reservoir in the area of dredging is 5.5 m; the area of unloading the soil along the O_x axis (along the length of the reservoir) is placed in the range from 200 to 250 m; the area of unloading the soil along the O_y axis (along the width of the reservoir) is placed in the range from 300 to 400 m; the flow velocity at depths from 4 to 10 m was 0.075 m/s (currents are directed from left to right); the density of fresh water under normal conditions is 1000 kg/m^3; the density of suspensions is 2700 kg/m^3; the particle shape coefficient for all three suspensions is 0.2222 (spherical shape); the initial viscosity of water is 1.002 MPa /s (at a temperature of 20 °C); the particle diameter of fraction A is 0.05 mm; the deposition rate of fraction A is 2.31 mm/s; the percentage of fraction A is 20 %; the particle diameter of fraction B — 0.04 mm; deposition rate of fraction B — 1.48 mm/s, percentage of fraction B — 30 %; particle diameter of fraction C — 0.03 mm; deposition rate of fraction C — 0.83 mm/s, percentage of fraction C — 50 %.

Fig. 1 shows the results of modeling the process of transport of three-component suspension in the water column. The horizontal axis is directed along the flow, the slice is presented in the middle of the calculated area, where the maximum concentration of suspended particles is observed (in the y = 360 m plane).

Fig. 1 shows that the heavier fraction A is deposited closer to the dredging zone than the lighter fractions B and C. The smaller fractions B and C are evenly distributed along the bottom of the water area.

Discussion and Conclusions. The paper presents a three-dimensional mathematical model of multicomponent suspension transport, supplemented by a three-dimensional model of hydrodynamics of a shallow reservoir. The presented model takes into account the composition of the soil (different diameter of the suspended particles), the flow rate of the water flow, the complex geometry of the coastline and bottom, overburden phenomena, wind currents and friction on the bottom, turbulent exchange, which allows to increase the accuracy of modeling.

The approximation of the proposed multicomponent suspension transport model based on the three-dimensional diffusion-convection equation is performed with the second order of accuracy relative to the steps of the spatial grid, taking into account the boundary conditions of the second and third kind. Approximation of a three-dimensional mathematical model of hydrodynamics is performed on a uniform rectangular computational grid using splitting schemes for physical processes.

For the numerical solution of the obtained discrete models, a software package has been developed that allows simulating the deposition of suspended particles of various diameters on the bottom, and assessing its effect on the bottom relief and changes in the composition of the bottom. The developed software package also allows you to analyze the process of sediment movement in the case of agitation of multicomponent bottom sediments of the reservoir, causing secondary pollution of the reservoir.

References

1. Matishov GG, Ilyichev VG. On optimal exploitation of water resources. The concept of internal prices. *Reports of the Academy of Sciences*. 2006;406(2):249–251. (In Russ.).

2. Kovtun II, Protsenko EA, Sukhinov AI, et al. Calculating the Impact on Aquatic Resources Dredging in the White Sea. *Fundamental and Applied Hydrophysics.* 2016;9(2):27–38. (In Russ.).

3. Sukhinov AI, Chistyakov AE, Atayan AM, et al. Mathematical model of process of sedimentation of multicomponent suspension on the bottom and changesin the composition of bottom materials, *Izvestiya Instituta Matematiki i Informatiki Udmurtskogo Gosudarstvennogo Universiteta*, 2022;60:73–89. (In Russ.). https://doi.org/10.35634/2226-3594-2022-60-05

4. Sukhinov AI, Kuznetsova IYu, Chistyakov AE. Study of the accuracy and applicability of the difference scheme for solving the diffusion-convection problem at large grid péclet numbers. *Computational Continuum Mechanics*. (In Russ.). https://doi.org/10.7242/1999-6691/2020.13.4.34

5. Kuznetsova IYu, Sukhinov AI, Chistyakov AE, et al. Mathematical model of hydrodynamics of estuarine areas. *Proceedings of the International scientific conference "Actual problems of applied Mathematics, computer science and Mechanics".* 2021:960–965. (In Russ.).

6. Samarskiy AA, Vabishevich PN. *Numerical methods for solving convection-diffusion problems*. Moscow: URSS. 2009:248. (In Russ.).

7. Samarskiy AA, Nikolaev ES. *Methods for solving grid equations*. Moscow: Nauka. 1978:592. (In Russ.).

8. Belotserkovsky OM, Gushchin VA, Schennikov VV. Splitting method applied to solving problems of dynamics of viscous incompressible fluid. *Journal of Computational Mathematics and Mathematical Physics*. 1975;15(1):197–207. (In Russ.). https://doi.org/10.1016/0041-5553(75)90146-9

9. Tikhonov AN, Samarskiy AA. *Equations of mathematical physics*. 7th ed. Moscow: Nauka: Moscow University Press, 2004:798. (In Russ.).

About the Authors:

Alexander I Sukhinov, Corresponding Member of the Russian Academy of Sciences, Doctor of Physical and Mathematical Sciences, Professor, Director of the Research Institute for Mathematical Modeling and Forecasting of Complex Systems, Don State Technical University (1, Gagarin Sq., Rostov-on-Don, 344003, RF), ORCID, MathSciNet, eLibrary.ru, ResearcherID, ScopusID, sukhinov@gmail.com

Inna Yu Kuznetsova, Senior Lecturer of the Department of Intelligent and Multiprocessor Systems, SIC Supercomputers and Neurocomputers (106, Italian Lane, Taganrog, 347900, RF), ORCID, ScopusID, elibrary.ru, ResearcherID, inna.yu.kuznetsova@gmail.com

Claimed contributorship:
all authors have made an equivalent contribution to the preparation of the publication.

Received 02.08.2023
Revised 24.08.2023
Accepted 25.08.2023

Conflict of interest statement
the authors do not have any conflict of interest.

All authors have read and approved the final manuscript.

Об авторах:

Сухинов Александр Иванович, член-корреспондент РАН, доктор физико-математических наук, профессор, директор НИИ Математического моделирования и прогнозирования сложных систем, Донской государственный технический университет (РФ, 344003, г. Ростов-на-Дону, пл. Гагарина, 1), ORCID, MathSciNet, eLibrary.ru, ResearcherID, ScopusID, sukhinov@gmail.com

Кузнецова Инна Юрьевна, старший преподаватель кафедры интеллектуальных и многопроцессорных систем, НИЦ супер-ЭВМ и нейрокомпьютеров (РФ, 347900, г. Таганрог, пер. Итальянский, 106), ORCID, Scopus ID, elibrary.ru, ResearcherID, inna.yu.kuznetsova@gmail.com

Заявленный вклад соавторов:
Все авторы сделали эквивалентный вклад в подготовку публикации.

Поступила в редакцию 02.08.2023
Поступила после рецензирования 24.08.2023
Принята к публикации 25.08.2023

Конфликт интересов
Авторы заявляют об отсутствии конфликта интересов.

Все авторы прочитали и одобрили окончательный вариант рукописи.

MATHEMATICAL MODELING
МАТЕМАТИЧЕСКОЕ МОДЕЛИРОВАНИЕ

UDC 519.6
https://doi.org/10.23947/2587-8999-2023-7-3-49-63

Original article

Comparison of Hydrodynamic Processes Modelling Results in Shallow Water Bodies Based on 3D Model and 2D Model Averaged by Depth

Sofia V Protsenko, Elena A Protsenko ✉, Anton V Kharchenko

Taganrog Institute named after A.P. Chekhov (branch) of RSUE, 48, Initiative St., Taganrog, Russian Federation

✉ eapros@rambler.ru

Abstract

Introduction. Two-dimensional hydrodynamic models have proven their ability to adequately describe the processes of runoff and transportation in rivers, lakes, estuaries, deltas and seas. Practice shows that even where significant three-dimensional effects are expected, for example, with wind flows, a two-dimensional approach can work effectively. However, in some cases, the two-dimensional model does not accurately reflect the actual flow structures. For example, in shallow waters with complex bathymetry, heterogeneous terrain and dynamics can lead to a non-uniform velocity profile. The aim of the study is to develop a basis for determining in which cases a two-dimensional model averaged in depth is sufficient for modelling hydrodynamic processes in shallow waters like the Azov Sea, and in which cases it is advisable to use a three-dimensional model to obtain accurate results.

Materials and Methods. Local analytical solutions have been obtained for the propagation of the predominant singular progressive wave in a shallow, well-mixed reservoir. Advective terms and Coriolis terms are neglected, the vortex viscosity is assumed to be constant, and the lower friction term is linearized. Special attention is paid to the latter, since the characteristics of the models significantly depend on the method of determining the coefficients of lower friction. The analytical method developed in the study shows that certain combinations of higher flow velocities ($u \approx> 1$ m/s) and water depths ($d > 50$ m) can cause significant differences between the results of the depth-averaged model and the model containing vertical information.

Results. The results obtained are verified by numerical simulation of stationary and non-stationary periodic flows in a schematized rectangular basin. The results obtained as a result of three-dimensional modelling are compared with the results of two-dimensional modelling averaged in depth. Both simulations show good compliance with analytical solutions.

Discussion and Conclusions. Analytical solutions were found by linearization of the equations, which obviously has its limitations. A distinction is made between two types of nonlinear effects — nonlinearities caused by higher-order terms in the equations of motion, i. e. terms of advective acceleration and friction, and nonlinear effects caused by geometric nonlinearities, this is due, for example, to different water depths and reservoir widths, which will be important when modelling a real sea.

Keywords: hydrodynamics, shallow water reservoir, wave motion, numerical modelling

Funding information. The study was supported by the Russian Science Foundation grant no. 22-71-00015. https://rscf.ru/project/22-71-00015/

For citation. Protsenko SV, Protsenko EA, Kharchenko AV. Comparison of hydrodynamic processes modelling results in shallow water bodies based on 3D model and 2D model averaged by depth. *Computational Mathematics and Information Technologies*. 2023;7(3):49–63. https://doi.org/10.23947/2587-8999-2023-7-3-49-63

Научная статья

Сопоставление результатов численного моделирования процессов гидродинамики в мелководных водоемах на основе трехмерной модели и двумерной модели, усредненной по глубине

С.В. Проценко, Е.А. Проценко✉, А.В. Харченко

Таганрогский институт имени А.П. Чехова (филиал) РГЭУ (РИНХ), Российская Федерация, г. Таганрог, ул. Инициативная, 48

✉ eapros@rambler.ru

Аннотация

Введение. Двумерные гидродинамические модели доказали свою способность адекватно описывать процессы стока и транспортировки в реках, озерах, эстуариях, дельтах и морях. Практика показывает, что даже там, где ожидаются значительные трехмерные эффекты, например, при ветровых потоках, двумерный подход может работать эффективно. Однако в некоторых случаях двумерная модель недостаточно точно отражает фактические структуры потока. Например, в мелководных водоемах со сложной батиметрией неоднородный рельеф и динамика могут привести к тому, что профиль скорости будет неоднородным. Целью исследования является разработка основы для определения того, в каких случаях двумерной модели, усредненной по глубине, достаточно для моделирования процессов гидродинамики в мелководных водоемах, подобных Азовскому морю, а в каких случаях для получения точных результатов целесообразно использование трехмерной модели.

Материалы и методы. Локальные аналитические решения получены для распространения преобладающей сингулярной прогрессивной волны в мелководном, хорошо перемешанном водоеме. Адвективными слагаемыми и слагаемыми Кориолиса пренебрегают, вихревая вязкость принимается постоянной, а слагаемое нижнего трения линеаризуется. Последнему уделяется особое внимание, поскольку характеристики моделей существенно зависят от способа определения коэффициентов нижнего трения. Аналитический метод, разработанный в исследовании, показывает, что определенные комбинации более высоких скоростей течения ($u \approx> 1$ м/с) и глубин воды ($d > 50$ м) могут вызывать значительные различия между результатами модели, усредненной по глубине, и модели, содержащей информацию по вертикали.

Результаты исследования. Полученные результаты проверяются численным моделированием стационарных и нестационарных периодических течений в схематизированном прямоугольном бассейне. Результаты, полученные в результате трехмерного моделирования, сравниваются с результатами двумерного моделирования, усредненного по глубине. Оба моделирования показывают хорошее соответствие аналитическим решениям.

Обсуждение и заключения. Аналитические решения были найдены путем линеаризации уравнений, что, очевидно, имеет свои ограничения. Отмечается два вида нелинейных эффектов — вызванных членами более высокого порядка в уравнениях движения, т. е. членами адвективного ускорения и трения и вызванных геометрическими нелинейностями, что связано, например, с различной глубиной воды и шириной водоема, что будет важно при моделировании реального моря.

Ключевые слова: гидродинамика, мелководный водоем, волновое движение, численное моделирование

Финансирование. Исследование выполнено за счет гранта Российского научного фонда № 22-71-00015. https://rscf.ru/project/22-71-00015/

Для цитирования. Проценко С.В., Проценко Е.А, Харченко А.В. Сопоставление результатов численного моделирования процессов гидродинамики в мелководных водоемах с аналитическим решением. *Computational Mathematics and Information Technologies*. 2023;7(3):49–63. https://doi.org/10.23947/2587-8999-2023-7-3-49-63

Introduction. Heterogeneous relief and dynamics in shallow waters with complex bathymetry can lead to the fact that the velocity profile will be heterogeneous, in this case, the two-dimensional model does not accurately reflect the actual flow structures. The main purpose of this study is to develop a theoretical basis for determining in which specific cases a two-dimensional model is sufficient to simulate flow processes in shallow seas such as the Azov Sea. To this end, it has been studied whether the reduction from 3D to 2D has a significant impact on the output data of the hydrodynamics model, such as water levels and depth-averaged flow velocities. It has been studied which simplifications are applied to the flow problem to allow the use of two-dimensional equations averaged over depth, rather than three-dimensional equations for shallow water. It is investigated which parameters are important when comparing a depth-averaged model with a model containing vertical information; in which cases a two-dimensional depth-averaged model is representative. The analytical approach made it possible to identify the effect of depth averaging using analytical solutions for highly simplified situations.

Despite conducting a wide range of studies focused on the problem under consideration, they do not fully reflect the totality of various factors and processes: hydrophysical, hydrodynamic, hydrobiological, meteorological and anthropogenic [1, 2]. The areas of application of the models presented in the study are tides caused by wind (for example, storm surges). River flows and stratified flows determined by density are beyond the scope of this study [3–5].

Let's consider the most important phenomena for shallow seas like the Azov Sea and determine the characteristic scales of length, time and speed. In the Azov Sea, the formation of currents is mainly due to three factors: the wind regime, the flow of flowing rivers and water exchange with the Black Sea. The great variability of currents is a consequence of the instability of the wind regime, the shallow waters of the sea and its relatively small area. In open areas of the sea, under the influence of wind, as a rule, there is a progressive movement of the aquatic environment, covering the entire thickness from the surface to the bottom horizons. The prevailing current velocity in the Azov Sea is 10–20 cm/s, the maximum velocity is 180–100 cm/s [6].

The mode of excitement of the Azov Sea is due to the small area of the sea, shallow depths and significant indentation of the shores. Wave heights of less than 1 m prevail in the described area (their repeatability reaches 75 %). The repeatability of wave heights of 1–2 m is 20–45 %, and wave heights of 2–3 m — no more than 13 %. In the central, deepest part of the sea, wave heights do not exceed 3.5 m and only in very rare cases they reach 4 m. In the stormiest months (December–March), the development of unrest in the described area is limited by the presence of ice [6]. As for overburden phenomena, before which there is often a powerful overclocking, strong waves are characterized by a slight decrease in the height of the waves before the start of the storm and then their rapid increase. Often, the processes of development and attenuation of run-up and storm phenomena in the Azov Sea are synchronous, thus dangerous phenomena arise.

In the Azov Sea, waves are observed with a length of mainly 15–25 m, and only sometimes 80 m. The wave period is usually less than 5 s, extremely rarely — 7–8 s. In the described area, short and very steep waves are noted, which pose a danger to small vessels.

In the shallow Azov Sea, seismic fluctuations occur constantly. Seiches are free fluctuations that occur in moderate–sized basins (harbors, lakes, bays, or even in the sea). These are standing waves with a frequency equal to the resonant frequency of the pool in which they occur. The duration of sessions can vary from a few minutes to several hours. The reason for their appearance in the Azov Sea is not only a change in wind or atmospheric pressure over the sea, but also waves of storm surges from the Black Sea. Since seiches are a resonant phenomenon, it is obvious that the size of the pool in relation to the wavelength is an important factor.

Materials and methods

1. Problem statement. 3D Navier-Stokes equations are used as a basis for solving fluid flow problems [7–8]. Assuming that water is an incompressible liquid, the continuity equation is applied:

$$\frac{\partial u}{\partial x}+\frac{\partial \upsilon}{\partial y}+\frac{\partial \omega}{\partial z}=0$$

with velocity components u, υ, ω in the direction x, y, z respectively. The conservation of momentum is expressed as follows:

$$\frac{\partial(pu)}{\partial t}+\frac{\partial\left(pu^2\right)}{\partial x}+\frac{\partial(pu\upsilon)}{\partial y}+\frac{\partial(\rho u\omega)}{\partial z}=-\frac{\partial p}{\partial x}+\rho f\upsilon+\frac{\partial \tau_{xx}}{\partial x}+\frac{\partial \tau_{xy}}{\partial y}+\frac{\partial \tau_{xz}}{\partial z},$$

$$\frac{\partial(p\upsilon)}{\partial t}+\frac{\partial(pu\upsilon)}{\partial x}+\frac{\partial(p\upsilon^2)}{\partial y}+\frac{\partial(p\upsilon\omega)}{\partial z}=-\frac{\partial p}{\partial y}-\rho fu+\frac{\partial \tau_{yx}}{\partial x}+\frac{\partial \tau_{yy}}{\partial y}+\frac{\partial \tau_{yz}}{\partial z},$$

$$\frac{\partial(p\omega)}{\partial t}+\frac{\partial(pu\omega)}{\partial x}+\frac{\partial(p\upsilon\omega)}{\partial y}+\frac{\partial(p\omega^2)}{\partial z}=-\frac{\partial p}{\partial y}-\rho g+\frac{\partial \tau_{zx}}{\partial x}+\frac{\partial \tau_{zy}}{\partial y}+\frac{\partial \tau_{zz}}{\partial z},$$

where ρ is the water density; p is the pressure; f is the Coriolis parameter; τ_{ij} is the viscous shear stress in the i-direction on the j-plane.

The stresses are defined as:

$$\tau_{ij}=\rho v\left(\frac{\partial u_i}{\partial x_j}+\frac{\partial u_j}{\partial x_i}\right),$$

where v is the kinematic viscosity.

The abbreviated designation is also used, where $x_i = (x, y, z)$, $u_i = (u, \upsilon, \omega)$ for $i = 1, 2, 3$.

To account for turbulence in the Navier-Stokes equations, the variables are decomposed into an average value and variation: $u=\bar{u}+u'$. We substitute the expansion over all variables into the momentum equations and the average results

into the Reynolds-averaged equations of motion, which have the same form as the original Navier-Stokes equations, with additional turbulent stresses called Reynolds stresses: $\tau_{ij} = \rho \overline{u_i' u_j'}$ [9].

The problem of closure is one of the main tasks of turbulence research. A simple turbulence model uses the Boussinesq hypothesis to describe turbulent motions similar to molecular motions, but with vortex viscosity coefficients ν_t^h и ν_t^υ for horizontal and vertical directions [10]. All of the above leads to the following equations:

$$\frac{\partial u}{\partial t} + u\frac{\partial u}{\partial x} + \upsilon\frac{\partial u}{\partial y} + \omega\frac{\partial u}{\partial z} = -\frac{1}{\rho_0}\frac{\partial p}{\partial x} + f\upsilon + \frac{\partial}{\partial x}\left(\nu_t^h \frac{\partial u}{\partial x}\right) + \frac{\partial}{\partial y}\left(\nu_t^h \frac{\partial u}{\partial y}\right) + \frac{\partial}{\partial z}\left(\nu_t^\upsilon \frac{\partial u}{\partial z}\right), \quad (1)$$

$$\frac{\partial \upsilon}{\partial t} + u\frac{\partial \upsilon}{\partial x} + \upsilon\frac{\partial \upsilon}{\partial y} + \omega\frac{\partial \upsilon}{\partial z} = -\frac{1}{\rho_0}\frac{\partial p}{\partial y} - fu + \frac{\partial}{\partial x}\left(\nu_t^h \frac{\partial \upsilon}{\partial x}\right) + \frac{\partial}{\partial y}\left(\nu_t^h \frac{\partial \upsilon}{\partial y}\right) + \frac{\partial}{\partial z}\left(\nu_t^\upsilon \frac{\partial \upsilon}{\partial z}\right), \quad (2)$$

$$\frac{\partial \omega}{\partial t} + u\frac{\partial \omega}{\partial x} + \upsilon\frac{\partial \omega}{\partial y} + \omega\frac{\partial \omega}{\partial z} = -\frac{1}{\rho_0}\frac{\partial p}{\partial z} - \frac{\rho}{\rho_0}g + \frac{\partial}{\partial x}\left(\nu_t^h \frac{\partial \omega}{\partial x}\right) + \frac{\partial}{\partial y}\left(\nu_t^h \frac{\partial \omega}{\partial y}\right) + \frac{\partial}{\partial z}\left(\nu_t^\upsilon \frac{\partial \omega}{\partial z}\right). \quad (3)$$

For a depth-averaged flow, it is assumed that the shear stress in the layer caused by the turbulent flow is determined by the quadratic law of friction:

$$\tau_b = \frac{\rho_0 g |U| U}{C_1^2} = \rho_0 c_{f_1} |U| U,$$

where $|U|$ is the value of the depth-averaged horizontal velocity, and C_1 is the Chezy coefficient for the depth-averaged model [11].

For models with vertical information (2DV or 3D), a quadratic formulation of stresses in the reservoir is used. The shear stress of the layer in 3D can be related to the current directly above the layer:

$$\tau_b = \rho_0 c_{f_2} |u_b| u_b,$$

where u_b — the value of the horizontal velocity directly above the layer.

2. Analytical research. Suppose that U characterizes the scales of horizontal velocities u and v, L characterizes the horizontal scales of length x and y, and H characterizes the vertical scale z. Then scaling the continuity equation leads to the expression for the vertical velocity scale W:

$$\frac{\partial u}{\partial x} + \frac{\partial \upsilon}{\partial y} + \frac{\partial \omega}{\partial z} = 0,$$

$$\frac{U}{L} + \frac{U}{L} + \frac{W}{H} = 0 \Rightarrow W \approx O\left(\frac{UH}{L}\right).$$

According to the data of the Unified State Information System on the Situation in the World Ocean [6], the horizontal component of the velocity is several orders of magnitude greater than the vertical component of the velocity for tides, storm waves and seiche in the Azov Sea. Consequently, the vertical component of the velocity can be neglected, it will not be considered in this study.

The vertical momentum equation reduces to a hydrostatic balance:

$$\frac{\partial p}{\partial z} = -\rho g.$$

Integrating this equation in the vertical direction gives:

$$p(z) = -\rho g(\zeta - z) + p_{atm}, \text{ in case of } \frac{\partial \rho}{\partial z} = 0,$$

where ζ is the height of the free surface (fig. 1); p_{atm} is the atmospheric pressure on a free surface.
Now:

$$\frac{\partial p}{\partial x} = \rho g \frac{\partial \zeta}{\partial x}, \quad \frac{\partial p}{\partial y} = \rho g \frac{\partial \zeta}{\partial y}, \text{ если } \frac{\partial \rho}{\partial x} = \frac{\partial \rho}{\partial y} = 0. \quad (4)$$

Substituting this into the horizontal momentum equations (1) and (2), we obtain:

$$\frac{\partial u}{\partial t} + u\frac{\partial u}{\partial x} + \upsilon\frac{\partial u}{\partial y} - \frac{\partial}{\partial z}\left(\nu_t \frac{\partial u}{\partial z}\right) = -g\frac{\partial \zeta}{\partial x} + f\upsilon, \quad (5)$$

$$\frac{\partial \upsilon}{\partial t} + u\frac{\partial \upsilon}{\partial x} + \upsilon\frac{\partial \upsilon}{\partial y} - \frac{\partial}{\partial z}\left(\nu_t \frac{\partial \upsilon}{\partial z}\right) = -g\frac{\partial \zeta}{\partial y} - fu. \quad (6)$$

Along with neglecting the vertical component of velocity and replacing the pressure gradient with the water level gradient, several other terms were ignored in order to move from equations (1) and (2) to (5)–(6). Viscous stresses are not taken into account due to the fact that turbulent stresses are many orders of magnitude higher than viscous stresses, because molecular viscosity is only important within a few millimeters of the boundary. In addition, horizontal turbulent stresses are not taken into account.

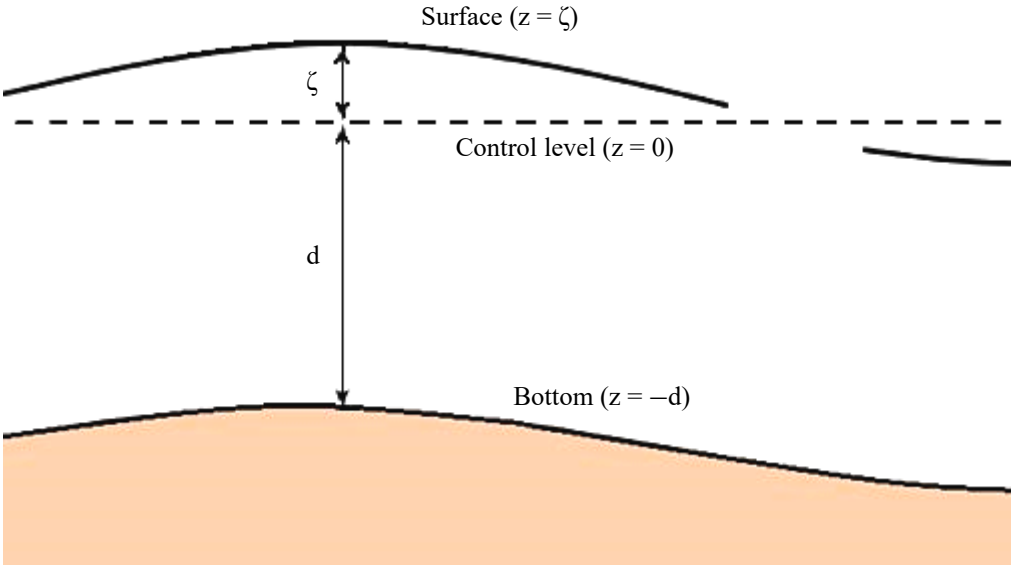

Fig. 1. Determination of surface height ζ and depth of undisturbed water *d*

Using equations (5)–(6), we determine the relative orders of magnitude of the terms in order to get an idea of the parameters that are most important in a certain situation, and which are insignificant. Let's consider each term separately and perform scaling:

– inertia: $\frac{\partial u}{\partial t} \approx \frac{U}{T}$;

– advection: $u\frac{\partial u}{\partial t} \approx \frac{U^2}{L}$;

– vertical momentum diffusion: $\frac{\partial}{\partial z}\left(\nu_t \frac{\partial u}{\partial z}\right) \approx \nu \frac{U}{H^2}$;

– pressure gradient: $-g\frac{\partial \zeta}{\partial y} \approx g\frac{\Delta H}{L}$;

– Coriolis force: $f\upsilon \approx fU$.

The term responsible for friction is important in the study, since it is defined differently in models. For 3D model, the ratio between the coefficient of friction and the coefficient of inertia can be expressed as:

$$\frac{friction}{inertia} \approx \frac{\nu U/H^2}{U/T} \approx \frac{\nu}{\omega H^2},$$

where $\omega \approx \frac{1}{T}$.

In addition, important parameters are viscosity ν, wave frequency ω and vertical length scale (for example, water depth d). A dimensionless combination of these parameters, widely used in the analytical approach, is described in [12], where the dynamic expression for the phase shift stress is compared with the expression in which the bottom stress is proportional to the depth-averaged velocity in the steady state. The result only depending on the parameter $\omega d^2/\nu$ (fig. 2).

When $\omega d^2/\nu$ very small, the ratio approaches unity, which means that the shear stress of the layer reacts to the periodic flow as if it were constant at each moment of time: $\omega d^2/\nu < 0.5$. It can also be written as $d^2/\nu < 0{,}5 \cdot T/2\pi \approx 0{,}08 \cdot T$, where T is the period of the oscillating flow. The value d^2/ν can be interpreted as the time required for a viscous flow to change the velocity profile at depth d. Thus, a quasi-stationary shear stress of the layer is expected when the adjustment time is less than 8 % of the period.

For turbulent flow in shallow water, the vortex viscosity estimate is [13]:

$$\nu = \frac{1}{6}\kappa d u_* = 0{,}067 d u_* .$$

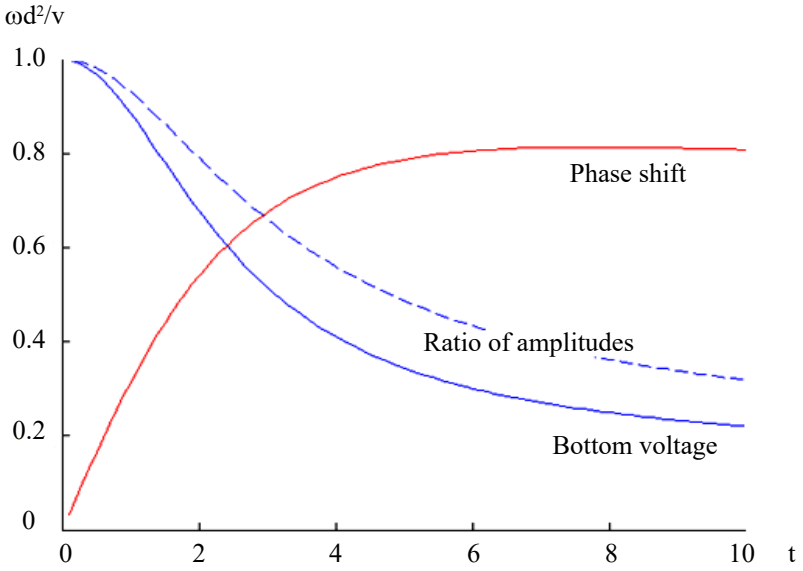

Fig. 2. The ratio of shear stresses of the layer at dynamic and steady flow

For the Azov Sea, with an average water depth $d \approx 7.4$ m and an average amplitude of the current at a depth $\bar{u} \approx 0.5$ m/s, the vortex viscosity estimate is ν = 0,00925 m/s.

Analytical solutions can be obtained only for significantly simplified forms of the equations of motion. Since the advection terms are nonlinear, it is necessary to exclude them from the momentum equation for an analytical approach. When the wave propagation velocity is defined as the wavelength over the wave period $c = L/T$, the ratio between the advection term and the inertia term leads to the Froude number, defined as $F_r = u/c$. $F_r << 1$ meaning that the inertia term is much more important than the advection term and therefore the advection term can be neglected. This refers to long waves with small amplitudes relative to the depth of the water. The set of equations without advective terms reduces to:

$$\frac{\partial u}{\partial t} - \nu_t \frac{\partial^2 u}{\partial z^2} = -g\frac{\partial \zeta}{\partial x} + f\upsilon, \tag{7}$$

$$\frac{\partial \upsilon}{\partial t} - \nu_t \frac{\partial^2 \upsilon}{\partial z^2} = -g\frac{\partial \zeta}{\partial y} - fu, \quad \frac{\partial p}{\partial z} = -\rho g.$$

We will consider a periodic flow bounded by one horizontal dimension given by equation (7). The main attention will be paid to the effect of changes in the plane (x, z). Taking into account these assumptions, the basic equation 2DV takes the form:

$$\frac{\partial u}{\partial t} - \nu_t \frac{\partial^2 u}{\partial z^2} = F, \tag{8}$$

$$F = -g\frac{\partial \zeta}{\partial x}.$$

Equation (8) can be integrated over the water depth d to obtain one-dimensional equation of momentum in the x direction:

$$d\frac{\partial U}{\partial t} - \nu_t \left(\frac{\partial \tilde{u}}{\partial z_{(z=0)}} - \frac{\partial \tilde{u}}{\partial z_{(z=-d)}} \right) = Fd,$$

where U is the depth-averaged velocity.

On the sea surface ($z = 0$), the shear stress is zero, since the free surface does not create any friction (in the absence of wind). In the formation ($z = -d$), it is customary to associate the shear stress with the velocity averaged over the depth with the coefficient of friction c_f for the model averaged over the depth. So, when:

$$\nu_t \frac{\partial u}{\partial z} = \tau_b \approx c_{f_1} |U| U,$$

the depth-averaged equation takes the form:

$$\frac{\partial U}{\partial t}+\frac{c_{f_1}|U|U}{d}=F. \tag{9}$$

Here the friction term is proportional $|U|U$ and, therefore, not linear. Since linear equations are much easier to solve analytically, it is convenient to use the linearization method. Lorenz [14] proposed such a linearization of the shear stress of the layer, which for many decades served as the basis for simple solutions. Suppose that the flow velocity changes sinusoidally in time:

$$U(t)=\hat{U}\cos(\omega t). \tag{10}$$

Only the real part of the expression for U, which is used further, is considered. Figure 3 shows the corresponding $|U|U/\hat{U}^2=|\cos(\omega t)|\cos(\omega t)$, which represents friction as a function of time, showing deviations from the pure cosine function.

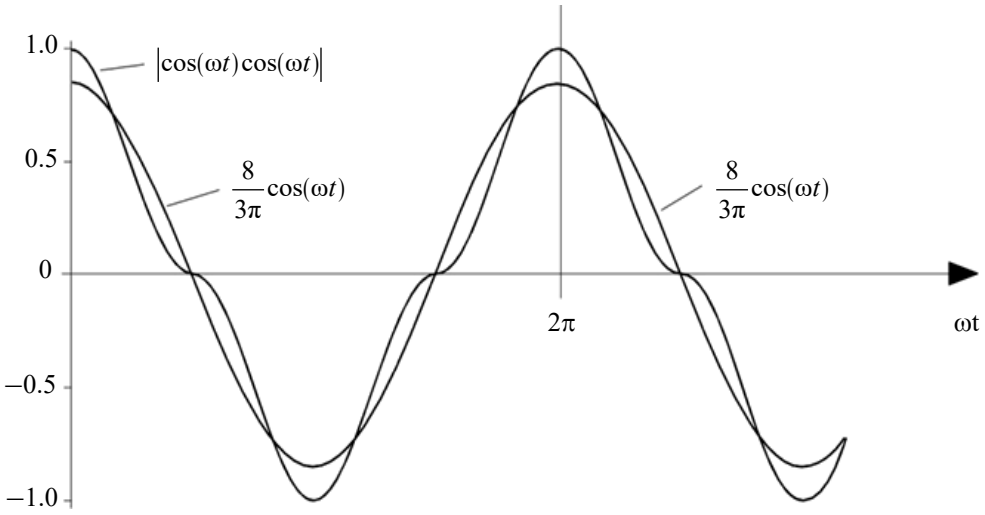

Fig. 3. Linearization of the quadratic friction term [15]

The rationale for linearization lies in the fact that, as is commonly believed, it does not reproduce the exact cosine function as long as the damping effect of friction persists. For this purpose, the energy that is lost per cycle due to friction is set equal for both cases. This approach allows us to obtain a suitable estimate of the linearization constant κ:

$$\kappa_1=\frac{8}{3\pi}c_{f_1}\frac{\hat{U}}{d}\approx c_{f_1}\frac{|U|}{d},$$

where the subscript "1" indicates a one-dimensional case. This expression contains the original velocity $\hat{U}$, which is unknown. Although iterative approaches to its definition have been proposed, this linearization constant is often accepted as a calibration parameter.

The shear stress of the linearized layer becomes: $\tau_b=c_{f_1}|U|U\approx\kappa_1 dU.$

Substituting this into equation (9), we obtain:

$$\frac{\partial U}{\partial t}+\kappa_1 U=F. \tag{11}$$

For dynamic flow in a one-dimensional situation, this linearized equation is used, while a complex representation of the flow velocity is introduced:

$$U(t)=\hat{U}e^{i\omega t}, \tag{12}$$

where $\hat{U}$ is the complex amplitude; $e^{i\omega t}=\cos(\omega t)+i\sin(\omega t)$, where i is an imaginary unit satisfying the equation $i=\sqrt{-1}$. The factor $e^{i\omega t}$ causes rotation in time with ω as the angular frequency, which is equal to $2\pi/T$.

Note that the velocity defined in (10) is equal to the real part of the expression:

$$U(t)=\mathrm{Re}\left[\hat{U}e^{i\omega t}\right]=\hat{U}\cos(\omega t).$$

Substituting the complex periodic solution (12) into equation (11), excluding the time change $e^{i\omega t}$ in each term gives:

$$i\omega\hat{U}+\kappa_1\hat{U}=\hat{F},\quad (i\omega+\kappa_1)\hat{U}=\hat{F},\quad \hat{U}=\frac{\hat{F}}{i\omega+\kappa_1},\quad \hat{U}=\frac{\hat{F}}{i\omega}\cdot\frac{1}{1+\kappa_1/i\omega},\quad \hat{U}=\hat{A}\cdot\frac{1}{1-i\sigma_1},$$

where $\hat{A}=\frac{\hat{F}}{i\omega}=-\frac{g}{i\omega}\frac{\partial\hat{\zeta}}{\partial x};\quad \sigma_1=\frac{\kappa_1}{\omega}=\frac{8}{3\pi}c_{f_1}\frac{\hat{U}}{\omega d}\cdot$

So, the expression for the depth-averaged velocity in the x direction is:

$$U=\hat{A}\cdot\left(\frac{1}{1-i\sigma_1}\right)e^{i\,\omega t}.$$

Thus, the expression for the depth-averaged velocity U is obtained by solving the depth-averaged momentum equation. Next, let's compare this expression with a similar solution for the depth-averaged velocity calculated using a model with vertical information.

The momentum equation $\frac{\partial u}{\partial t}-\nu_t\frac{\partial^2 u}{\partial z^2}=F$ with a periodic solution $u(z,t)=\tilde{u}(z)e^{i\,\omega t}$ (now $\tilde{u}$ is the complex amplitude as a function of the vertical coordinate) and elimination $e^{i\omega t}$ takes the form:

$$i\omega\tilde{u}(z)-\nu_t\frac{\partial^2}{\partial z^2}\tilde{u}(z)=\hat{F}$$

and is a differential equation with a homogeneous and partial solution:

$$\tilde{u}(z)=C_1e^{bz}+C_2e^{-bz}+\hat{A},\quad b=\sqrt{\frac{i\omega}{\nu_t}}\quad \hat{A}=\frac{\hat{F}}{i\omega}.$$

On the sea surface ($z = 0$) shear stress $\tau = 0$ since the free surface does not create friction (in the absence of wind):

$$\left.\frac{\partial\tilde{u}}{\partial z}\right|_{(z=0)}=0\ \Rightarrow\ C_1=C_2\ \Rightarrow$$
$$\Rightarrow\ \tilde{u}(z)=C\cosh(bz)+\hat{A}. \tag{13}$$

There are several variants of the boundary condition in the layer to find an expression for the C integration constant. The partial slip condition assumes velocity in the layer $u \neq 0$. It is assumed that the shear stress in the layer ($z = –d$) is described by the linearized quadratic law of friction:

$$\nu_t\left.\frac{\partial\tilde{u}}{\partial z}\right|_{(z=-d)}=\tau_b\approx\kappa_2 d\,\tilde{u},$$

where $\kappa_2=\frac{8}{3\pi}c_{f_2}\frac{\tilde{u}_b}{d}\cdot$

The subscript "2" indicates a two-dimensional case. Substituting the expression for the flow velocity (13) into equation (14), we obtain:

$$\nu_t\cdot(Cb\sinh(-bd))=\kappa_2 d\cdot\left(C\cosh(-bd)+\hat{A}\right),$$
$$C\cdot(-\nu_t b\sinh(-bd)-\kappa_2 d\cdot\cosh(bd))=\kappa_2 d\hat{A}\ \Rightarrow$$
$$\Rightarrow C=-\hat{A}\cdot\left(\frac{\nu_t b}{\kappa_2 d}\sinh(bd)+\cosh(bd)\right)^{-1}.$$

The solution for the vertical velocity profile becomes:

$$\tilde{u}(z)=\hat{A}\cdot\left(1-\frac{\cosh(bz)}{\frac{\nu_t b}{\kappa_2 d}\sinh(bd)+\cosh(bd)}\right), \tag{15}$$

$$\tilde{u}(z)=\hat{A}\cdot\left(1-\hat{\gamma}\frac{\cosh(bz)}{\cosh(bd)}\right),$$

where $\hat{\gamma}=\left(1+\frac{\nu_t b}{\kappa_2 d}\tanh(bd)\right)^{-1}=\left(1+\frac{i}{\sigma_2 bd}\tanh(bd)\right)^{-1}\cdot$

So, the velocity profile described by equation (15) is a function of a dimensionless parameter:

$$bd = \sqrt{i\omega d^2/\nu_t}, \tag{16}$$

and dimensionless parameter σ_2:

$$\sigma_2 = \frac{\kappa_2}{\omega} = \frac{8}{3\pi} c_{f_2} \frac{\hat{u}_b}{\omega d}.$$

The parameter similar to the parameter in equation (16) has already been discussed in the context of the shear stress of the layer $\omega d^2/\nu$.

The depth-averaged velocity is obtained:

$$\bar{u} = \frac{1}{d}\int_{-d}^{0} \tilde{u}(z)dz = \frac{1}{d}\int_{-d}^{0} \hat{A}\left(1 - \hat{\gamma}\frac{\cosh(bz)}{\cosh(bd)}\right)dz = \frac{\hat{A}}{d}\left[z - \frac{\hat{\gamma}}{b}\frac{\cosh(bz)}{\cosh(bd)}\right]_{-d}^{0};$$

$$\bar{u} = \hat{A}\cdot\left(1 - \frac{\hat{\gamma}}{bd}\tanh(bd)\right)e^{i\omega t}.$$

The equation for a one-dimensional steady-state flow model with linearized bottom friction (11) reduces to:

$$\kappa_1 U = F, \tag{17}$$

where $\kappa_1 \approx cf_1|U|/d$ is the linearized coefficient of friction for a depth-averaged flow (for a steady flow, the coefficient $8/3\pi$ is not taken into account); U is the depth-averaged horizontal velocity and $F = -g\partial\zeta/\partial x$ is an abbreviated designation of the water level gradient. The expression for the depth-averaged velocity U follows from equation (17):

$$U = \frac{F}{\kappa_1}. \tag{18}$$

In a two-dimensional steady-state flow model with linearized bottom friction, equation (18) reduces to:

$$-\nu_t \frac{\partial^2 u}{\partial z^2} = F.$$

Since it is assumed that F is independent of z, integration gives:

$$\nu_t \frac{\partial u}{\partial z} = -Fz + C_1.$$

On the sea surface ($z = 0$) the shear stress $\tau_0 = \nu_t \partial u/\partial z = 0$ means that the integration constant $C_1 = 0$ and, therefore:

$$\nu_t \frac{\partial u}{\partial z} = -Fz. \tag{19}$$

Thus, the shear stress is linearly distributed vertically with the maximum shear stress τ_b in the layer ($z = -d$):

$$\tau_b = Fd. \tag{20}$$

Assuming a constant vertical vortex viscosity, the velocity profile is determined by integrating equation (19):

$$u(z) = C_2 - \frac{Fz^2}{2\nu_t}. \tag{21}$$

This is a parabolic velocity profile, where the integrating constant C_2 is equal to the maximum velocity on the sea surface ($z = 0$). To find the constant C_2, it is necessary to impose a boundary condition on the layer. Various approaches are possible to implement the lower boundary condition.

The combination of the linearized boundary condition $\tau_b = \kappa_2 du_b$, $\kappa_2 \approx c_{f_2}|u_b|/d$ and equation (20) will result in an expression for the velocity in the layer. Substituting this into equation (21), we obtain an expression for C_2. Then the speed profile becomes:

$$u(z) = \frac{F}{2\nu_t}\left(d^2 - z^2\right) + \frac{F}{\kappa_2}.$$

Integration by depth gives:

$$\bar{u} = \frac{1}{d}\int_{-d}^{0} u(z)dz = \frac{1}{d}\int_{-d}^{0}\left(\frac{F}{2\nu_t}\left(d^2 - z^2\right) + \frac{F}{\kappa_2}\right)dz = \frac{Fd^2}{3\nu_t} + \frac{Fd^2}{\kappa_2}. \tag{22}$$

Thus, in the stationary case, there are also two solutions, (18) and (22), with two different bottom friction coefficients, where $\kappa_1 \neq \kappa_2$ since the shear stress of the layer is determined differently in both cases. Assume that the depth-averaged velocities for both models are equal $\overline{u} = U$. This leads to the following relation between κ_1 and κ_2:

$$\frac{1}{\kappa_1} = \frac{1}{\kappa_2} + \frac{d^2}{3\nu_t}.$$

Applying $\sigma = \kappa / \omega$:

$$\frac{1}{\sigma_1} = \frac{1}{\sigma_2} + \frac{\omega d^2}{3\nu_t}. \quad (23)$$

In the relation between σ_1 and σ_2 there is a dimensionless parameter $\omega d^2/\nu$ now choosing a certain range for σ_1 will result in obtaining σ_2 as dimensionless parameter function for each σ_1. σ-ratio (23) helps comparing the amplitudes and phases of depth-averaged velocities calculated using a one-dimensional and two-dimensional model, respectively.

Figures 4 and 5 show the ratio of the velocity amplitude and phase for several values σ_1. The relations of amplitudes and phases for the corresponding physical phenomena are indicated by dots. Thus, the application of the σ-relation is limited to situations $\omega d^2/\nu_t > /\sigma_1$.

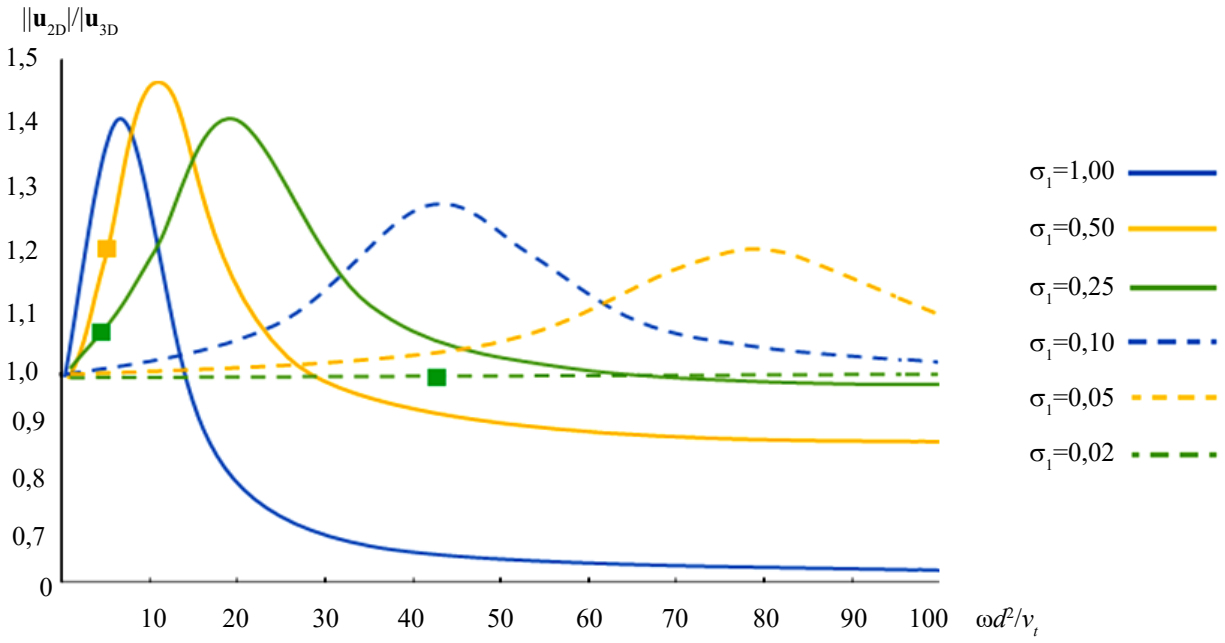

Fig. 4. The ratio of amplitudes between U and $\overline{u}$ as a function $\omega d^2/\nu_t$ and σ_1

The ratio of velocity amplitudes is greater than 1, provided that $\omega d^2/\nu_t < 65$, this means that the velocity calculated using a depth-averaged model will be greater than the amplitude of the velocity that contains information about the vertical than vice versa. In addition, it should be noted that for seas like the Azov Sea (green dot on the line $\sigma_1 = 0.25$) the ratio of the velocity amplitude to 1.06 and the phase ratio to 1.01. An amplitude deviation of 6 % is expected for parameter values that are likely to occur in practice. At the same value $\omega d^2/\nu_t$ but a higher value σ_1 the differences increase (yellow dot on the line $\sigma_1 = 0.50$). The only reason for the increase , when ω, d and ν_t remain constant would be an increase in velocity $\widehat{U}$. So, the initial initial velocity was estimated as $\widehat{U}$ = 0.5 m/s, for $\widehat{U}$ = 1 m/s the yellow dot indicates the ratio of the velocity amplitudes 1.23 and the phase ratio 0.94.

At lower values of the ratio of velocity amplitudes is almost always greater than 1, regardless of the value $\omega d^2/\nu_t$. In the case of inertia dominance (for example, for a seiche) one should not expect any difference between calculations with vertical information and without it. This is indicated by a green dot on the line $\sigma_1 = 0{,}02$.

The result of the amplitude-phase ratio seems to be significantly sensitive to the estimation of velocity amplitudes $\widehat{U}$, as well as to the bottom friction coefficient c_f. It can be concluded that the regions in which significant differences (more than 20 %) should be expected are difficult to quantify in a general sense, in addition, there are certain combinations of flow velocity and depth water, which can lead to a significant difference in results.

In a one-dimensional steady- state flow model with quadratic bottom friction, the momentum equation reduces to:

$$\frac{c_{f_1}|U|U}{d} = F,$$

where c_{f1} is the coefficient of friction for the flow averaged over depth.

Since U can be considered positive at steady flow, the expression for the depth-averaged velocity becomes:

$$U = \sqrt{\frac{Fd}{c_{f_1}}}.$$

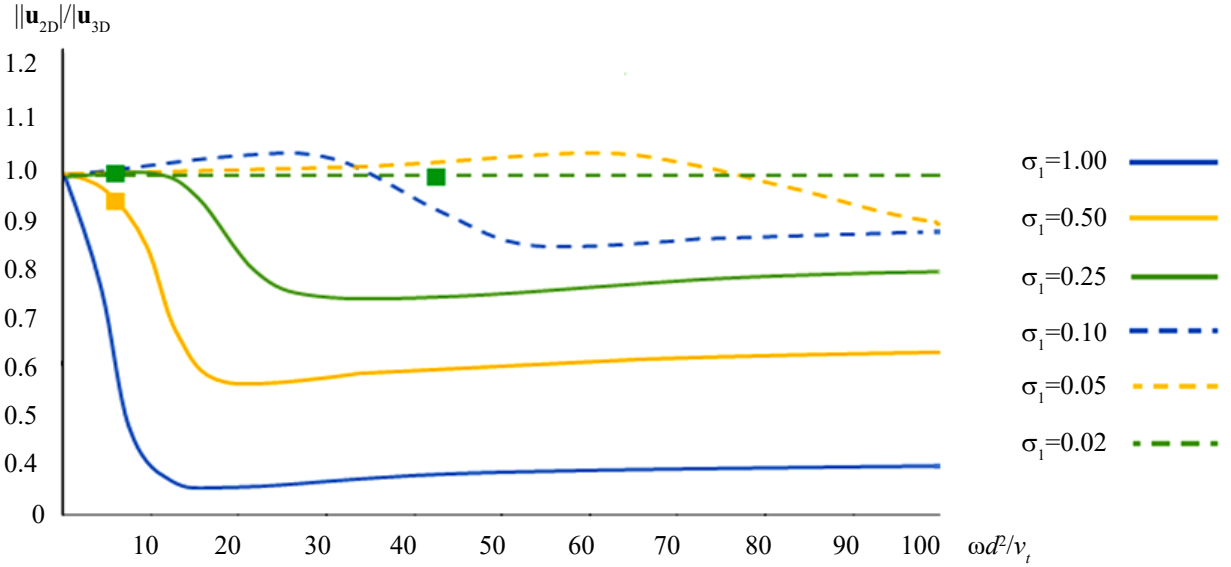

Fig. 5. The phase ratio between U and $\bar{u}$ as a function $\omega d^2/v_t$ and σ_1

The starting point for a steady flow with quadratic bottom friction for a two-dimensional model is equation (21). The integration constant is again found by superimposing a boundary condition on the layer. The combination of the quadratic boundary condition $(\tau_b = c_{f_2}|u_b|u_b)$ and equation (20) will result in an expression for the velocity in the layer. Substituting this into equation (21), we obtain an expression for C_2, thus, the velocity profile becomes:

$$u(z) = \frac{F}{2\nu_t}\left(d^2 - z^2\right) + \sqrt{\frac{Fd}{c_{f_2}}},$$

where c_{f2} is the coefficient of friction for the model containing information in the vertical direction. Integration by depth gives:

$$\bar{u} = \frac{1}{d}\int_{-d}^{0} u(z)dz = \frac{1}{d}\int_{-d}^{0}\left(\frac{F}{2\nu_t}\left(d^2 - z^2\right) + \sqrt{\frac{Fd}{c_{f_2}}}\right)dz = \frac{Fd^2}{3\nu_t} + \sqrt{\frac{Fd}{c_{f_2}}}.$$

Similarly, to the linearized case, under the assumption $\bar{u} = U$ follows the relation between c_{f1} and c_{f2}:

$$\frac{1}{\sqrt{c_{f_1}}} = \frac{1}{\sqrt{c_{f_2}}} + \frac{\sqrt{Fd^3}}{3\nu_t},$$

also $c_{f1} \neq c_{f2}$ and c_{f2}, since the shear stress of the layer is determined differently. The elevation function of the level can be included in this analysis using the continuity equation:

$$\frac{\partial u}{\partial x} + \frac{\partial v}{\partial y} + \frac{\partial \omega}{\partial z} = 0.$$

The depth–averaged version of the continuity equation is:

$$\frac{\partial \zeta}{\partial t} + d\frac{\partial U}{\partial x} = 0, \qquad (24)$$

where ζ is the height above sea level on a free surface; *d* is the depth of the water; *U* is the depth-averaged velocity. The height of the surface can be found by substituting an expression for the depth-averaged velocity calculated using two models.

The previously obtained one-dimensional depth averaged velocity *U* is equal to:

$$U = A\left(\frac{1}{1-i\sigma_1}\right)e^{i\,\omega t},$$

where $A = F/\,iw$ и $F = -g\partial\zeta\,/\,\partial x$.

Substituting this into the depth-averaged continuity equation (24), we obtain:

$$i\omega\tilde{\zeta} - \frac{dg}{i\,\omega}\frac{\partial^2\tilde{\zeta}}{\partial x^2}\left(\frac{1}{1-i\sigma_1}\right)e^{i\,\omega t} = 0.$$

Substituting $\zeta(x,t) = \tilde{\zeta}(x,t)e^{i\,\omega t}$, we obtain: $i\omega\tilde{\zeta} - \frac{dg}{i\,\omega}\frac{\partial^2\tilde{\zeta}}{\partial x^2}\left(\frac{1}{1-i\sigma_1}\right)e^{i\,\omega t} = 0.$

This differential equation has the following homogeneous solution:

$$\tilde{\zeta}(x) = C_+\,e^{-p\,x} + C_-\,e^{p\,x},$$

where $\pm\,p_1 = \pm ik_0\sqrt{1-i\,\sigma_1}$, $k_0 = \omega/c_0$ is the wave number without friction; $c_0 = \sqrt{gd}$ is the speed of the wave without friction.

The general periodic solution given by equation (25) contains two exponentially decaying waves propagating in the opposite direction. Here $\pm ik_0$ represents propagation in the absence of friction, $\sqrt{1-i\sigma_1}$ represents the effect of friction. Rewriting *p* as $p_1 = \mu + ik$:

$$\mathrm{Im}(p) = k_1 = \frac{k_0}{\sqrt{1-\tan^2\delta}},\quad \mathrm{Re}(p) = \mu_1 = k_1\tan\delta,$$

where $\tan^2\delta \equiv \sigma_1 = \frac{k_1}{\omega}$ or $\tan 2\delta \equiv \sigma_1 = \frac{k_1}{\omega}$.

Here, instead of working with σ (the ratio of friction to inertia), the friction angle δ is determined, since this seems more convenient. The general periodic solution of equation (25) can be written as:

$$\tilde{\zeta}(x) = C_+\,e^{-p_1 x} + C_-\,e^{p_1 x},\quad \tilde{\zeta}(x) = C_+\,e^{-\mu_1 x}\,e^{-i\,k_1 x} + C_-\,2e^{\mu_1 x}\,e^{-i\,k_1 x},\quad \tilde{\zeta}(x) = \tilde{\zeta}_+ + \tilde{\zeta}_-. \tag{26}$$

This is an abbreviated designation for two waves propagating in the opposite direction.

Similarly, $\bar{u}$ substituted into the continuity equation, which leads to the following complex root:

$$\pm\,p_2 = \pm ik_0\left(1 - \frac{\tilde{\gamma}}{bd}\tanh(bd)\right)^{-1/2},$$

where $\tilde{\gamma} = \left(1 + \frac{i}{\sigma_2 bd}\tanh(bd)\right)^{-1}$, $\sigma_2 = \frac{\kappa_2}{\omega}$, $bd = \sqrt{\frac{i\omega}{\nu_t}}d$.

The following section illustrates some of the previous developments for a singular translational wave and waves in a pool closed at one end, both for the two-dimensional and three-dimensional case.

Results. To interpret the solution for a singular progressive wave, we will use:

$$\zeta(x,t) = Re\left\{\tilde{\zeta}e^{i\,\omega\,t}\right\}.$$

A singular traveling wave is considered, so we will use from equation (26):

$$\zeta_+(x,t) = \mathrm{Re}\left\{\tilde{\zeta}_+(x)e^{i\,\omega t}\right\} = \mathrm{Re}\left\{C_+e^{-\rho x}e^{i\,\omega\,t}\right\}.$$

Substituting $p_2 = \mu + ik$ and taking C_1 modulo and argument, we get:

$$\zeta_+(x,t) = \mathrm{Re}\left\{\left|C_+\right|e^{-\mu x}\,e^{i(\omega\,t - kx + \arg C_+)}\right\}\ \text{ or }\ \zeta_+(x,t) = \tilde{\zeta}_+(x)e^{i\,(\omega\,t - kx + \arg C_+)},$$

where $\tilde{\zeta}_+(x) = \left|C_+\right|e^{-\mu x}$.

This solution shows the surface height of a singular translational wave with k (the imaginary part of p) as the wave number (phase change per unit length). Since the phase varies with x and t through $\omega t - kx$, this refers to a progressive wave in the positive direction x, with a phase velocity $c = \omega/k$ an argument C_+ is the initial phase (phase when $\omega t = 0$) ζ_+ for $x = 0$. The amplitude $\zeta_+(x, t)$ for $x = 0$ is given through $|C_+|$ decreases exponentially in the positive direction along the x axis with a decay rate of μ.

The results of numerical experiments are presented in Table 1. Case 1 illustrates a situation in which bottom friction does not significantly contribute to the solution ($\sigma_1 = 0.05$; $d = 60$ m); for case 2, friction is essential ($\sigma_1 = 0.50$; $d = 20$ m).

Table 1

Calculated parameters of a wave with constant viscosity $v_t = 0.05$ m^2/s

Parameter	Formula	Case 1	Case 2
σ_1		0.05	0.50
σ_2		0.06	0.62
d		60 [м]	20 [м]
c_0	$\sqrt{gd}$	24.3 [м/с]	14.0 [м/с]
k_0	ω / c	$5.80 \cdot 10^{-6}$	$1.00 \cdot 10^{-5}$
k_1	Im (p_1)	$5.80 \cdot 10^{-6}$	$1.03 \cdot 10^{-5}$
k_2	Im (p_2)	$5.81 \cdot 10^{-6}$	$8.79 \cdot 10^{-6}$
μ_1	Re (p_1)	$1.45 \cdot 10^{-7}$	$2.44 \cdot 10^{-6}$
μ_2	Re (p_2)	$1.50 \cdot 10^{-7}$	$1.56 \cdot 10^{-6}$

The amplitude of the surface rise decreases with a coefficient $e^{i-\mu\Delta x}.\exp(-\mu\Delta x)$. At a distance of $\Delta x = 10$ km one-dimensional reduction coefficient for case 1 is equal $e^{(-0,015)} \approx 0.99$, two-dimensional one is also equal $e^{(-0,015)} \approx 0.99$. For case 2, the one-dimensional reduction coefficient is $\exp(-0.24) \approx 0.78$, 2D — $\exp(-0.16) \approx 0.86$. It can be concluded that the differences between one-dimensional and two-dimensional results are not significant when bottom friction does not significantly contribute to the solution.

Discussion and Conclution. Analytical solutions for a depth-averaged model and a model that contains vertical information are:

$$U = \widetilde{A} \cdot \left(\frac{1}{1 - i\sigma_1} \right) e^{i\omega t}, \quad \overline{u} = \widetilde{A} \cdot \left(1 - \frac{\widetilde{\gamma}}{bd} \tanh(bd) \right) e^{i\omega t},$$

where $\widetilde{\gamma}$ is the function of σ_2 and bd. Thus, the depth-averaged velocities in both models look very similar and can be described by a function of a dimensionless σ_1-parameter or σ_2-parameter and a dimensionless parameter bd, respectively, where:

$$\sigma_1 = \frac{8}{3\pi} c_{f_1} \frac{\widehat{U}}{\omega d}, \quad \sigma_2 = \frac{8}{3\pi} c_{f_2} \frac{\widetilde{u}_b}{\omega d}, \quad bd = \sqrt{\frac{i\omega d^2}{\nu_t}}.$$

In order to link the above solutions, it was decided to assume that the depth-averaged velocities in both cases are equal for a steady flow.

Concentrating on the propagation of one predominant singular progressive wave, the analytical approach shows that certain conditions can cause significant differences between the depth-averaged velocities calculated using two-dimensional and three-dimensional models. However, a thorough study has led to the conclusion that it is quite difficult to find such conditions in practice. Thus, in combination with the uncertainties associated with the relationship between the two models, the greatest differences should be expected in places with greater water depth ($d > 60$ m) and high speeds ($u \approx> 1$ m/s). It should also be noted that the ratio of amplitudes is almost always greater than 1, and the ratio of phases < 1 for seas.

Analytical solutions were found by linearization of the equations, which obviously has its limitations. A distinction is made between two types of nonlinear effects:

1. Non-linearities caused by higher-order terms in the equations of motion, i.e. the terms of advective acceleration and friction. The linearization of the kU friction term is based on optimal reproduction of the prevailing singular progressive wave. Although such linearization is effective for the purposes of this study, it distorts the propagation and generation of other components of the motion of the aquatic environment.

2. Nonlinear effects caused by geometric nonlinearities that result from the dependence of the cross-section on the height of the surface ζ. This is due, for example, to the different depth of water and the width of the reservoir, which will be important when modelling a real sea.

References

1. Bijlsma AC, Uittenbogaard RE, Blokland T. Horizontal large eddy simulation applied to stratified tidal flows. *Proceedings of the International Symposium on Shallow Flows*. Delft, Netherlands. 2003:559–566. https://doi.org/10.1201/9780203027325.ch70

2. Chamecki M, Chor T, Yang D, et al. Material transport in the ocean mixed layer: recent developments enabled by large eddy simulations. *Reviews of Geophys*. 2019;57:1338–1371. https://doi.org/10.1029/2019RG000655

3. Gushchin VA, Mitkin VV, Rozhdestvenskaya TI, et al. Numerical and experimental study of the fine structure of a stratified fluid flow over a circular cylinder. *Applied Mechanics and Technical Physics*. 2007;48(1(281)):43–54. (In Russ.). https://doi.org/10.1007/s10808-007-0006-y

4. Jirka GH. Large scale flow structures and mixing processes in shallow flows. *Journal of Hydraulic Research*. 2001;39(6):567–573. https://doi.org/10.1080/00221686.2001.9628285

5. Smit PB, Janssen TT, Herbers TH. Nonlinear wave kinematics near the ocean surface. *Journal of Oceanography.* 2017;47:1657–1673. https://doi.org/10.1175/JPO-D-16-0281.1

6. Unified state information system on the situation in the World Ocean. URL: http://portal.esimo.ru (Accessed 10.06.2023).

7. Alekseenko E, Roux B, Sukhinov A, et al. Nonlinear hydrodynamics in a mediterranean lagoon. *Nonlinear Processes in Geophysics.* 2013;20(2):189–198. https://doi.org/10.5194/npg-20-189-2013

8. Battjes J, Labeur R. *Unsteady Flow in Open Channels*. Cambridge University Press, 2017. 312 p. https://doi.org/10.1017/9781316576878

9. Belocerkovskij OM. *Turbulence: new approaches*. Moscow: Nauka, 2003. 285 c.

10. Monin AS. Turbulence and microstructure in the ocean. *Soviet Physics Uspekhi*. 1973;109(2):333–354. (In Russ.). https://doi.org/10.1070/PU1973v016n01ABEH005153

11. Breugem WP. The influence of wall permeability on laminar and turbulent flows. PhD thesis. *Delft University of Technology*, 2004. 206 p.

12. Vreugdenhil CB. *Numerical Methods for Shallow-Water Flow*. Springer, Berlin; Heidelberg, New York, 1994. 262 p.

13. Fischer H. *Mixing in Inland and Coastal Waters.* Academic Press, 1979. 483 p.

14. Lorentz HA. Sketches of his work on slow viscous flow and some other areas in fluid mechanics and the background against which it arose. *Journal of Engineering Mathematics*. 1996;30(1–2):1–18. https://doi.org/10.1007/BF00118820

15. Sukhinov AI, Chistyakov AE, Alekseenko EV. Numerical realization of the three-dimensional model of hydrodynamics for shallow water basins on a high-performance system. *Matematicheskoe modelirovanie*. 2011;3(5): 562–574. (In Russ.). https://doi.org/10.1134/S2070048211050115

16. Suhinov AI, Chistyakov AE. Parallel implementation of a three-dimensional hydrodynamic model of shallow water basins on supercomputing systems. *Numerical methods and programming*. 2012;13(1):290–297. (In Russ.).

17. Suhinov AI, Chistyakov AE, Fomenko NA. A Method of Constructing Difference Scheme for Problems of Diffusion-Convection-Reaction, Takes Into the Degree of Filling of the Control Volume. Proceedings of the Southern Federal University. *Technical sciences*. 2013;4(141):87–98. (In Russ.).

18. Sukhinov AI, Chistyakov AE, Procenko EA. Sediment Transport mathematical modeling in a coastal zone using multiprocessorComputational. *Numerical methods and programming*. 2014;15:610–620. (In Russ.).

19. Vasil'ev VS, Suhinov AI. Precise Two-Dimensional Models for Shallow Water Basins. *Matematicheskoe modelirovanie*. 2003;15(10):17–34. (In Russ.).

20. Samarskiy AA. *The Theory of difference schemes*. Moscow: Nauka, 1989. 553 p. (In Russ.).

21. Samarskiy AA, Vabishevich PN. *Numerical methods for solving convection-diffusion problems*. Moscow : Nauka, 2015. (In Russ.).

About the Authors:

Sofia V Protsenko, Candidate of Physical and Mathematical Sciences, Associate Professor of the Department of Mathematics, Researcher, A. P. Chekhov Taganrog Institute (branch) Rostov State University of Economics (48, Initiative St., Taganrog, Rostov region, 347936, RF), ORCID, rab5555@rambler.ru

Elena A Protsenko, Candidate of Physical and Mathematical Sciences, Associate Professor of the Department of Mathematics, Leading Researcher, A. P. Chekhov Taganrog Institute (branch) Rostov State University of Economics (48, Initiative St., Taganrog, Rostov region, 347936, RF), ORCID, eapros@rambler.ru

Anton V Kharchenko, Master's student, A. P. Chekhov Taganrog Institute (branch) Rostov State University of Economics (48, Initiative St., Taganrog, 347936, RF), av.kharchenko91@mail.ru

Claimed contributorship:
all authors have made an equivalent contribution to the preparation of the publication.

Received 19.07.2023
Revised 10.08.2023
Accepted 11.08.2023

Conflict of interest statement
the authors do not have any conflict of interest.

All authors have read and approved the final manuscript.

Об авторах:
Проценко Софья Владимировна, кандидат физико-математических наук, доцент кафедры математики, научный сотрудник, Таганрогский институт им. А. П. Чехова (филиал) Ростовского государственного экономического университета (347936, РФ, г. Таганрог, ул. Инициативная, 48), ORCID, rab5555@rambler.ru

Проценко Елена Анатольевна, кандидат физико-математических наук, доцент кафедры математики, ведущий научный сотрудник, Таганрогский институт им. А. П. Чехова (филиал) Ростовского государственного экономического университета (347936, РФ, г. Таганрог, ул. Инициативная, 48), ORCID, eapros@rambler.ru

Харченко Антон Владимирович, магистрант, Таганрогский институт им. А. П. Чехова (филиал) Ростовского государственного экономического университета (347936, РФ, г. Таганрог, ул. Инициативная, 48), av.kharchenko91@mail.ru

Заявленный вклад соавторов:
все авторы сделали эквивалентный вклад в подготовку публикации.

Поступила в редакцию 19.07.2023
Поступила после рецензирования 10.08.2023
Принята к публикации 11.08.2023

Конфликт интересов
Авторы заявляют об отсутствии конфликта интересов.

Все авторы прочитали и одобрили окончательный вариант рукописи.